



Calhoun: The NPS Institutional Archive DSpace Repository

Theses and Dissertations

1. Thesis and Dissertation Collection, all items

1995-09

Operating characteristics of a propylene charged loop heat pipe with potential spacecraft applications

Gherlone, Joseph A.

Monterey, California. Naval Postgraduate School

<http://hdl.handle.net/10945/35135>

This publication is a work of the U.S. Government as defined in Title 17, United States Code, Section 101. Copyright protection is not available for this work in the United States.

Downloaded from NPS Archive: Calhoun



<http://www.nps.edu/library>

Calhoun is the Naval Postgraduate School's public access digital repository for research materials and institutional publications created by the NPS community.

Calhoun is named for Professor of Mathematics Guy K. Calhoun, NPS's first appointed -- and published -- scholarly author.

**Dudley Knox Library / Naval Postgraduate School
411 Dyer Road / 1 University Circle
Monterey, California USA 93943**

NAVAL POSTGRADUATE SCHOOL

Monterey, California



THESIS

**OPERATING CHARACTERISTICS OF A
PROPYLENE CHARGED LOOP HEAT PIPE
WITH POTENTIAL SPACECRAFT
APPLICATIONS**

by

Joseph A. Gherlone, Jr.

September, 1995

Co-Advisors:

Matthew D. Kelleher
Paul J. Marto

Approved for public release; distribution is unlimited.

19960304 078

DTIC QUALITY INSPECTED 1

DISCLAIMER NOTICE



THIS DOCUMENT IS BEST
QUALITY AVAILABLE. THE
COPY FURNISHED TO DTIC
CONTAINED A SIGNIFICANT
NUMBER OF PAGES WHICH DO
NOT REPRODUCE LEGIBLY.

REPORT DOCUMENTATION PAGE			Form Approved OMB No. 0704-0188
<p>Public reporting burden for this collection of information is estimated to average 1 hour per response, including the time for reviewing instruction, searching existing data sources, gathering and maintaining the data needed, and completing and reviewing the collection of information. Send comments regarding this burden estimate or any other aspect of this collection of information, including suggestions for reducing this burden, to Washington Headquarters Services, Directorate for Information Operations and Reports, 1215 Jefferson Davis Highway, Suite 1204, Arlington, VA 22202-4302, and to the Office of Management and Budget, Paperwork Reduction Project (0704-0188) Washington DC 20503.</p>			
1. AGENCY USE ONLY <i>(Leave blank)</i>	2. REPORT DATE September, 1995	3. REPORT TYPE AND DATES COVERED Master's Thesis	
4. TITLE AND SUBTITLE OPERATING CHARACTERISTICS OF A PROPYLENE CHARGED LOOP HEAT PIPE WITH POTENTIAL SPACECRAFT APPLICATIONS		5. FUNDING NUMBERS	
6. AUTHOR(S) Gherlone, Joseph A. Jr.			
7. PERFORMING ORGANIZATION NAME(S) AND ADDRESS(ES) Naval Postgraduate School Monterey CA 93943-5000		8. PERFORMING ORGANIZATION REPORT NUMBER	
9. SPONSORING/MONITORING AGENCY NAME(S) AND ADDRESS(ES)		10. SPONSORING/MONITORING AGENCY REPORT NUMBER	
11. SUPPLEMENTARY NOTES The views expressed in this thesis are those of the author and do not reflect the official policy or position of the Department of Defense or the U.S. Government.			
12a. DISTRIBUTION/AVAILABILITY STATEMENT Approved for public release; distribution unlimited		12b. DISTRIBUTION CODE	
<p>13. ABSTRACT</p> <p>Heat pipes have been in use for spacecraft thermal control since the early 1970s. They offer the advantages of high thermal conductance with relatively low mass, but suffer the liabilities of a rigid configuration and sensitivity to adverse acceleration (exemplified by the evaporator raised over the condenser in earth's gravity field). The Loop Heat Pipe was developed in Russia specifically to address these concerns. Using a metal matrix wick with relatively high capillary pumping capacity and careful fluid inventory management, the Loop Heat Pipe is claimed to be fully self-priming and capable of withstanding high adverse acceleration. The above factors also allow the vapor and liquid to travel through very small lines (3 mm OD), providing a highly flexible installation.</p> <p>The Loop Heat Pipe appears to be a valuable technology for future spacecraft development, but little performance data is available. Martin Marietta has purchased two Loop Heat Pipes (one charged with propylene and one with ammonia) from the Lavochkin Association in Russia. The ammonia pipe was tested by Martin Marietta Astronautics Group in Denver, and the propylene pipe by the author at Philips Laboratory under a Memorandum of Agreement between Martin Marietta and the Air Force Materiel Command. The results presented show that while the propylene charged pipe is not capable of transferring the heat carried by the ammonia pipe, it has otherwise similar characteristics. Failure modes and recovery procedures are documented, and recommendations for further study are included.</p>			
14. SUBJECT TERMS Spacecraft Thermal Control, Heat Pipes, Capillary Pumped Loops		15. NUMBER OF PAGES 150	16. PRICE CODE
17. SECURITY CLASSIFICATION OF REPORT Unclassified	18. SECURITY CLASSIFICATION OF THIS PAGE Unclassified	19. SECURITY CLASSIFICATION OF ABSTRACT Unclassified	20. LIMITATION OF ABSTRACT UL

Approved for public release; distribution is unlimited.

**OPERATING CHARACTERISTICS OF A PROPYLENE CHARGED LOOP
HEAT PIPE WITH POTENTIAL SPACECRAFT APPLICATIONS**

Joseph A. Gherlone, Jr.
Lieutenant, United States Navy
B.S., Rensselaer Polytechnic Institute, 1987

Submitted in partial fulfillment of the requirements for the degree of

**MASTER OF SCIENCE IN SYSTEMS TECHNOLOGY
(SPACE SYSTEMS OPERATIONS)**

and

**MASTER OF SCIENCE IN ENGINEERING SCIENCE
(ASTRONAUTICS)**

from the

**NAVAL POSTGRADUATE SCHOOL
September, 1995**

Author:

Joseph A. Gherlone, Jr.

Approved by:

Matthew D. Kelleher, Co-Advisor

Paul J. Marto, Co-Advisor

Conrad F. Newberry, Second Reader

Daniel J. Collins, Chairman

Department of Aeronautics/Astronautics

Rudolph Panholzer, Chairman
Space Systems Academic Group

ABSTRACT

Heat pipes have been in use for spacecraft thermal control since the early 1970s. They offer the advantages of high thermal conductance with relatively low mass, but suffer the liabilities of a rigid configuration and sensitivity to adverse acceleration (exemplified by the evaporator raised over the condenser in earth's gravity field). The Loop Heat Pipe was developed in Russia specifically to address these concerns. Using a metal matrix wick with relatively high capillary pumping capacity and careful fluid inventory management, the Loop Heat Pipe is claimed to be fully self-priming and capable of withstanding high adverse acceleration. The above factors also allow the vapor and liquid to travel through very small lines (3 mm OD), providing a highly flexible installation.

The Loop Heat Pipe appears to be a valuable technology for future spacecraft development, but little performance data is available. Martin Marietta has purchased two Loop Heat Pipes (one charged with propylene and one with ammonia) from the Lavochkin Association in Russia. The ammonia pipe was tested by Martin Marietta Astronautics Group in Denver, and the propylene pipe by the author at Philips Laboratory under a Memorandum of Agreement between Martin Marietta and the Air Force Materiel Command. The results presented show that while the propylene charged pipe is not capable of transferring the heat carried by the ammonia pipe, it has otherwise similar characteristics. Failure modes and recovery procedures are documented, and recommendations for further study are included.

TABLE OF CONTENTS

I. INTRODUCTION	1
A. EXECUTIVE SUMMARY	1
B. PROBLEM STATEMENT	3
C. SPACECRAFT THERMAL CONTROL	3
1. Heat Balance Equations	4
2. Space Environmental Thermal Considerations	5
a. Direct Solar Heating	5
b. Earth Albedo	7
c. Earth Radiated Infrared	8
d. Free Molecular Heating	8
e. Charged Particle Heating	8
f. Spacecraft Emission	8
3. Spacecraft Thermal Considerations	9
a. Electronic Equipment	10
b. Propulsion	11
c. Batteries	11
d. Solar Arrays	12
e. Antennas	12
4. Passive Thermal Control Methods	13
a. Surface Finishes and Coatings	13
b. Insulation	13
c. Radiators	14
d. Heat Sinks	14
e. Phase Change Material	14
f. Thermal Doubler	15
5. Active Thermal Control Methods	15
a. Louvers	15
b. Heaters	15
c. Thermo-Electric and Thermo-Acoustic Coolers	16
d. Fluid Heat Exchange Loops	16
D. HEAT PIPES	16

a. Working Fluids	17
b. Wick Designs and Structures	18
c. Thermal Transport Limits	19
II. LOOP HEAT PIPE	23
A. LOOP HEAT PIPE TECHNOLOGY	23
1. LHP Elements	24
a. Evaporator	24
b. Compensation Chamber	26
c. Condenser	26
d. Transport Lines	26
2. Loop Heat Pipe Operating Principles and Theory	27
B. CAPILLARY PUMPED LOOP TECHNOLOGY	31
1. CPL Elements	31
a. Evaporator	31
b. Condenser	32
c. Transport Lines	33
d. Reservoir	33
e. Subcooler	33
f. Mechanical Components	33
2. Capillary Pumped Loop Operating Characteristics	34
C. PREVIOUS LHP EXPERIMENTS	34
III. EXPERIMENT DESCRIPTION	37
A. TEST PROGRAM	37
1. Objectives	37
B. TEST ARTICLE	38
1. Description and Specifications	38
2. Propylene Properties	40
C. TEST CONFIGURATION	41
1. Physical Layout	41
2. Evaporator End	42
3. Condenser End	43
4. Instrumentation	43
a. Temperature	43
b. Power	44

5. Data Acquisition	44
a. Temperature	44
b. Power	44
D. TESTS CONDUCTED	44
E. TEST AND SAFETY PROCEDURES	46
1. Safety	46
2. Testing	47
F. POST-TEST DATA HANDLING	47
IV. DATA REDUCTION AND DISCUSSION	49
A. TEST DATA	49
B. PERFORMANCE CHARACTERISTICS	50
1. Startup and Transient Behavior	51
a. Anomalous Runs	55
b. Reverse Flow	57
c. Complex Flow	58
2. Thermal Transport	58
a. Operating Range	58
b. Evaporator Equilibrium Temperature	59
c. Delta T	62
d. Conductance Characteristics	64
e. Adverse Height Effects	66
C. FAILURE MODES	69
D. RECOVERY MODES	70
E. EXPERIMENTAL FLAWS	71
1. Control of Temperature	71
2. Heat Balance	71
3. External Sensors	71
4. Temperature Sensors Only	72
V. CONCLUSIONS AND RECOMMENDATIONS	73
A. SUITABILITY	73
1. Usable Operating Range and Criteria	73
2. Advantages	73
3. Disadvantages	74
B. FURTHER RESEARCH	75

1. Interior Sensors	75
2. Propylene Properties	75
3. Destructive Testing	76
4. Low Temperature Testing	76
5. Thermal Vacuum Testing	76
6. Tests with Vapor and Liquid Lines Coiled/Bent	77
REFERENCE LIST	79
BIBLIOGRAPHY	81
APPENDIX A. PREVIOUS LHP EXPERIMENTATION RESULTS.	83
APPENDIX B.	
LHP-93-2-PROP TEST INFORMATION, AND SELECTED RESULTS.	89
APPENDIX C. LHP-93-2-PROP EXPERIMENTAL DATA.	105
INITIAL DISTRIBUTION LIST	135

ACKNOWLEDGMENTS

The author would like to thank Dr. Matthew Kelleher and Dr. Paul Marto for their inexhaustible patience and firm guidance during the production of this thesis. Despite heavy workloads as Department Chairman and Dean of Research, respectively, they brought out my best.

The author would also like to thank Lt. Eric Critchley and Dr. Don Gluck of the Space Thermal Technologies Branch (VTPT) of Phillips Laboratory for their inestimable help in commencing testing and "working out the bugs," and Mary Corrigan, formerly of VTPT, for coordinating many details that made the author's trip there a success.

Thanks to Jane Baumann of Lockheed Martin Astronautics Group for the photographs used on pages 38 and 39.

Finally, thanks to the Joeys.

I. INTRODUCTION

A. EXECUTIVE SUMMARY

Heat pipes have been in use for the thermal control of spacecraft since the early 1970s. They offer the advantages of high heat transfer rates and relatively low weight, but suffer the liabilities of cessation of heat transfer under adverse acceleration (the acceleration force oriented axially toward the condenser end), and a rigid configuration. The Loop Heat Pipe (LHP) design was developed in Russia to address these concerns. Using a metal matrix wick with a high capillary pumping capacity and careful fluid inventory management, the loop heat pipe is advertised to be fully self-priming, and capable of operation even under high adverse accelerations. These factors also allow the evaporator and condenser to exchange fluid (and thus heat) by very small (3 mm) lines, solving the configuration issue as well.

The LHP appears to be a valuable technology for future spacecraft development, but little performance data is available. Lockheed Martin has purchased two LHPs (one charged with ammonia, and one with propylene) from the Lavochkin Association in Russia. The ammonia LHP was tested by the Lockheed Martin Astronautics Group (LMAG) in Denver, CO, and an agreement was completed with Phillips Laboratory (part of the Air Force Material Command) to test the propylene LHP, with assistance from the Naval Postgraduate School.

This thesis discusses the background of spacecraft thermal control and the heat pipe as a thermal control device in spacecraft, the propylene-charged LHP, and the test setup. The data gathered is presented in its entirety, and the following conclusions are drawn:

- ♦ The propylene-charged LHP has a fairly limited range of operation, roughly 10-150 watts. Over this range, temperature control is fairly stable.
- ♦ The LHP tested exhibits variable conductance properties, maintaining 20-30°C evaporator temperature for a range of heat loads and condenser temperatures.
- ♦ The adverse conditions (evaporator above condenser to simulate an adverse

acceleration) specified in the acceptance test documents could not be replicated, but successful runs were achieved with approximately half the specified adverse height. As expected, equilibrium temperature at the evaporator climbs by 5-10 degrees.

- ◆ Startup appears reliable over the range of loads specified, but anomalous failures which remain unexplained were experienced. Failure was more likely when a significant temperature difference existed between evaporator and condenser.
- ◆ When failures occurred, subsequent startup was difficult, especially when in adverse orientation. Recovery mode involved returning the LHP to a horizontal orientation and applying 70 W to achieve vapor/liquid redistribution.

During the course of experimentation and analysis, shortcomings in setup and method were identified for correction in later research, and recommendations were developed for further study.

- ◆ No heat balance determination was performed at the heat sink. All power figures used were based on electrical input to the attached heater. Determining heat removed by the chiller would refine experimental accuracy.
- ◆ No internal sensors were possible for this testing. Internal sensors for direct vapor/liquid temperature, pressure, and flow rate measurement would greatly enhance the value of the experiments and the analysis process.
- ◆ There was initial difficulty in locating propylene thermophysical properties. Further research should be done to locate additional data, especially regarding surface tension in the anticipated working range.
- ◆ Anomalous startup failures are an item of concern. While the quantity of data collected is significant, the inability to explain these incidences makes the expense of a flight experiment a high risk. Further ground study with internal sensors is recommended.

B. PROBLEM STATEMENT

This investigation intends to rectify in part the lack of characterization data on the Loop Heat Pipe design. In particular the propylene-charged LHP has had little attention due to difficulties in locating sufficient ranges of thermophysical property data [6, App. C]. The intent of the project is to compare the performance of the propylene charged LHP to the ammonia charged LHP with regard to such properties as startup, range of evaporator heat loads, condenser temperatures, effect of insulation, adverse heights, and rotation of the evaporator. The propylene pipe is to be evaluated for variable conductance behavior, control of performance by applying small heat loads to the compensation chamber, and low power performance and reliability. As testing is still ongoing as this thesis is written, the issues of startup, load range, condenser temperature, adverse height, and variable conductance will be addressed. Conclusions will be presented regarding the utility of the LHP, and recommendations for improvements to experimentation and for further investigation.

C. SPACECRAFT THERMAL CONTROL

Heat transfer occurs by three basic mechanisms: conduction, convection, and radiation. All of these mechanisms are in operation on earth, but the space environment constrains the processes in use, complicating thermal control.

As the environment in space is essentially a vacuum, convection does not provide a mode for heat removal from the spacecraft. This eliminates one of the most significant mechanisms for equalizing temperatures normally experienced in an atmosphere. Heat is readily conducted within the vehicle, but while differing temperatures between components may provide a heat flow path, the heat load will remain internal to the vehicle, and may cause equipment to exceed operating temperature limits. Ordinarily, components are placed carefully in order to minimize harmful interactions, but there are definite bounds to this method. What is required is a path for removal of excess heat from the spacecraft to some sink. Radiation is the only mode which normally results in heat transfer from the spacecraft to the environment.

1. Heat Balance Equations

Spacecraft absorb heat from and emit heat to the environment, and carry equipment aboard which produce heat by power dissipation (i.e., electronic components). In *Design of Geosynchronous Spacecraft*, Agrawal refers to a simple but elegant formula for heat balance in spacecraft [1, p. 280]:

$$\text{heat stored} = \text{heat in} - \text{heat out} + \text{heat dissipated} \quad (1-1)$$

If the heat stored remains constant, so will temperature. Therefore, the internal power and absorbed radiation must balance the heat radiated to space to maintain the temperature within desired limits. To perform the thermal control design process, the spacecraft will usually be broken down into various sections, or nodes, which have similar characteristics. The above formula applies to each node individually as it does to the entire vehicle -- if temperature is to be maintained, heat in and out must balance. Since some items with high dissipation are located inside the shell where they cannot radiate excess heat, or others requiring minimum temperature are not sunlit, some heat must be moved from place to place inside the spacecraft. An enormous radiator does no good if heat dissipated inside the spacecraft is not routed to it.

If we treat all external heat sources except direct sunlight as negligible, the above equation can be written:

$$mc_p \frac{dT}{dt} = \alpha_s S A_{\text{sunlit}} + P_{\text{dissip}} - \epsilon_{\text{rad}} \sigma T^4 A_{\text{rad}} \quad (1-2)$$

(A) (B) (C)

where m = mass of the node,

c_p = specific heat of the node,

$\frac{dT}{dt}$ = the time change of temperature of the node,

α_s = solar absorptance of node,

S = incident solar energy per unit area (incl. angle and seasonal variations),

A_{sunlit} = area of the node receiving solar radiation,

P_{dissip} = power generated (internally dissipated) in the node,

ϵ_{rad} = emittance of the node,

T = absolute temperature of the node, and

A_{rad} = area of the node emitting at thermal wavelengths.

It can be seen in Eqn. 1.2 that the goal should be to cause the right side of the equation to go to zero, effectively eliminating temperature change since m and c_p are constants. We do this by manipulating each of the terms on the right. Obviously, S and σ cannot be altered, but they vary over time, and the remaining factors are design criteria for the elements of thermal control described below.

2. Space Environmental Thermal Considerations

Heat transfer by radiation is a two-way path. Heat input comes from sunlight (both direct and reflected from earth and other bodies), the earth's infrared emissions, and interaction of the spacecraft with free molecules and charged particles in earth orbit. Heat outflow is due to emission from the spacecraft outer surfaces. None of these is constant; each varies by wavelength of the radiation, orbital placement, time of day, season, sunspot cycle, and surface properties of spacecraft components.

a. Direct Solar Heating

The direct input of the sun is the most significant heat load for most spacecraft. The sun's emissions are constant to within 1 % of the annual average solar flux (1353 W/m^2) at all times, but a spacecraft in earth orbit will experience a variation of approximately ± 3.5 % of the mean due to the eccentricity of the earth's orbit around the sun. Spacecraft are also subject to eclipse by the bulk of the earth and variation of the sun's angle (as viewed from the spacecraft), dependent on the characteristics of their orbital parameters, causing different components to receive heat at different times. For a geosynchronous spacecraft, which remains above the same point on the earth, the eclipse will be short (or non-existent in some seasons), and vary daily based on the day-night cycle. The angle between the earth's equator and the plane of the ecliptic causes a seasonal variation of $\pm 23.5^\circ$ as depicted in Fig. 1.1.

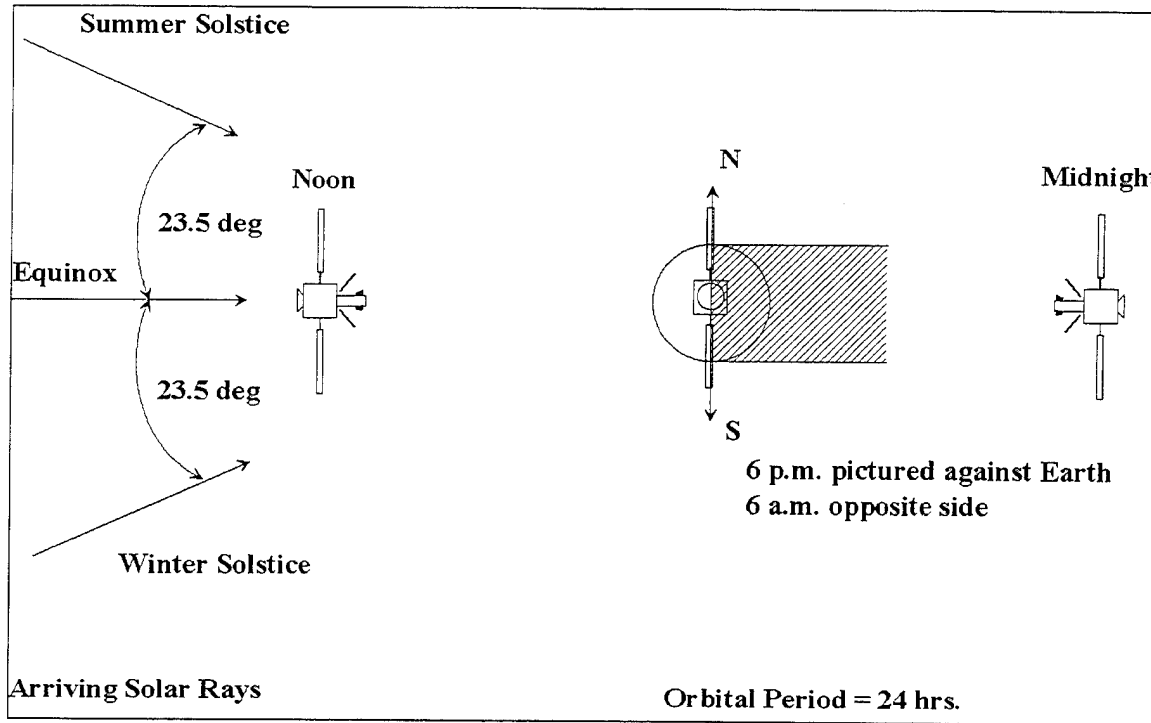


Figure 1.1. Solar Incidence Angle Variation. [after 1, p. 279]

A low-earth orbiting (LEO) spacecraft will experience eclipse once per orbit due to its relative closeness to the earth, and an angular variation related to its altitude and orbital inclination (Figs. 1.2 and 1.3). A special case is the sun-synchronous orbit; its orbital parameters are gauged to maintain a certain time of equatorial passage at a certain longitude, for optical observations. [3, p. 2-3]

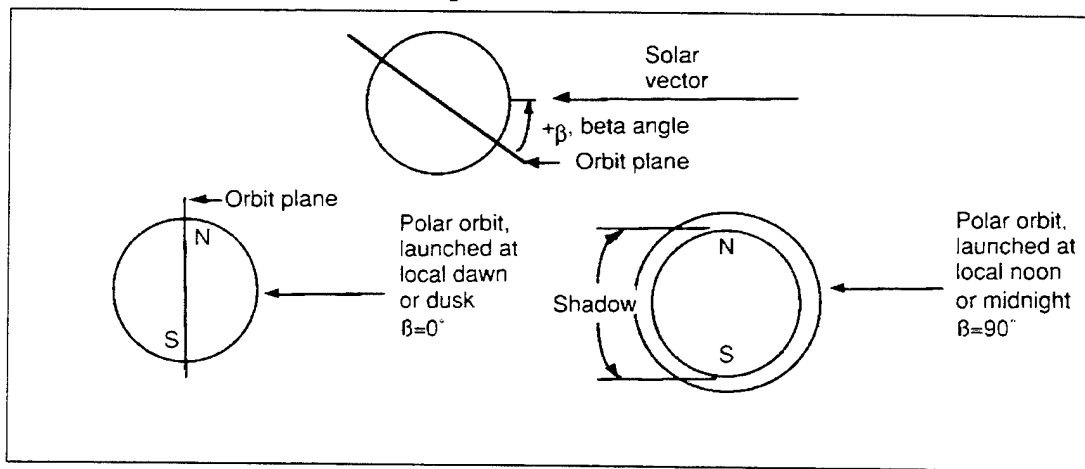


Figure 1.2. Beta Angle Related To Orbital Inclination. [3, p. 2-18]

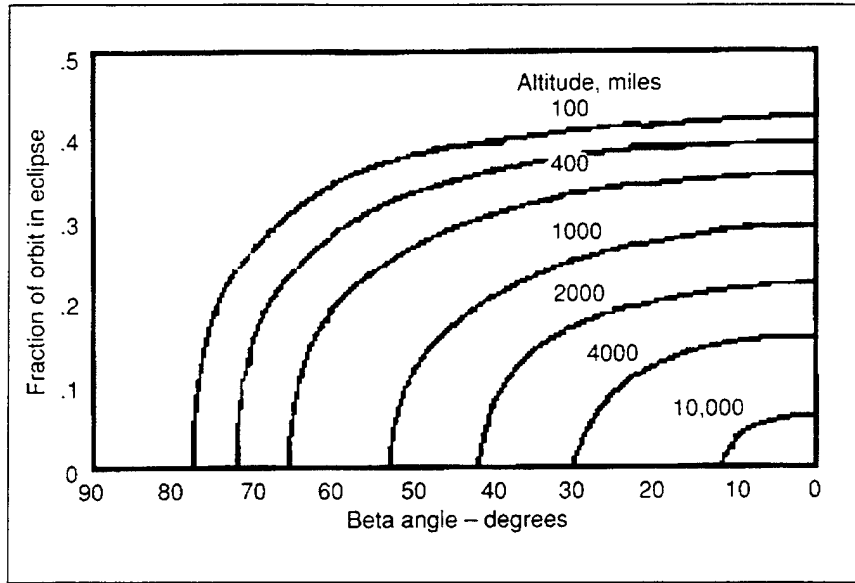


Figure 1.3. Beta Angle Related to Altitude. [3, 2-19]

Solar radiation also varies by wavelength and properties of the surface irradiated. The amount of energy absorbed by surfaces on the spacecraft is largely dependent on the wavelength of the incident radiation. Thus, a surface with higher absorptivity for the predominant wavelengths in solar radiation (Fig. 1.4) will become hotter than a surface with high absorptivity in another range of wavelengths. [1, p. 273] This assumes that the surfaces emit similarly, as discussed below.

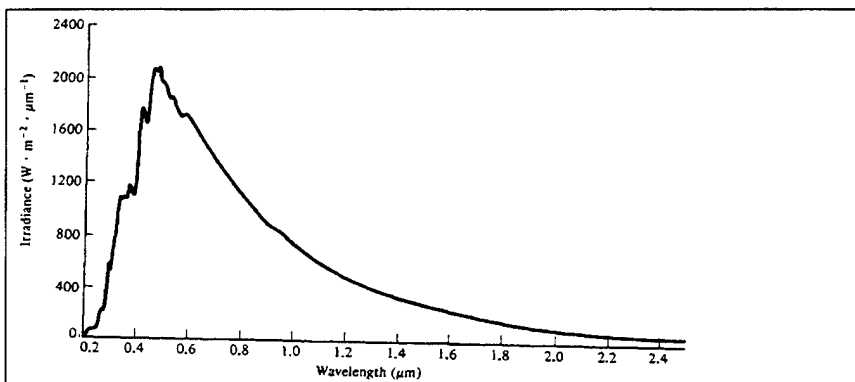


Figure 1.4. Solar Spectral Irradiance Curve. [1, p.274]

b. Earth Albedo

Albedo refers to incident energy flux reflected from a body. It is normally expressed as a percentage of incident radiation, and varies significantly with atmospheric

conditions, land or ocean surfaces, and solar incident angle to the terrestrial area of interest. Even when the albedo itself is constant, the motion of the satellite causes a change in intensity due to the change in reflection angle between sun, subsolar point on the earth, and the satellite. Generally, albedo is considered a minor factor in spacecraft thermal control, but especially in LEO can have repercussions due to its viability.

c. Earth Radiated Infrared

While some of the incident solar radiation is reflected by the earth as albedo, a much larger share is absorbed by the atmosphere and surface of the planet. This places the earth in the same situation as a satellite, subject to a significant but varying heat load, and able to maintain balance only by radiation to space. This radiation is in the form of long-wave infrared (IR) emissions. The satellite will receive some of this radiation, just as it receives solar input, although this is again a very small factor. [3, p. 2-8]

d. Free Molecular Heating

The kinetic energy transfer effected by the bombardment of the satellite by molecules in the outer reaches of the atmosphere is termed free molecular heating (FMH). It is considered negligible unless the perigee of the satellite is within 185 km [3, p.2-10], but may be a consideration for launch phase or a highly elliptical orbit (HEO) design.

e. Charged Particle Heating

A similar effect to FMH is the transfer of energy from charged particles in the Van Allen radiation belts. This factor is even less significant than the others discussed, but may have influence in cryogenic applications. [3, p. 2-11]

f. Spacecraft Emission

The sole permanent loss of heat from the spacecraft is by radiation from its outer surfaces. It is governed by the Stephan-Boltzmann Law, written

$$E = \epsilon \sigma T^4, \quad (I-3)$$

where the Stephan-Boltzmann Constant, $\sigma = 5.67 \times 10^{-8} \text{W/m}^2 \cdot \text{K}^4$,
 ϵ is the emittance of the surface, and

T is the absolute temperature of the surface, in K.

Thus, the heat ejected from the spacecraft is dependent on both the temperature of the outer surfaces, and their relative ability to emit at a given wavelength. Like absorptivity, emissivity varies with wavelength, so external surfaces can be optimized to minimize solar wavelength absorption, and maximize thermal wavelength emission if heat load exceeds heat output. [1, p. 271]

3. Spacecraft Thermal Considerations

Nearly every component on a spacecraft has some temperature requirements. Temperature limits may be necessary to prevent freezing of liquids, warping of structure due to temperature differentials, or damage to components. Certain other items may require a particular temperature range for most efficient operation, but not suffer permanent degradation if those limits are exceeded. Table 1.1 provides typical temperature ranges for a variety of spacecraft subsystems, and specifics for some critical subsystems are discussed below.

Component	Initialization	Operating
Communication Receiver	-30 to +55	+10 to +45
RF Multiplexer	-30 to +55	-10 to +40
TWTA	-30 to +55	-10 to +55
Antenna	-170 to +90	-170 to +90
Solar Array	-160 to +80	-160 to +80
Battery	-10 to +25	0 to +25
Electrical Shunt Assembly	-45 to +65	-45 to +65
Earth/Sun Sensor	-30 to +55	-30 to +50
Angular Rate Sensor	-30 to +55	+1 to +55
Momentum Wheel	-15 to +55	+1 to +45
Propellant Tank	+10 to +50	+10 to +50
Thruster Catalyst Bed	+10 to +120	+10 to +120
Pyrotechnic Separation Mechanism	-170 to +55	-115 to +55
Separation Clamp	-40 to +40	-15 to +40

Table 1.1. Typical Equipment Temperature Limits in Degrees Celsius. [1, p. 266]

Since the heat transfer provided by atmosphere is not available in space, the main path for heat transfer is by conduction between subsystems or by radiation to space or other systems. Conduction occurs readily, but without careful attention to equipment placement and methods for insulation or provision of an alternate heat path, the equipment requiring a low temperature for successful operation becomes a "heat sink," its lower temperature allowing all other subsystems to transfer heat to it. Radiation external to the spacecraft allows excess heat to be emitted, but since most of the equipment in a spacecraft is inside a shell, ordinarily a box or cylinder shape, radiation can become a path to those cooler components. The problem worsens if there are insufficient paths to external surfaces for radiation, as heat becomes trapped inside the shell, and the radiative or conductive coupling between the cooler and hotter components tends to equalize temperatures between them.

a. Electronic Equipment

Solid state electronic devices generate heat. The semiconductor-based processing systems in common use today may have power efficiencies anywhere between 50 percent and 10 percent, meaning that for every Watt of electrical power consumed, between half and nine-tenths of a Watt must be shed as heat. These devices also have an optimum temperature range, outside which the switching functions which allow high performance and high speed are severely hampered.

Some electronic devices have non-solid state components which generate orders of magnitude additional heat. A good example of this is the Traveling Wave Tube Amplifiers (TWTA) used for high power radar and communications applications. These consume in the hundreds of Watts, and are roughly 40 percent efficient, so that a 200 W TWTA must dissipate 120 W of thermal energy. [1, p. 423]

Almost every spacecraft requires attitude determination and control systems (ADCS) to maintain instrument or communication pointing knowledge and direction, flight path determination, and correction for orientation or position disturbances. These systems are largely based on sun, earth, or star sensors, which contain high precision optical devices. Very small temperature changes can induce disproportionately large

errors into the ADCS by changing focal length or alignment. [3, p. 3-16]

Some attitude sensors and payload instruments use IR wavelength to locate the earth, or to gather data. Some communications gear depends on low noise amplifiers to reduce power usage or antenna size. Extraneous IR radiation from sources on the spacecraft will introduce noise into the subsystem, or make it difficult for the sensor to detect the earth. These systems are generally designed to operate at cryogenic temperatures, and thus must be carefully shielded, and isolated from all sources of internal heat. [3, p. 3-17]

b. Propulsion

Satellites use two main types of on-orbit propulsion systems: monopropellant, or bipropellant. The activation of either system has temperature requirements for successful start-up, and both systems release considerable heat. Monopropellant systems use a catalyst to convert a liquid to a rapidly expanding gas for thrust. The catalytic bed must be maintained within certain temperature limits or it will suffer degradation, and the working fluid must be able to flow so that the reaction can be initiated. Bipropellant systems are based on the "burning" of a fuel with an oxidizer, both of which must be able to flow smoothly so that mixture rates can be maintained.

In either case, the propellant tank must be kept from freezing, or warmed prior to use, and the flow lines must be kept clear. In some cases, power dissipating equipment may be conductively coupled with the propulsion system, but this is complicated by the exothermic nature of the operation of the propulsion system, and the temperature requirements of the coupled system. Ordinarily, temperature maintenance is accomplished using heaters. [3, p. 3-5 to 3-8]

c. Batteries

The two types of batteries commonly used on spacecraft are Nickel-Cadmium (NiCd), and Nickel-Hydrogen (NiH₂). NiCd batteries require temperatures between 0°C and 20°C, as higher temperatures degrade life, and lower temperatures may freeze the electrolyte, damaging the cell. NiH₂ require 0°C to 20°C, since they are pressurized, and

either higher or lower temperatures may damage the pressure vessel. Both types require all cells to be isothermal to within about $\pm 5^{\circ}\text{C}$, to balance charge/discharge rates. These rates are temperature dependent, so significant temperature differences could cause imbalances and current shifts across the spacecraft bus, potentially damaging electrical equipment or the batteries themselves. Future battery designs being tested include Sodium-Sulphur (NaS) cells, in which the electrolyte is solid at room temperature, which will require even greater attention to thermal control. [3, p. 3-10]

d. Solar Arrays

Solar arrays function due to sunlight impinging on a juxtaposition of two materials, referred to as a P-N junction. This requires a high solar absorptance, but the efficiency of electron flow in and between these materials is highly temperature dependent. Thus, there is a need to radiate great quantities of heat to keep the temperatures low, while reflective coatings to reduce heating from incoming radiation would defeat the purpose of the cells. In practice, some method of controlling voltage must be established, which will usually involve the dissipation of heat, while array panels will be exposed to a range of temperatures from -75°C to $+65^{\circ}\text{C}$ in LEO, and -145°C to 55°C in GEO. [3, p. 3-21]

e. Antennas

Antennas are among the largest structures on any spacecraft, and cannot be shielded completely from sunlight, as they must maintain proper pointing. They ordinarily have temperature limits based on the amount of distortion caused in the material of which reflectors or structural components are made. Distortions in the shape or fit of components could affect the beam shape, gain, or pointing accuracy of an antenna, breaking a vital communication link. Additionally, any coatings or components used for thermal control must be free of adverse interaction with radio frequency radiation (RF), to avoid interference. [3, p.3-13]

4. Passive Thermal Control Methods

a. Surface Finishes and Coatings

Surfaces may be manufactured into the material of a component or applied afterward, and are intended to affect terms A and C. Kirchoff's Law states that at any given wavelength, absorptance and emittance must be equal. Thermal coatings are designed to minimize absorption of wavelengths which result in power input, and maximize emission of thermal IR wavelengths. A "cold" coating, for instance could be a white paint which has a low absorptance in solar (visible light) wavelengths (~ 0.2), but high thermal emittance (~ 0.9). Gold foil or paint is considered a "warm" coating, since its absorptance is nearly as low as the white paint (~ 0.25), but its thermal emittance is also fairly low (~ 0.45). Optical Solar Reflectors (OSR) are second-surface mirrors composed of a quartz or Teflon film backed with a metallic coating. These devices can be attached to a smooth surface with conductive epoxy, to provide an even colder surface finish as shown in Fig. 1.5. They typically have absorptance in the range of 0.05 to 0.1, and an emittance near 0.8. [3, p. 4-8]

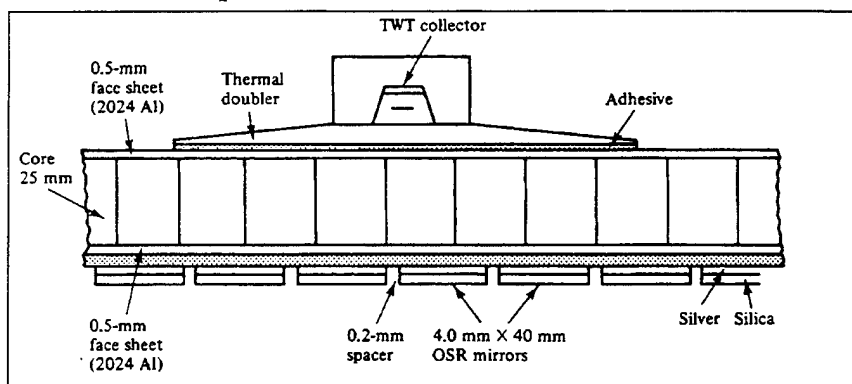


Figure 1.5. Example of Passive Control Methods. [3, p. 298]

b. Insulation

Insulation for spacecraft normally comes in the form of a "blanket," which may be multiple layers (called multi-layer insulation, or MLI) or single layer. MLI is used to either retain heat, or prevent heating from the outside (either environmental or from elsewhere on the spacecraft -- propulsion motor plumes are the best example). Single

layer barriers are used to save mass and bulk when isolation need not be as rigorous. Either type of insulation is composed of some type of low-emittance film with some form of reflective finish. This reduces the effective solar absorptance in term A of Eqn. 1-3, or the effective emittance in term C. In the case of MLI, a "spacer" material may be included between layers to minimize conduction transfer through the barrier. [3, p. 4-75]

c. Radiators

Radiators are the main means of eliminating waste heat from a spacecraft, and are therefore a critical component in thermal design. Placement is important to minimize solar flux, as well as to minimize difficulty in transferring waste heat from components which generate it. A radiator requires a "cold" coating as described above to maximize heat rejection (term C of Eqn. 1-3), and to minimize environmental impact on efficiency (term A of Eqn. 1.3). [3, p. 4-125]

d. Heat Sinks

For transient heat loads, such as intermittent operation of a TWTA, heat may be controlled by creating a node specifically for storage. Conductive coupling is intentionally established between the node generating the heat, and a node called a heat sink. In this way, the heat stored on the left side of Eqn. 1-3 is not stored in the node that generated it, but in the sink. If the mass and the specific heat of the sink are correctly selected, the temperature will rise in the sink, but not in the equipment dissipating the power. Conduction rates are temperature dependent, so a limit will be reached if the temperature difference between source and sink becomes too small, and then source temperature will also rise. If the time for which the load is active is short, the limit will not be reached and loss to the environment (if necessary via a radiator) can eliminate the heat absorbed over time, provided that the sink is isolated from solar input. [3, p. 156]

e. Phase Change Material

Transient heat loads can also be controlled using a material which uses absorbed heat to effect a change of state, referred to as a Phase Change Material (PCM). Rather

than simply having sufficient mass to absorb heat without significant temperature change, PCM is selected to have a melting point (in rare cases, boiling point) in the desired range. Heat absorbed once this range is reached will cause no further temperature change, but is used as the "heat of fusion" for the material. When all of the material has melted, the absorbed heat energy will again cause a rise in temperature. This method has the advantage over a simple heat sink of being closer to an isothermal process since the rate of heat absorbed is not dependent on a narrowing temperature differential. [3, p. 4-149]

f. Thermal Doubler

A thermal doubler has some of the characteristics of a heat sink, but it has a somewhat different purpose. Rather than simply absorbing the heat, it is made to absorb the heat from a small area, and spread it out over a larger area so that it can be eliminated via OSR or another surface finish. A typical use is shown in Fig. 1.5. [1, p. 297]

5. Active Thermal Control Methods

a. Louvers

Louvers are mechanically actuated devices, normally either slatted (like venetian blinds) or rotating pinwheels with cutouts. They are used to selectively hold or release heat by radiation, and can provide about a six-to-one variation in temperature from full open to full closed position. They are used in concert with surface finishes to maintain desired temperatures, and can be integrated with a thermostatic controller if the actuators are bimetallic spring type. These devices allow fairly fine control of radiating surfaces, but heat must be brought to them to be of use. [3, p. 4-99]

b. Heaters

Heaters are available in many sizes and shapes, and are usually highly flexible for space applications. They can then be attached directly to whatever they are heating to minimize collateral effects. They are mentioned here only for completeness. [3, p. 4-89]

c. Thermo-Electric and Thermo-Acoustic Coolers

Thermo-electric coolers are simple, rugged devices based on the Peltier Effect, by which an electric current will cool a junction of dissimilar metals. They are limited by size, low efficiency when large temperature differentials are required between the hot and the cold stages, and relatively high power consumption for cooling achieved.

Thermo-acoustic coolers depend on the relation between an acoustic standing wave and the time lag of heat diffusion through the working fluid to effect cooling. Testing of a unit developed at NPS was accomplished on the Space Shuttle *Discovery* (STS-42), and the concept shows promise for future spacecraft use. For current space applications, most designs rely on the ability to radiate into space, which provides a ready sink. [3, p. 4-141]

d. Fluid Heat Exchange Loops

Fluid heat exchange loops are devices which use a pumped fluid and a series of heat exchangers for efficient transfer of waste heat from the source to the radiator. The elements of such a loop are a pump, coolant fluid, heat exchangers, and radiator. The coolant fluid is pumped to the heat exchanger at the source, where it absorbs heat, ordinarily from multiple fluid line passes either in a helical coil or a "snake" pattern. The fluid is then carried through the return line to the radiator. Since the radiator is constantly shedding heat to space, heat is efficiently transferred by convection to the radiator body, and then to space by radiation. These systems are generally limited by the size and mass of the pump and the piping system. They work very well, but can only be fielded in space for fairly large systems. [3, p. 4-161]

D. HEAT PIPES

A heat pipe is a two phase fluid flow device which provides high efficiency heat transfer. As shown in Fig. 1.6, it consists of a cylindrical body containing the working fluid and a wick. Heat is absorbed by conduction through the pipe wall and wick structure, generating vapor which flows under its own pressure through the center duct. At the condenser end, heat is removed (for our purposes, generally using a radiator) and the cooled vapor condenses against the pipe wall. The wick structure forms menisci in

the deposited liquid, providing capillary pressure which pumps the liquid back to the evaporator. As long as there is sufficient capillary pressure developed by liquid surface tension in the wick structure, condensate will continue to return to the evaporator, and natural flow will be maintained.

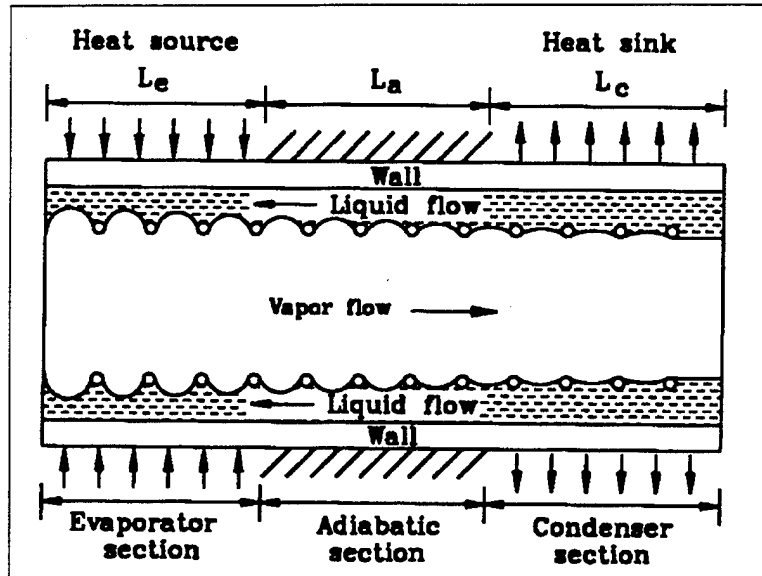


Figure 1.6. Generic Heat Pipe Schematic. [2, p. 5]

The advantage to using a heat pipe vice a strap, bar, or doubler to provide the path for heat removal to the radiator is mass. To illustrate, I refer back to the TWTA as a thermal control problem -- I previously mentioned one which dissipates 120 W thermal (W_t) of 200 W electrical (W_e). If the maximum operating temperature for the TWTA is 55°C or 328 K, and the excess heat will be removed by conduction through a path with a very high conductance like an aluminum bar (assume conductivity of 200 W/m·K) to a sink at absolute 0, the diameter of the bar would be about 5 cm, or 2 inches. The mass for such a bar would be in excess of 17 kg/m³ -- this is nearly 2 kg for each centimeter the heat needs to be transported. A heat pipe 1 m long might weigh only about 2 kg and transport the same amount of heat.

a. Working Fluids

Working fluid is the major design factor for a heat pipe which determines the operating temperature range. Boiling point, critical temperature and pressure, and surface

tension as a function of temperature all contribute to a working fluid's useful range. A rule of thumb provided by Amir Faghri holds that useful range extends between a saturation pressure of 0.1 atm and 20 atm. Below that range, low vapor pressure limits capacity, and above it, the pipe wall material must be made so thick that thermal resistance in the material becomes the limiting factor [3, p. 21]. Figure 1.7 shows typical working fluids, divided into four categories by temperature of useful range.

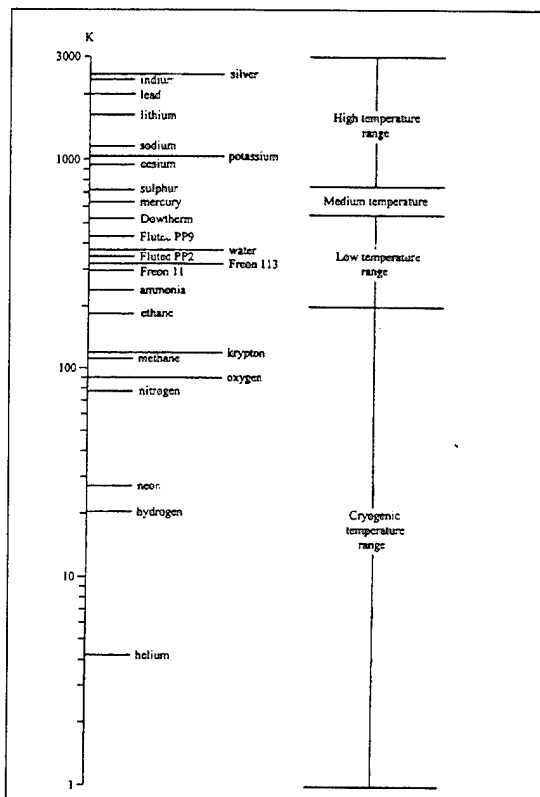


Figure 1.7. Working Fluids Grouped By Temperature Range. [2, p.23]

b. Wick Designs and Structures

From a design standpoint, there are three main characteristics of wicks : capillary radius, permeability (to axial liquid flow), and thermal conductivity (to minimize thermal resistance across the wick). These are frequently contradictory requirements; for example, small pores are needed at the liquid-vapor interface to achieve high capillary pumping pressure, but may impede the flow of liquid through the wick. Due to these requirements, wicks may be homogeneous, consisting of one wick material

or structure, or may be composite, utilizing multiple materials or methods. Figure 1.8 shows several typical homogenous wick designs, and Fig. 1.9 depicts a variety of composite wicks.

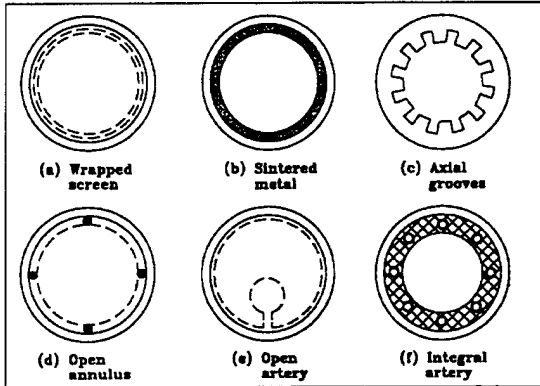


Figure 1.8. Homogeneous Wick Designs. [2, p. 120]

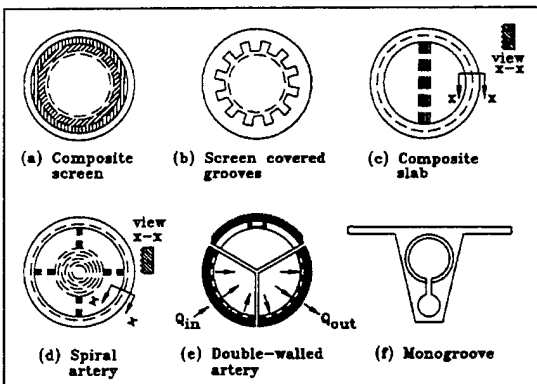


Figure 1.9. Composite Wick Designs. [2, p. 122]

c. Thermal Transport Limits

There are a number of mechanisms which serve to limit the transfer capacity of a heat pipe. The capillary limit refers to the ability of the wick to pump against the pressure drops created by fluid flow, gravity head, passage through the wick, and temperature differences across the wick. The sonic limit applies for high temperature applications with very high vapor velocities -- the velocity as the vapor leaves the evaporator section cannot exceed the local speed of sound. The boiling limit is reached if vapor generation happens too rapidly and bubbles form in the wick, preventing liquid flow and drying out the evaporator. The entrainment limit refers to high vapor velocities carrying sufficient

liquid to dry out the evaporator. Other limits exist for frozen startups and situations where vapor pressure is insufficient to maintain pressure at the condenser end.

The limit of interest to us is the capillary limit, as it is the only one which applies under normal circumstances in other than high temperature applications. The limit is described by the following pressure summation, which must be satisfied for the heat pipe to operate:

$$\Delta p_{cap,max} \geq \Delta p_l + \Delta p_v + \Delta p_{e,\delta} + \Delta p_{c,\delta} + \Delta p_g \quad (1-4)$$

where $\Delta p_{cap,max}$ = capillary pumping pressure,
 Δp_l = liquid flow pressure drop,
 Δp_v = vapor flow pressure drop,
 $\Delta p_{e,\delta}$ = evaporation interface pressure drop,
 $\Delta p_{c,\delta}$ = condensation interface pressure drop, and
 Δp_g = gravity head pressure drop.

The evaporation and condensation losses are relatively small enough to be neglected, and the following allow calculation of the capillary pumping pressure and the gravity head.

$$\Delta p_{cap,max} = \frac{2\sigma_t}{r_{eff}} \quad (1-5)$$

$$\Delta p_g = \rho_1 g L_t \sin \phi \quad (1-6)$$

where σ_t = surface tension coefficient of working fluid,
 r_{eff} = effective pore radius as determined from the menisci radii,
 ρ_1 = liquid density of working fluid,
 g = acceleration due to gravity,
 L_t = total length of the heat pipe, and
 ϕ = the angle of the heat pipe from horizontal.

With these refinements, we can rewrite Eqn. 1.4 as a general expression of the capillary limit for a generic heat pipe:

$$\frac{2\sigma_t}{r_{eff}} \geq \Delta p_l + \Delta p_v + \rho_1 g L_t \sin \phi \quad (1-7)$$

This reinforces the earlier statements about wick design and working fluid. The left side of Eqn. 1.7 is dependent on selection of wick material and design, while the

pressure drops on the right side are all contingent on the thermophysical properties of the working fluid. [2, chap. 4]

A final way of looking at the general heat pipe design problem is to simply model the pipe as a conductance device [1, p. 301]. This allows the development of a relative transfer capacity coefficient which I will call a conductance coefficient. The model is very simple:

$$Q = C_{HP}\Delta T \quad (1-8)$$

where Q = heat flow,

C_{HP} = conductance coefficient,

ΔT = the temperature difference between the evaporator and condenser ends of the heat pipe.

This provides a means of comparing similar heat pipes in terms of performance. It must be remembered that the internal mechanics of the conductive and convective processes are in reality far more complex than indicated by this simple formulation, but that level of depth exceeds the scope of this investigation.

II. LOOP HEAT PIPE

The loop heat pipe and capillary pumped loop (CPL) are very similar in structure and function, having been separately developed to address the same issues. A description of both designs and their operating characteristics is provided for comparison.

A. LOOP HEAT PIPE TECHNOLOGY

A conventional heat pipe has the advantage of a high thermal conductance with low mass compared to solid conductors such as straps or bars, and no moving parts or power requirements, unlike a fluid heat exchange loop. It also has the disadvantages of high sensitivity to axial accelerations, low transport capacity over long distances, and a rigid physical configuration. [3, p. 581] The Loop Heat Pipe was developed to address some of the drawbacks of a conventional heat pipe. Figure 2.1 shows an idealized LHP functional and physical configuration diagram. The device consists of an evaporator, condenser, separate vapor and liquid transport lines, and a compensation chamber (CC).

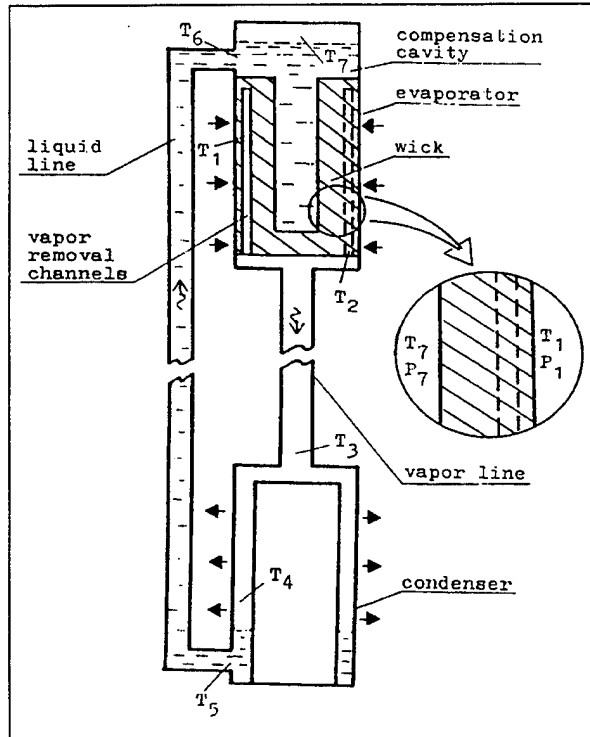


Figure 2.1. LHP Physical Configuration. [5, Fig. 2]

The Loop Heat Pipe is a two-phase fluid flow device developed in 1971 by Gerasimov and Maidanik at the Urals Technical University in the Russian Federation (at the time, the USSR). A patent was granted in the United States for the device in 1985. It has a high heat transfer capacity, over longer distances and in various acceleration conditions. In addition, it is mechanically flexible, allowing more advantageous installations. [3, p. 585]

1. LHP Elements

a. Evaporator

The evaporator of an LHP consists of a casing, ordinarily cylindrical, and the wick. Unlike a conventional heat pipe, the wick is entirely contained in the evaporator, and does not extend throughout the device. Some designs call for a portion of the wick to extend into the compensation chamber to facilitate wetting, but in most cases the wick is only the length of the evaporator. The wick structure is composed of either titanium or nickel sintered powder, and reportedly can reach 300 mm in length and 50 mm in diameter. Nickel wicks can be constructed with an effective pore radius between 0.6 and 3.0 μm , and porosity in the 60-70% range, while titanium yields 4.0 to 7.0 μm and 50 to 70%, respectively. The wicks are grooved on their outer surface for vapor removal (Fig. 2.2), and constructed with a central penetration to allow liquid flow along most of the length of the wick (Fig. 2.1 and 2.3). Liquid flows radially through the wick absorbing heat, and evaporates from the wick menisci into the vapor channels. According to Maidanik, the capillary pressure generated by these wicks can be as high as 60 kPa with ammonia as the working fluid, theoretically allowing operation against an adverse height of 6 m [6, p. 3].

Figure 2.3 shows some alternative evaporator arrangements. As can be seen from the detail drawings, the vapor collection channels may run axially or around the circumference of the cylinder, and the vapor line may attach at the side or the end of the evaporator. The liquid line may simply terminate at the compensation chamber, or, as pictured farthest left, may penetrate at the vapor end of the wick, and go all the way

through the length of the evaporator to introduce the return liquid to the CC. There are also designs for some applications which use multiple evaporators. [6, p. 2]

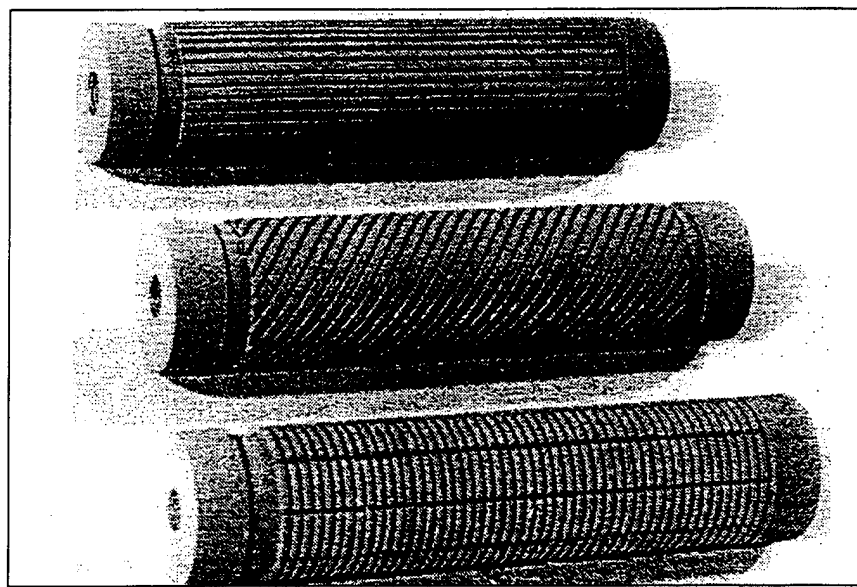


Figure 2.2. LHP Titanium Wick Configurations. [5, Fig. 10]

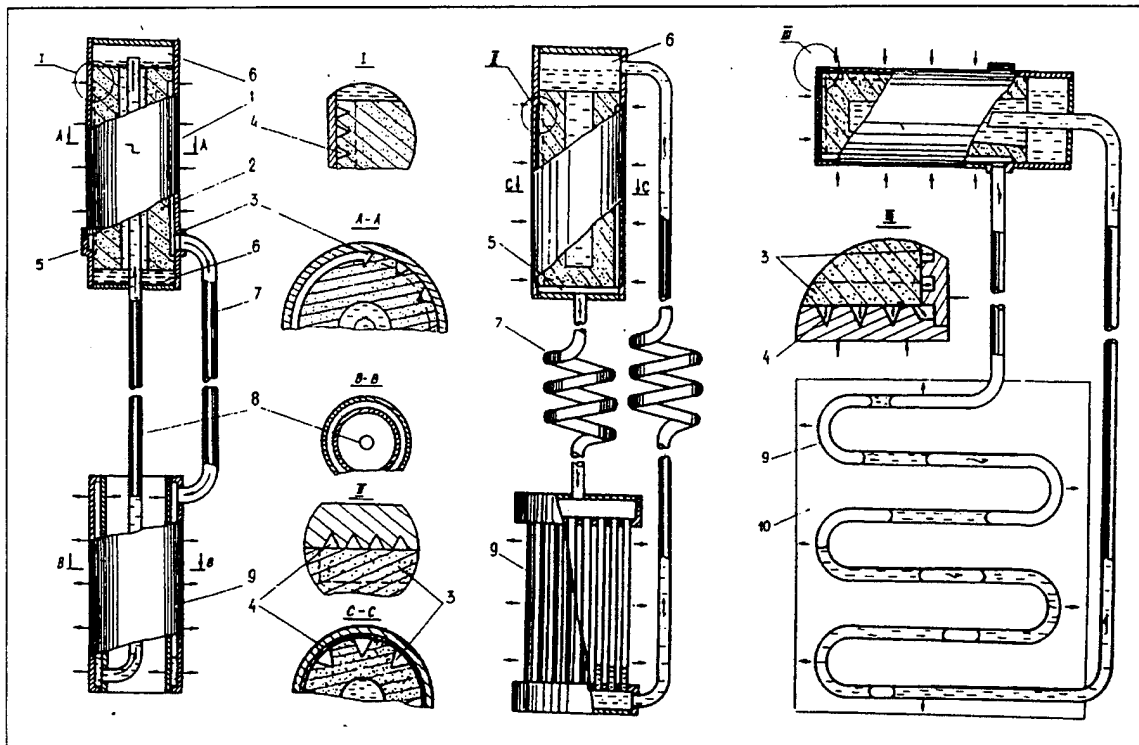


Figure 2.3. Diagram Showing Configuration Variations. 1- Evaporator; 2 - Sintered Metal Wick; 3 - Axial Vapor Removal Ducts; 4 - Azimuthal Vapor Removal Ducts; 5 - Vapor Collection Space; 6 - Compensation Chamber; 7 - Vapor Line; 8 - Liquid Line; 9 - Condenser; 10 - Radiator. [5, Fig. 3]

b. Compensation Chamber

The compensation chamber (also variously termed a compensation cavity, accumulator, or hydroaccumulator) serves as a reservoir for liquid returned from the condenser, and is placed to ensure that the wick remains wetted by the working fluid at all times. Its radius is generally larger than the evaporator, to allow sufficient liquid storage, but this is not always the case. The CC is attached to the head of the evaporator, so that returning liquid passes through it, and so that it receives parasitic heat leaks from the evaporator. When a heat load is applied to the evaporator, vapor begins to form, and liquid is displaced from the vapor line into the condenser. The fluid inventory of the LHP is such that the liquid is accumulated in the CC, ensuring that the wick remains wetted. Some experimentation has been done to use a small heater to control liquid volume redistribution in the CC, inducing variable conductance behavior. [6]

c. Condenser

The purpose of the condenser is heat removal. It permits condensation of the working fluid vapor, and provides some degree of subcooling to the liquid returned to the CC, as required by the heat load and orientation of the LHP. As can be seen in Fig. 2.3, the condenser for an LHP can take on virtually any form. It must be sufficiently sized, and allow proper speed of fluid flow, to permit dissipation of the entire heat load for the system. An undersized condenser will cause pressure to build up, causing cessation of circulation and therefore heat transport, and will also provide insufficient subcooling to the liquid being returned to the CC. [5]

d. Transport Lines

The vapor and liquid lines in an LHP are very small, smooth-walled, and highly flexible. The experimental models documented by Maidanik all have lines of stainless steel, with internal diameter (ID) ranging from 2 to 8 mm. The lines need not be identical in diameter, in fact, as vapor pressure losses in the vapor spaces are a significant portion of the total pressure losses for the loop. A larger diameter vapor line eases the magnitude of these losses. [5]

2. Loop Heat Pipe Operating Principles and Theory

The following discussion is a compilation of descriptions of the LHPs intended operation from several papers [5, 6, 7] written by Yury Maidanik, one of the inventors. The papers were translated from the Russian, and unclear at times, and provided few of the background derivations for the formulas presented.

Figure 2.4 portrays an idealized pressure-temperature curve for the processes involved in the operation of the LHP. Point 1 refers to the vapor pressure and temperature above the vapor-liquid interface in the meniscus formed in the wick structure. Section 1-2 exhibits vapor motion from the evaporating surface and through the vapor removal channels. This is a superheated state, resulting from both the pressure drop accompanying the flow of vapor to the base of the evaporator, and from increasing temperature due to additional heat absorbed from the evaporator wall. Vapor motion in the vapor line is rapid enough to be considered very nearly isothermal, and subject only to pressure losses (ΔP_v), as shown in section 2-3. Section 3-4 represents the condensation of the vapor, and 4-5 the subcooling provided by the condenser. Liquid motion in the liquid line is, like the vapor line, considered isothermal (section 5-6; ΔP_l), and point 6 shows the entry of subcooled liquid into the CC. Since the CC is thermally linked to the evaporator, a portion of the evaporator heat load is experienced in the CC, causing the temperature rise, section 6-7. Again, pressure losses within the CC may be neglected, as well as the possibility of a temperature gradient across the CC. It should be noted that these characteristics allow the possibility of saturated vapor at T_7 and P_6 or P_7 with a vapor-liquid phase boundary within the CC. The final section depicts liquid passage through the wick structure to the evaporation surfaces provided by the vapor removal channels. It displays liquid superheat both as a result of the pressure drop, and due to a temperature rise from evaporator heat load. Point 8 is the liquid state under the vapor-liquid boundary at the evaporating wick menisci. [6]

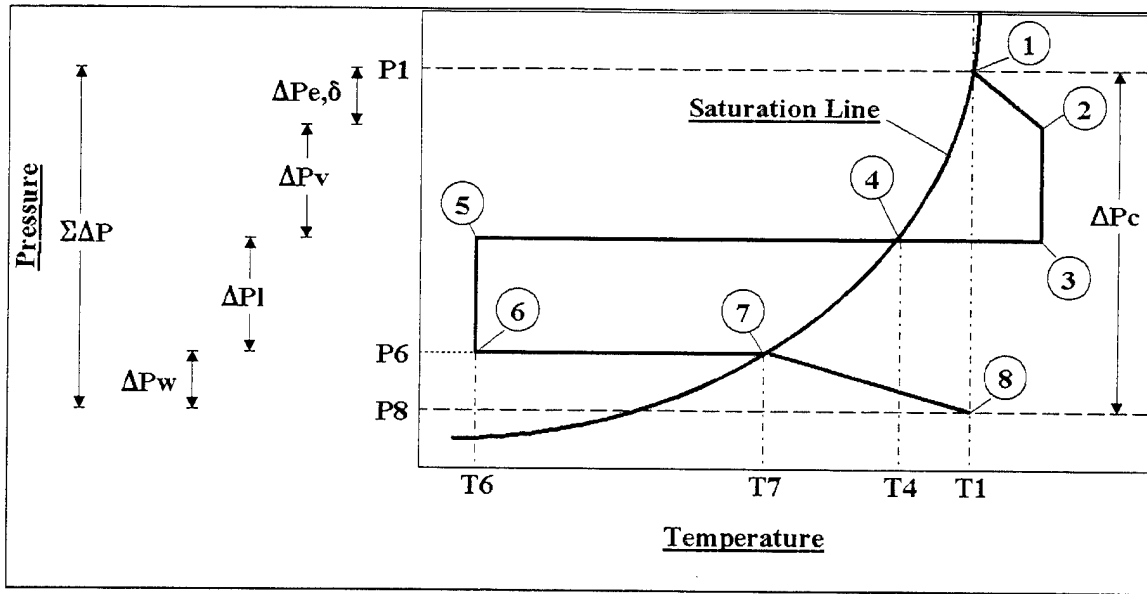


Fig. 2.4. Pressure-Temperature Curve For LHP. [after 4, Fig. 2]

As with any heat pipe, the basic operational condition is that stated in Chap. 1, that the capillary pumping pressure generated in the wick must exceed the sum of the pressure losses experienced in the operation of the loop, or in terms of Fig. 2.4:

$$\Delta P_c \geq \Sigma \Delta P \quad (2-1)$$

Eqn. 2-1 may be directly related back to Eqn. 1-4, and it is with that relation that we can look again at the effect of gravity head. The losses in the vapor and liquid lines, shown by sections 1-3 and 5-6, are dependent in part on the gravity head, expressed in Eqn. 1-4 and 1-6 as ΔP_g . Additionally, Maidanik has developed the following to describe the major pressure losses in an LHP [7, p. 3]:

$$\Sigma \Delta P(Q) = A \cdot Q + \Delta P_g \quad (2-2)$$

where A is a coefficient determined by the geometry of the vapor line, and the properties of the working fluid. For this treatment, he assumes that liquid line losses, and the contributions of vapor spaces and condenser are negligibly small compared to the vapor line losses. These are determined using the coefficient A , as determined by Eqn. 2-3:

$$A = 128 \rho_v l_v / \pi \mu_v h_{fg} d_v^4 \quad (2-3)$$

where ρ_v, μ_v, h_{fg} = density, viscosity, and latent heat of vaporization of the

vapor phase of the working fluid, and

d_v, l_v = diameter and length of the vapor line. [7, p. 3]

For LHPs, two additional considerations are required for proper operation. The first is expressed:

$$\frac{dP}{dT} \Big|_T \Delta T_{1-7} = \Delta P_{1-7} \quad (2-4)$$

where $\frac{dP}{dT} \Big|_T$ = the slope of the saturation curve at the point with temperature T^* , and

T is between T_1 and T_7 .

The left side of Eqn. 2-4 then refers to the temperature change predicted by the Clausius-Clapeyron relationship for the pressure change existing across the loop. This results in a pressure differential between the vapor above the boundary in the evaporation zone, and the vapor existing in saturated state in the CC. This condition is valid when the slope of the saturation line can be considered a straight line in the range between T_1 and T_7 , which is to say that ΔT_{1-7} is small. Achieving this can be managed by careful selection of a working fluid with a suitable working range. This is required for reliable start and operation of the LHP at low temperature differentials between points 1 and 7.

[6, p. 3-4]

The third condition is also specific to LHPs, and simply refers to the degree of subcooling required in the liquid entering the CC.

$$\Delta T_{4-5} = \frac{\Delta P_{5-6}}{\frac{dP}{dT} \Big|_T} \quad (2-5)$$

The relationship specified shows that subcooling must be provided to prevent boiling of the working fluid in the liquid line and interfering with the circulation of the loop. This factor is not as compelling as the first two, as the CC contains two-phase fluid, but excessive vapor can cause either a "dry-out" phenomenon, in which the wick is insufficiently supplied with liquid, or the inhibition of flow, in which the $\Sigma \Delta P$ exceeds the wick's pumping capacity. [6, p. 4]

* dP/dT may be calculated from the Clausius-Clapeyron relation, $dP/dT \Big|_T = h_{fg}/T v_{fg}$.

The overall vapor temperature relationship developed by Maidanik shows a phenomenon he calls as "autoregulation," which is based on factors already discussed. [7, p. 3] The liquid balancing which occurs due to the pressure differential across the wick, and the heat leak afforded into the CC, allows the system to absorb a certain amount of change in heat load. The resulting change in vapor temperature at the evaporator will be very small over a relatively wide range of heat input. This is based on Maidanik's expression [7]:

$$T_v = T_l + (T_{v,cc} - T_l) \left(\frac{r_o}{r_i} \right)^{\left(c_p Q / 2\pi L_w h_{fg} k_{eff} \right)} \quad (2-6)$$

(A)

(B)

where T_v = vapor temperature in the vapor spaces and line,

T_l = liquid temperature entering CC,

$T_{v,cc}$ = vapor temperature in CC,

r_o, r_i = outer and inner radii, respectively, of wick,

c_p = constant pressure heat capacity of working fluid,

L_w = length of wick, and

k_{eff} = effective thermal conductivity of the wick. [3, p. 614]

Equation 2-6 has no known closed form solution, but it can be seen that the heat load, Q , plays a relatively small role in the change on T_v , within a certain range. This is true since the wick radius ratio is small by design, and $T_{v,cc}$ is intended to be near T_l . Outside that range, if the parasitic heat leak into the CC is too small to maintain vapor in the CC, term (B) collapses to nearly eliminate ΔT . If the heat leak is large enough to create a significant gradient between the entering liquid and the vapor above the phase boundary, the temperature of the evaporator will also rise. One technique to lengthen the range of minimum variation in T_v is to actively control (by either heating or cooling) the parameters in the CC. Using an appropriate feedback controller and a small heater attached to the CC, gains can be realized in both temperature stability, and width of the "flat" region [6, p. 5-6].

B. CAPILLARY PUMPED LOOP TECHNOLOGY

The CPL is a two-phase fluid flow heat transfer device first proposed by Stenger at NASA Lewis Research Center in 1966. It was developed to address the same concerns as the LHP, and in fact, there was some early confusion between the two as they were both described as "capillary pumped loops." The major difference between them is the location and design of the reservoir. [3, p. 585] Fig. 2.5 shows an idealized configuration for a CPL.

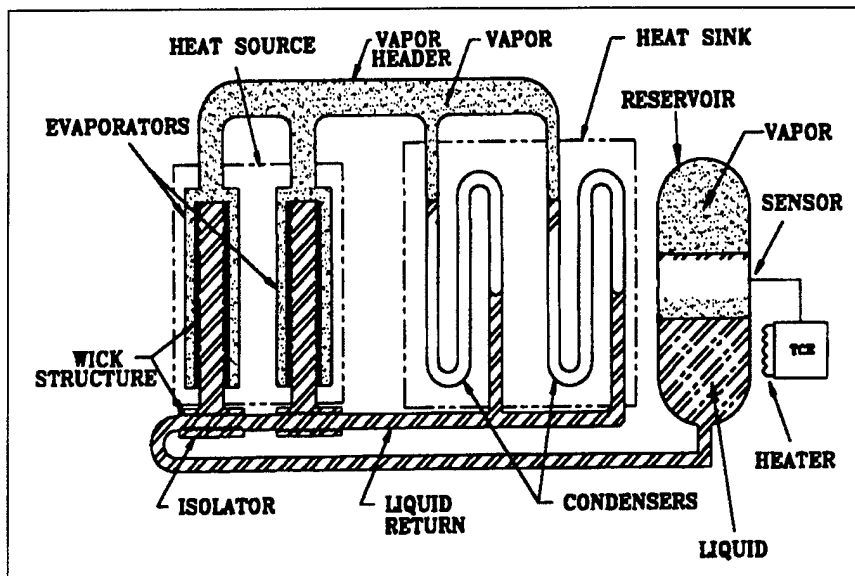


Fig. 2.5. CPL Functional Diagram. [3, p. 583]

1. CPL Elements

a. Evaporator

The evaporator for a CPL serves the same purpose as that of an LHP, providing pumping power for the entire loop, and thus requiring capillary pressure from the wick. CPLs have been designed with various types of wicks, while LHPs have strictly used the sintered metal powder structure. Multiple evaporator designs require the use of an isolator to prevent vapor backflow from causing the depriming of an adjacent operating evaporator. Figure 2.6 depicts a typical design, using a conventional wick material (polyethylene mesh), force-fitted into an axially grooved aluminum extrusion. Liquid

flows through the center penetration, just as in the LHP evaporator. As shown in section B of Fig. 2.6, the direct contact between the extruded fins and the evaporating liquid allows the creation of the meniscus, and since the heat need not be transferred through a liquid layer, the heat transfer is two to three times that achieved in a conventional heat pipe. [3, p. 590]

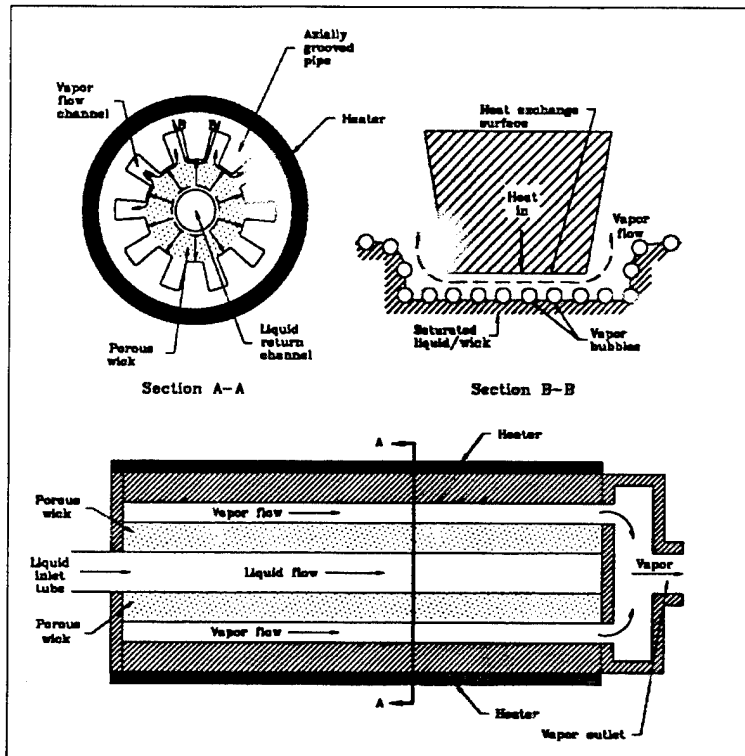


Figure 2.6. Typical CPL Evaporator Design. [3, p. 588]

b. Condenser

The condenser in a CPL, much as discussed regarding LHPs, may take on many forms. The main requirement is that it must be appropriately sized and configured to remove the imposed heat load. Since CPLs frequently utilize multiple parallel condensers, other criteria for design include ease of flow regulation between condensers, small pressure drop across the condenser, and minimum weight. [3, p. 591]

c. Transport Lines

The transfer lines in a CPL follow the same requirements as for an LHP. They are smooth-walled, and are intended to minimize frictional flow losses. They may be identically sized, or sizes may be optimized to further reduce pressure loss. [3, p. 592]

d. Reservoir

The reservoir in a CPL serves as an accumulator for excess fluid, and a control device for the rest of the loop. It is intended to contain two-phase fluid, and has a heater attached to provide thermostatic control of the temperature of the mixture. Pressure imbalances created by shifting conditions in the loop are automatically adjusted to form a new equilibrium state by inflow or outflow to the reservoir. A new equilibrium based on a different operating temperature can also be forced by adjusting the temperature, and thus the fluid balance in the operating loop. This ability is critical for provision of priming for the evaporators at startup.

e. Subcooler

The subcooler is not pictured in Figure 2.5, but many CPL designs include this device. It allows stable operation of the CPL by ensuring that the condensation of the working fluid is complete, and the state of the fluid entering the evaporator is well below saturation. Most CPLs are considerably more sensitive to vapor formation on the liquid side of the wick than are LHPs, so bubble formation can deprime the evaporator.

f. Mechanical Components

Some CPLs are designed with mechanical pumps to assist in startup and high power applications, where capillary pumping is insufficient. In this way most of the operating characteristics of a CPL may be employed, while some of the drawbacks are ameliorated.

2. Capillary Pumped Loop Operating Characteristics

The operating characteristics for the CPL are very similar to the LHP. Both are subject to the capillary pressure limitation, the requirement for subcooling, and the need for the temperature differential-induced pressure differential across the wick. The difference is in the means of addressing these issues. Both use high efficiency wick designs to increase pumping capacity, while the CPL may add the use of a mechanical pump. The subcooling requirement is met in the condenser design in the LHP, while the CPL adds a component specifically to provide that requirement. The LHP is also less prone to deprime from bubble formation, since the CC is intended to maintain vapor in a saturated state, and the sintered metal wick is less prone to blockage by bubble accumulation. The use of the CC is also very different from the reservoir: the former is intended to function based on careful matching of physical design and working fluid properties and inventory, while the reservoir is meant to be actively controlled via thermostat.

C. PREVIOUS LHP EXPERIMENTS

Experimentation has been performed on LHP designs in Russia, Germany, and the United States. Summary information for these tests is included in Appendix A. Key performance characteristics of the LHP shown in these experiments include:

- ◆ Start-up with a high degree of reliability.
- ◆ Capability to operate against significant adverse elevations.
- ◆ Ability to operate in one gravity acceleration with rotated (tilted) evaporators with nearly unchanged performance characteristics.
- ◆ Increased ΔT_{1-7} at low heat loads.
- ◆ Variable conductance capability.
- ◆ Active control using applied heat load on the CC.
- ◆ A similar curve for T_{evap} plotted against heat load in most results.

The testing accomplished by LMAG on the ammonia-charged LHP designated LHP-93-1-Ammon is of particular interest, as the design of the LHP is identical to the propylene-charged device investigated at Phillips Laboratory. Thirty-six test were conducted by LMAG on the ammonia LHP in which the following parameters were varied:

- ♦ heat loads (10 W to 200 W)
- ♦ adverse (evaporator above condenser) elevations from 1 inch to 111 inch
- ♦ environmental effects [bare lines with and without forced convection (fan flow) cooling]
- ♦ insulated lines versus bare lines
- ♦ time varying heat loads (step function)
- ♦ heating of the compensation cavity (5 W to 15 W) at 100 W load
- ♦ evaporator rotation to 90 degrees such that the compensation cavity (CC) was below the evaporator
- ♦ load power cycling from 25 W to 200 W (step function)
- ♦ condenser temperature cycling from -15°C to +14°C
- ♦ heat load and condenser cycling tests with the compensation cavity heater holding the evaporator at a constant temperature.

Data obtained during these tests were startup transients (success or failure to start) and evaporator minus condenser temperature difference (ΔT). The curves developed for these characteristics are displayed as Fig. A.6 to A.8 in App. A. Variable conductance mode performance for various CC heating levels was presented at various heat loads and condenser temperatures (one significant result is depicted in Fig. A.9).

III. EXPERIMENT DESCRIPTION

A. TEST PROGRAM

The testing accomplished by LMAG on the ammonia-charged LHP was completed in 1993 and 1994 shortly after receipt of the two LHPs from the Lavochkin Association in Russia. The second LHP, charged with propylene and designated LHP-93-2-Prop, was lent to the United States Air Force, under a Memorandum of Agreement completed in February 1995. Testing began in early March 1995 at Philips Laboratory, Kirtland Air Force Base, Albuquerque, NM, at the Space Power and Thermal Technologies Directorate, Thermal Management Branch (VTPT). Testing was continued throughout summer 1995, and during the preparation of this thesis, Dr. Don Gluck at VTPT indicated that the testing would continue until October 1995, at which time the LHP would be returned to LMAG in Denver, Colorado.

1. Objectives

The goal of the test program was to begin where the LMAG program ended, and determine the differences in operating characteristics between the two LHPs. The objectives of the program, as stated in the test plan, were to:

- ♦ Compare performance of the propylene filled LHP with the ammonia filled LHP tested by LMAG.
- ♦ Characterize the propylene LHP startup and performance over a range of evaporator heat loads, insulation options, condenser temperatures, adverse heights (evaporator above condenser), rotations (compensation chamber both above and below evaporator).
- ♦ Characterize low power performance at several adverse heights.
- ♦ Study effects of load and condenser temperature cycling on response and stability.

- ♦ Investigate the variable conductance behavior of the LHP.
- ♦ Demonstrate that evaporator temperature can be controlled using feedback to the CC heater. Develop methods to provide control at reduced CC heater power.
- ♦ Further investigate the difficulty in starting the LHP with a cold condenser after long inoperative periods reported by LMAG.
- ♦ Conduct tests in a thermal vacuum chamber under simulated space conditions.

B. TEST ARTICLE

1. Description and Specifications

The test article, LHP-93-2-Prop, is pictured in Figs. 3.1 and 3.2. The evaporator is cylindrical, and embedded in an aluminum block with dimensions of 48 x 120 x 19 mm (1.9 x 4.7 x 0.76 inches) to increase heat absorption area. The condenser cylinder was embedded in an aluminum block with dimensions 48 x 176 x 19 mm (1.9 x 6.9 x 0.76 inches).

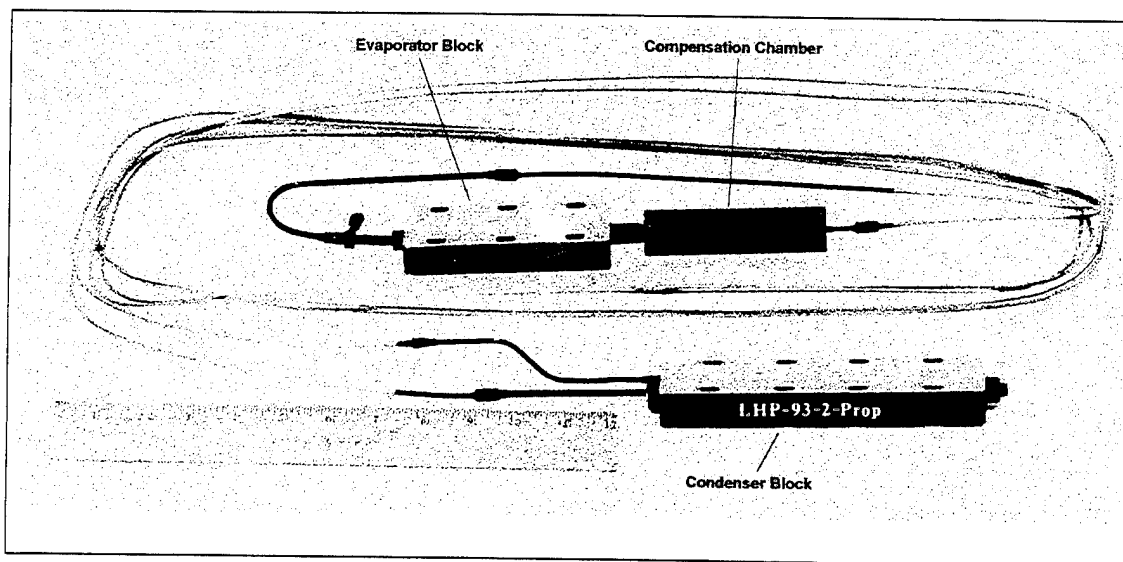


Fig. 3.1. Test LHP In "As-Shipped" Configuration. [LMAG]

The contract between LMAG and the Lavochkin Association called for the specifications listed in Table 3.1.

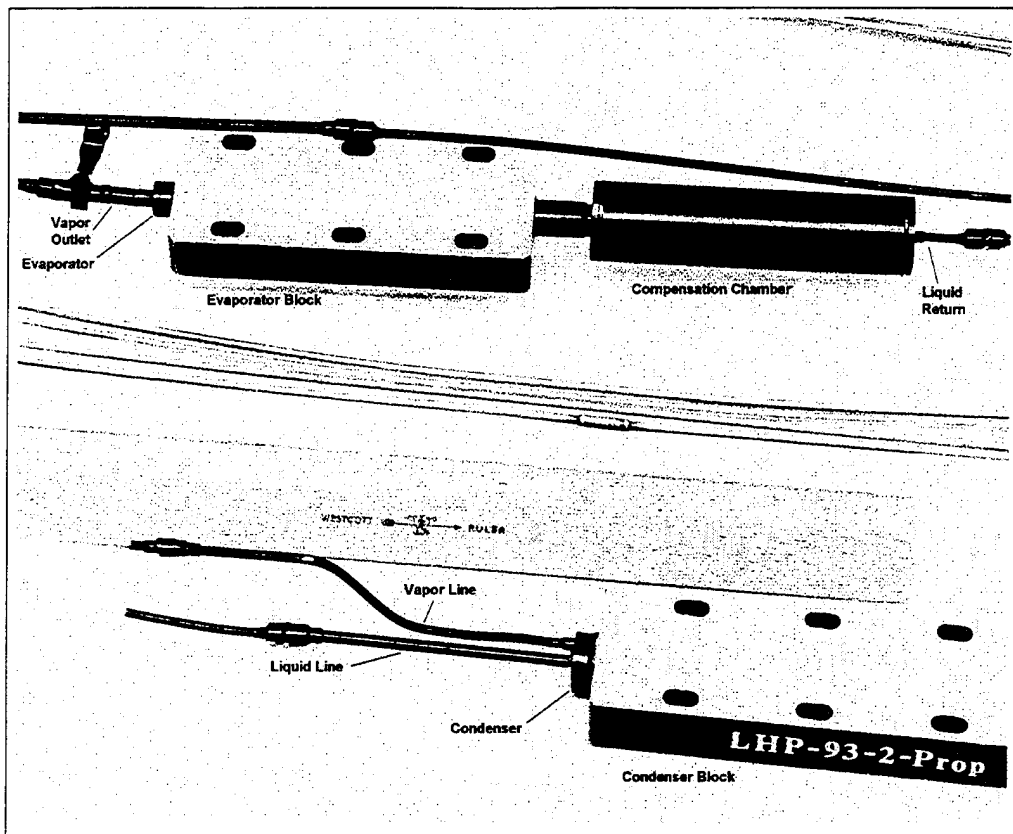


Fig. 3.2. Detail of Test LHP. [LMAG]

Part Number	LHP-93-2-Prop
Casing Material	Stainless Steel
Wick Material	Nickel
Wick Pore Size	1 μ m
Working Fluid	Propylene (C_3H_6)
Fill Quantity	30 ± 5 g
Maximum Heat Load	100 W
Evaporator Outer Diameter (OD)	12 mm
Evaporator Length (Active Zone)	112 mm
Vapor Line OD	3 mm
Condenser OD	14 mm
Condenser Length (Active Zone)	176 mm
Liquid Line OD	3 mm

Table 3.1. Specifications for LHP-93-2-Prop. [8]

In addition to the physical characteristics in the specification, the following tests were required by the contract:

- Prove that LHP-93-2-Prop can transport 30 W with no greater than 10°C difference between evaporator and condenser, maintaining the evaporator in the 20-30°C temperature range, and
- Subject the LHP to an internal pressure test of not less than 6.205×10^6 Pa.

The acceptance test results are included in Appendix B.

2. Propylene Properties

Propylene is an organic compound, composed of three carbon and six hydrogen atoms, with the configuration $\text{CH}_3\text{-CH=CH}_2$. Designated R-1270 by the American Society of Heating, Refrigeration, and Air-Conditioning Engineers, Inc. (ASHRAE), it has a critical temperature (T_c) of 364.9 K and critical pressure (P_c) of 4.6 MPa, and a melting point and boiling point at 1 atm of -185.25°C and -47.7°C, respectively. Using Faghri's rule of thumb mentioned in Chap. I, and a table of vapor pressure values [10, p. 313], the working range for a propylene-charged heat pipe should be from about -80 to +50°C. This compares favorably with the recommended working range of -70 to +50°C given by Yury Maidanik via email to Don Gluck on 10 March 1995. While Faghri cites pressure vessel construction as the reason for his upper limit, the properties of propylene provide another. Using the Eötvös equation, surface tension can be approximated well, except within 20-30°C of T_c . Considering a 40 degree range just outside this limit, a the rise from 26.85 to 46.85°C results in a 37% loss in surface tension, while the next twenty degree rise causes a further 55% decrease. As the upper temperature limit is approached, surface tension decreases sharply, and at an increasing rate of decline, and pumping power is lost in the wick.

C. TEST CONFIGURATION

1. Physical Layout

The physical setup for the experiments was as depicted in Fig. 3.3. The evaporator and condenser were each supported by a cinder block, with two more blocks supporting the liquid and vapor lines. The active parts of the LHP were isolated from the supports by 0.5 inch foam insulation; the same insulation was used to cover the entire assembly. Insulation was secured and sealed with duct tape in cases where access was not required, or steel wire, where removal was necessary. For the portions of the testing requiring differences in elevation between evaporator and condenser, parachute cord was attached to the blocks, and strung over the rafters in the experiment bay. This allowed easy adjustment and access, while the weight of the blocks maintained stability, and preserved fixed level orientation of the evaporator and condenser.

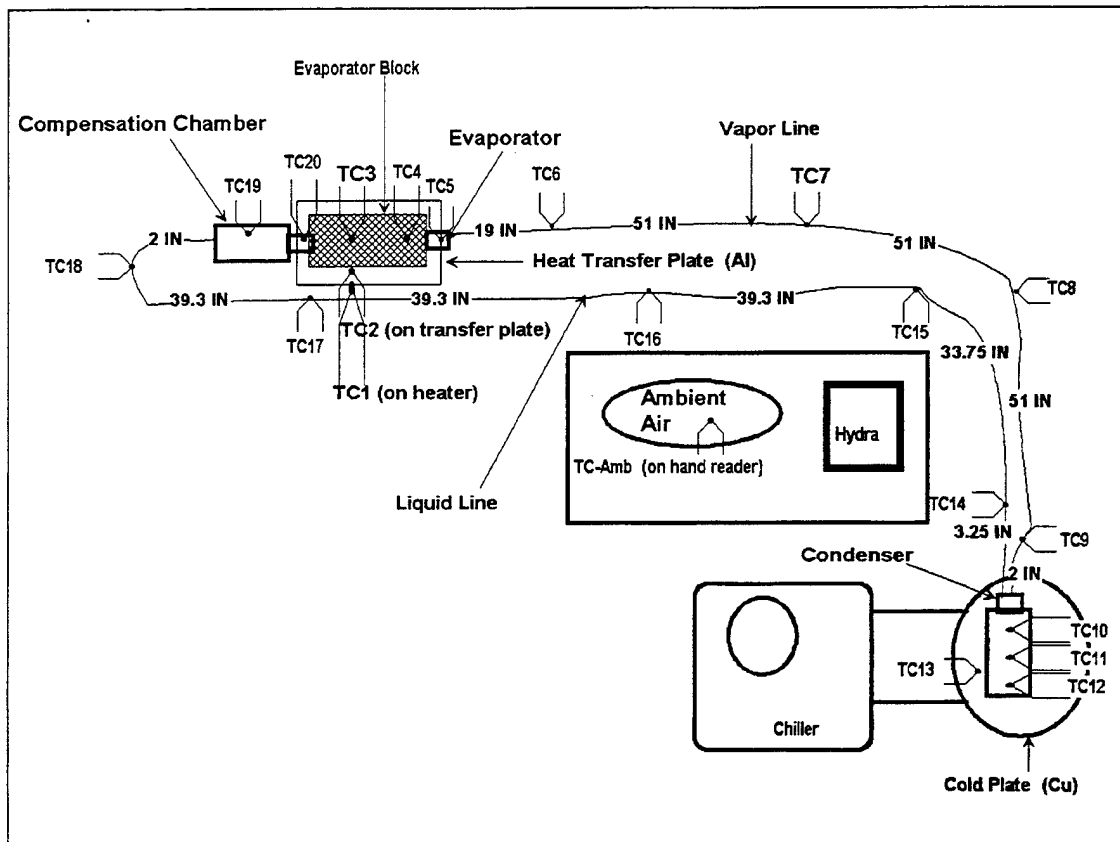


Figure 3.3. Experiment Setup.

2. Evaporator End

An aluminum heater plate was fabricated with dimensions 75 x 175 x 6 mm (3 x 6.9 x 0.25 inches) to serve as a junction between the evaporator and heater. Holes were drilled and threaded to allow the evaporator block to be attached using 1/4-20 steel bolts. Figure 3.4 shows the size and layout of the attachment holes in the evaporator and condenser blocks. The air gap between the two surfaces was filled with thermal grease (Type Z9 Silicone Heat Sink Compound; GC Electronics, Rockford, IL) The surface opposite the evaporator block was smoothed and all bolt protrusions removed, to allow attachment of a Kapton-backed foil heater. The heater was a Minco Thermofoil™ Heater Model #5172, rated for 61.6 ohms, with dimensions of 2 x 6 inches. This rating allowed a total theoretical power rating for the heater of 215 W at 115 VAC. Power applied to the evaporator block was controlled by a variable capacity resistor (Variac), allowing control to within ± 2 W. A 2 x 4 inch heater of the same brand and characteristics as the evaporator heater was procured for the compensation chamber.

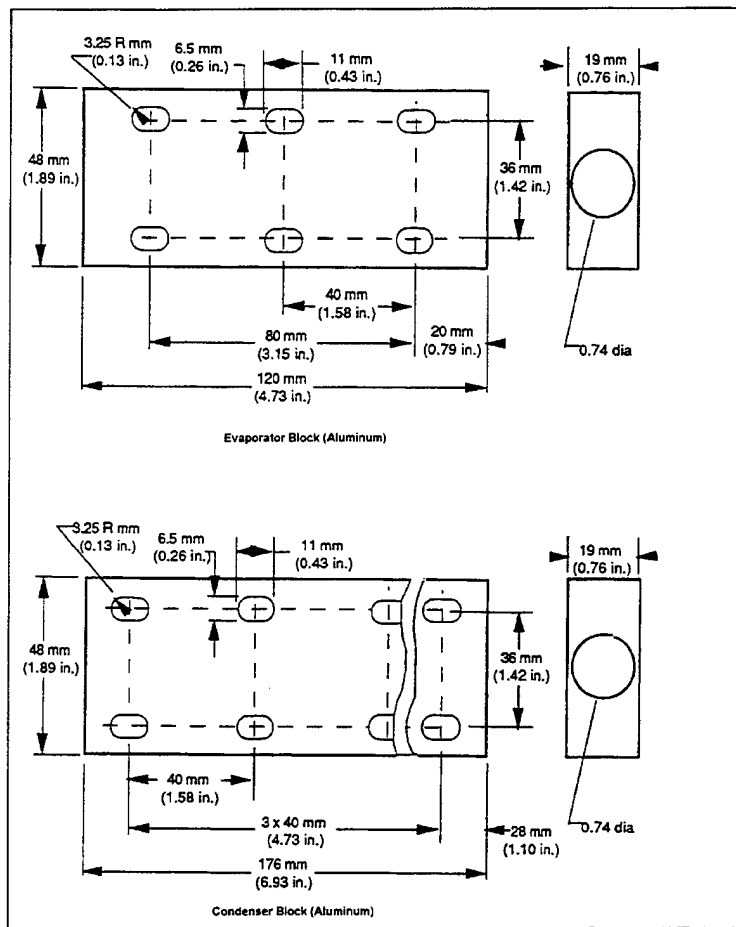


Figure 3.4. Evaporator and Condenser Block Configuration for LHP-93-2-Prop.

3. Condenser End

The condenser block was affixed to a copper cold plate 300 mm in diameter, using the same attachment method as the evaporator block. The interior cooling coil of the plate was a 6 mm copper tube, following a serpentine pattern. An FTS Model RC-50A chiller unit, rated at 250 W, with a coolant mixture of 50-50 industrial grade ethylene glycol and water provided the heat sink.

4. Instrumentation

a. Temperature

Thermocouples were fabricated from type "K" thermocouple (TC) wire, and attached to the point indicated on Fig. 3.1 using Kapton tape. Care was taken to keep the

TCs as uniform as possible, with 3 twists prior to the weld bead. Type "K" TC wire is rated for -200 to 1250°C, with NiCr anode lead, and NiAl cathode.

b. Power

Power input to the heater was measured indirectly, using two voltage measurements. V_1 refers to the voltage obtained across the heater leads. V_2 is the voltage across a 5 ohm shunt resistor placed in the line, allowing a determination of current. The power input for any run was the product of the voltages divided by 5.

5. Data Acquisition

a. Temperature

Data acquisition was performed using a Hydra 2620A Data Acquisition Unit. This device provides 20 analog channels for any voltage, current, resistance or frequency, either AC or DC. The product manual gives a temperature error using "K" type TC wire of approximately $\pm 0.6^\circ\text{C}$. The Hydra will internally reject 60 Hz and other common interference modes in TC readings, preventing electro-magnetic interference (EMI) on the Hydra due to the proximity of the AC heater. A Fluke TC reader was used to monitor ambient temperature, allowing an error of 2.2°C .

b. Power

Voltage measurements required for the determination of applied power were taken by hand using a Fluke Digital Multimeter. The accuracy cited on the cover plate was 0.1 V in the operating range.

D. TESTS CONDUCTED

The complete program of tests to be conducted is given in the spreadsheet of App. B, Table 1. The basic phases of the test program are discussed in the following paragraphs.

The "A" series was intended to determine the general operating characteristics and limitations of LHP-93-2-Prop. The initial series of "A" runs was expanded early in the

testing when the original parameters, selected based on the LMAG experience with LHP-93-1-Ammon, were found to be unrealistic for the propylene design. The "A" runs include:

- ♦ A1 - No Insulation - To permit comparison with insulated runs, and a determination as to the significance of ambient effects.
- ♦ A2 - Basic parametrization - Runs were completed at 100 and 70 W. The 70 W heat load was adopted as a standard load, as the 100 W load required extremely low temperatures to maintain the goal evaporator temperature of 20-30°C.
- ♦ A3 - Effect of Load - The effective load range of the LHP was determined.
- ♦ A4 - Effect of Condenser Temperature - The effect of variations in sink temperature at two selected heat loads, 30 and 70 W, was investigated.
- ♦ A5 - Effect of Adverse Height Conditions - The effect of placing evaporator above the condenser was investigated. This series was expanded when startup could not be achieved at greater than 1 m (40 inches) adverse height. The added runs investigated a range of heat loads at 1 m adverse, and attempted to find a load which would induce startup at greater heights.
- ♦ A6 - Reflux operations - Investigated the ability of the LHP to operate with the condenser raised above the evaporator, flooding the CC.
- ♦ A7 - Effect of Rotation - Determine the effect of orientation of evaporator alone on ability to pump effectively.

The "B" series of tests was to characterize the performance of LHP-93-2-Prop at low heat loads when in slightly adverse gravitational situations. The sensitivity of performance noted by LMAG in low loading conditions was to be characterized in 5 W increments and at heights of 0.305, 0.4572, and 0.61 m (12, 18, and 24 inches) adverse.

The "C" series was designed to test the LHP's response to both power and temperature cycling. Power was to be varied from 100 W down to 5 W and back, with all other factors constant, at adverse heights of 1 and 2 m (40 and 80 inches). The test was to

be repeated at a constant 100 W, varying condenser temperature from -20°C to above ambient at +30°C.

Series "D" involved the application of small amounts of heat load to the CC, to verify and expand upon the LMAG results. The later runs of this series would attempt to characterize the requirements to control evaporator temperature using heat applied to the CC.

LMAG reported some difficulty achieving successful startup after long pauses, so the "E" series was to provide minimum 24 hour cooldown periods, attempting to duplicate and characterize the failure mechanisms. The runs would include starts at 100 and at 50 W, as well as varying condenser start temperature, in order to determine if either parameter was a significant factor.

The "F" series was to be the final series, performed in a thermal vacuum environment to verify significant results in a highly controlled environment. The runs were to duplicate a sample of significant results from the open air testing.

E. TEST AND SAFETY PROCEDURES

1. Safety

A minimum of additional safety procedures were imposed for working with the propylene. The LHP was sealed and never intended to be opened, so handling was not necessary. Prior to commencement of testing, the potential for an explosive atmosphere were evaluated, and placards posted to provide warnings. Propylene is not dangerous unless in sufficient quantity to displace air, or form an explosive mixture (Lower Explosive Limit - 2% by volume; Upper Explosive Limit - 10.5%). It is heavier than air, so greater attention must be paid to lower spaces, and expanding vapor escaping from the LHP can cause frostbite due to the heat absorbed as the liquid becomes vapor. The quantity contained in the LHP was on the close order of 30 g, and the bay in which it was housed was on the order of 300 cubic meters, so the concerns were minimal.

2. Testing

The testing procedure for each run was as below. The LMAG testing found that the majority of their failed starts occurred when the condenser was colder than the evaporator [9, p. 6-1], but few problems were incurred using the following method.

- ◆ Ensure all power cords connected; all switches to OFF
- ◆ Visually inspect for abnormal conditions/loose TCs/etc.
- ◆ Hydra - Power On
- ◆ Verify all channels active
- ◆ Activate Hand Reader; let TC settle to ambient
- ◆ Visually inspect chiller; verify no leaks/abnormal conditions
- ◆ Position both switches on chiller console to "1"
- ◆ Check for leaks/abnormal conditions
- ◆ Adjust dial on chiller console to temperature indicated in test plan
- ◆ Allow cold plate to attain desired temperature; monitor via channel 13 (cold plate) until delta T is less than 0.1°C in 5 min.
- ◆ Adjust Variac to provide heater power level indicated in test plan
- ◆ Monitor and record temperatures every two minutes until transients slow to 0.1°C in 2 minutes; then monitor and record temperatures every five minutes until evaporator block and condenser block temperatures are stable (approx. 40 min.), defined as delta T on channels 3 (evaporator block) and 12 (condenser block) less than 0.1°C in 5 minutes.

F. POST-TEST DATA HANDLING

All test data was recorded by hand on data sheets; a sample is provided in App. B. After all the data had been collected, the numbers were transcribed by hand into Lotus

1-2-3 worksheets, one for each run. The standard settings for each temperature and voltage cell of the worksheet were numerical input with one decimal place, as that was the maximum display precision of the Hydra. The power cells allow three decimal places to account for the multiplication of the voltage values. All results shown are in that format, and the charting function was used to present graphical information. The naming conventions permitted in 1-2-3 , Excel, or other modern spreadsheets are of great help in collating large quantities of data for reduction.

IV. DATA REDUCTION AND DISCUSSION

A. TEST DATA

As stated in Chap. III, the "A" series of tests was intended to determine the general operating characteristics and limitations of LHP-93-2-Prop. The initial series of "A" runs was expanded early in the testing when the original parameters, selected based on the MMAG experience with LHP-93-1-Ammon, were found to be unrealistic for the propylene design. The runs included in this thesis are:

- ♦ A2 - Baseline Parametrization; Insulated - Runs were completed at 100 and 70 watts. The 70 W heat load was adopted as a standard load, as it did not require extremely low temperatures to maintain the goal evaporator temperature of 20-30°C.
- ♦ A3 - Effect of Load - Heat loads from 5 to 200 watts were applied to establish the operating range of the LHP.
- ♦ A4 - Effect of Condenser Temperature - Sink temperature was varied from 0°C to above ambient at two selected heat loads, 30 and 70 watts.
- ♦ A5 - Effect of Adverse Height Conditions - This series was expanded when startup could not be achieved at greater than 1 m (40 inches) adverse height. The added runs investigated a range of heat loads at 1 m adverse, and attempted to find a load which would induce startup at greater heights.

The runs not included in this thesis, some of which were subsequently completed by personnel at VTPT include:

- ♦ A1 - Baseline Parametrization; No Insulation - The runs without insulation were completed, but subsequent to their execution, a contact problem was located at the condenser end of the device. Investigation revealed that the dissimilar metals of cold plate, condenser block, and bolts allowed a gap of over 1 mm to develop between the condenser block and cold plate, interfering with heat transfer.

Figure B.13 in App. B shows the equilibrium temperatures for all thermocouples for these runs. The data collected were used in several of the comparisons which follow -- all comparisons use the condenser temperature for reference, vice that of the cold plate, allowing the poor heat transfer to be ignored. They are unusable for their initial purpose of determination of ambient air effects. The runs are to be repeated after all other testing is completed.

- A6 to A7 - This testing was accomplished during June and July 1995, during the writing of this thesis. The only change to the experimental setup was the automation of data acquisition and handling using a PC. An equilibrium data sheet is included in Appendix C, as some of the data is used in this thesis.
- B1 to F11 - The personnel at VTPT deviated from the test plan designations, but continued some of the programmed testing.

B. PERFORMANCE CHARACTERISTICS

In discussing the performance of LHP-93-2-Prop, the taxonomy used in the LMAG report on the ammonia-charged LHP is adopted with some further clarification [8, p.6-1]. A good start is evidenced by the rapid rise of the vapor line temperature to match the evaporator, and a drop in the liquid line temperature; it is further defined by a trend in the condenser to rise in temperature prior to a similar rise in cold plate temperature, and a decrease or reversal in the rate of rise of the evaporator temperature. A bad start is denoted by unchanging vapor and liquid line temperatures, a decreasing or steady condenser, and steady or accelerating temperature rise at the evaporator. An anomalous start is one which appears to be successful, but displays some unusual behavior.

In this chapter, figure legend will refer to specific thermocouple (TC) numbers only when they are discussed in the text. Otherwise, functional labels are employed for ease of reference. If specific TCs are not discussed in the accompanying text, the following labels match the listed TCs from Fig. 3.3:

Evaporator = TC03,

Condenser = TC12 if listed singly, or TC10, TC11, and TC12 if all three are included,

Cold Plate = TC13, and

CC = TC19.

1. Startup and Transient Behavior

The startup profile demonstrated by LMAG using LHP-93-1-Ammon was replicated by the test article, as shown in Fig. 4.1. Startup was immediate in all cases, with the exception of the 5 watt load runs, which are discussed further below. In horizontal orientation, two failures to start were observed for LHP-93-2-Prop. In the first case, the evaporator had not yet cooled to ambient, and the condenser temperature was at -18°C; in the second instance, the run was not a test, but was intended to force redistribution of the liquid in the LHP after a failed adverse height run was suspected of drying out the wick; the evaporator was again warm, and the condenser temperature was at about -18°C. In each case, when condenser temperature was allowed to rise to about -12°C and the application of heat load was repeated, an immediate startup was observed. One potential explanation is that under the pressure conditions extant in the LHP, temperatures lower than -12°C result in sufficient resistance from liquid viscosity. Another line of reasoning would be that the greater than normal difference in temperature between the evaporator and condenser may have upset the balance called for in Eqn. 2-4. This relation was stated to be valid only for small ΔT_{1-7} , and the second order effects involved when linearity could no longer be assumed may have been responsible for the failure to start.

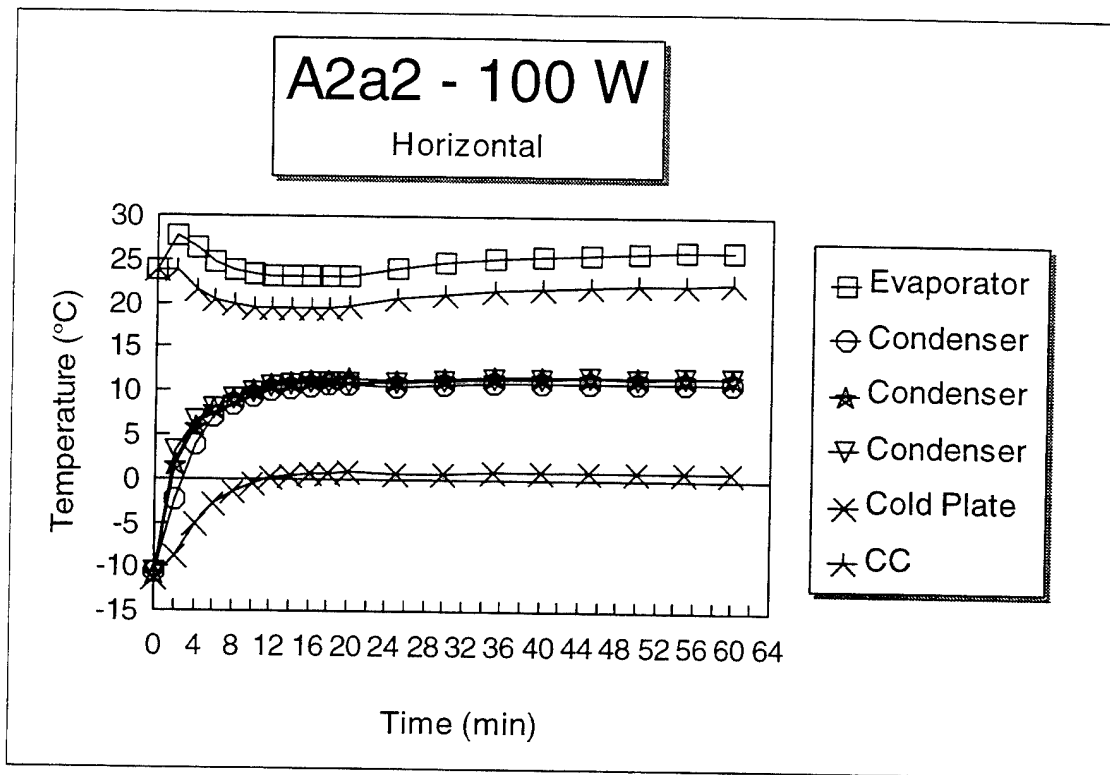


Figure 4.1. Typical Startup Profile for LHP-93-2-Prop.

The time plot looks similar for each heat load tested, with minor variation. The "overshoot" phenomenon, in which the evaporator temperature rises and falls several times before reaching equilibrium came as a surprise; it is rare in the LMAG data, and has not been pointed out in other previous testing. This phenomenon could be the result of the flow rates induced by the heat load. It could also be related to the liquid redistribution described by Maidanik, which he described as "autoregulation." [7] This phenomenon could be important to investigate further, as the liquid redistribution is critical to maintenance of the evaporator within a narrow range of temperatures in the transient case. Fig. 4.2 shows another example of an excursion of evaporator temperature, in this case a much smaller rise from time 12 to time 72. Note that this rise is effected while the ambient temperature remains constant (the ambient temperature at $t=12$ was 23.5°C , and at $t=72$, 23.3°C). This indicates an internal phenomenon, and not something associated with linkage to the environment.

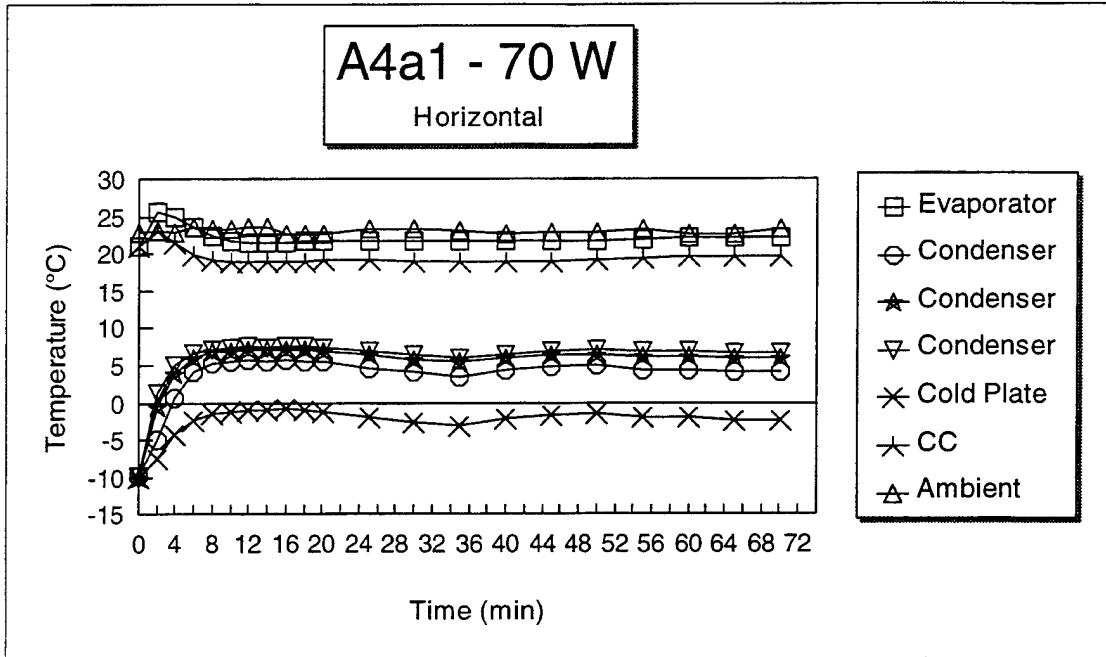


Figure 4.2. Seventy Watt Heat Load, Condenser at 5°C.

Figure 4.3 shows a 70 watt run completed by allowing the condenser temperature to rise above ambient. The "overshoot" can still be observed between $t=4$ and $t=10$.

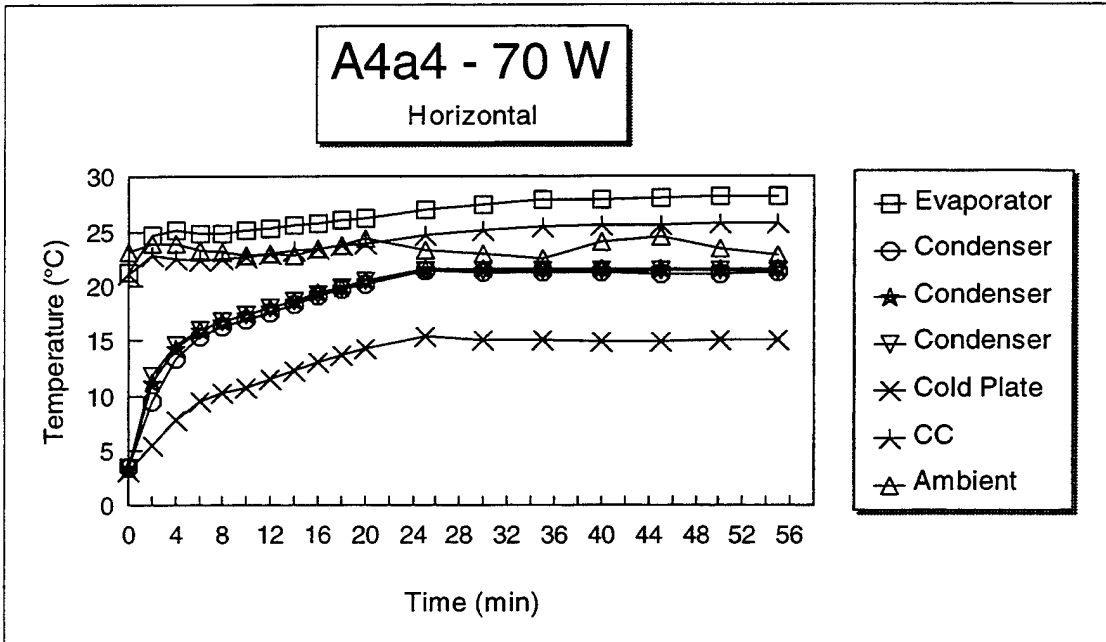


Figure 4.3. Seventy Watt Heat Load, Condenser at 20°C.

Figure 4.4 depicts a 30 watt run which demonstrates little or no overshoot. Below 50 W, the phenomenon is rarely seen. It is possible that the lower vapor and liquid flow

velocities created during operation at the lower heat load cause less transient redistribution of fluid, and thus a smoother transition to equilibrium.

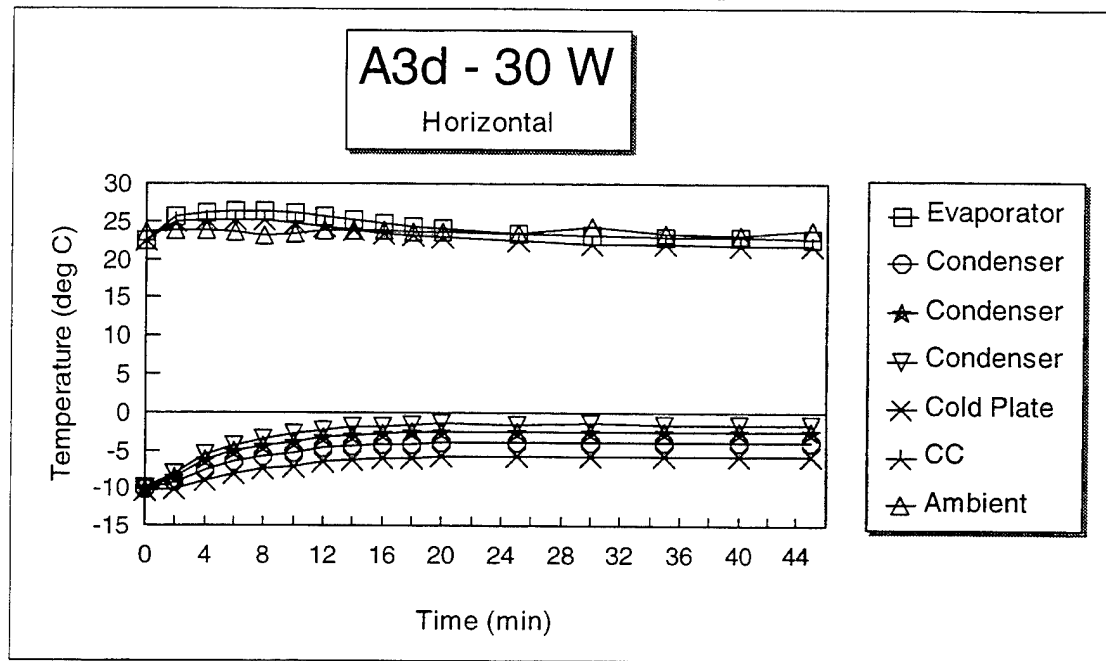


Figure 4.4. Thirty Watt Heat Load, Condenser below 0°C.

Figures 4.5 and 4.6 show two runs with identical setup but slightly differing results. The difference may be partly due to environmental interaction. The ambient temperature at equilibrium for the first run was lower by 1.4°C than for the second, and this corresponded exactly to the difference between the evaporator equilibrium temperatures. Other explanations could be simply the accuracy of the instrumentation or the chiller unit motor controller, or small differences in the state of the fluid existing in the transport lines prior to startup.

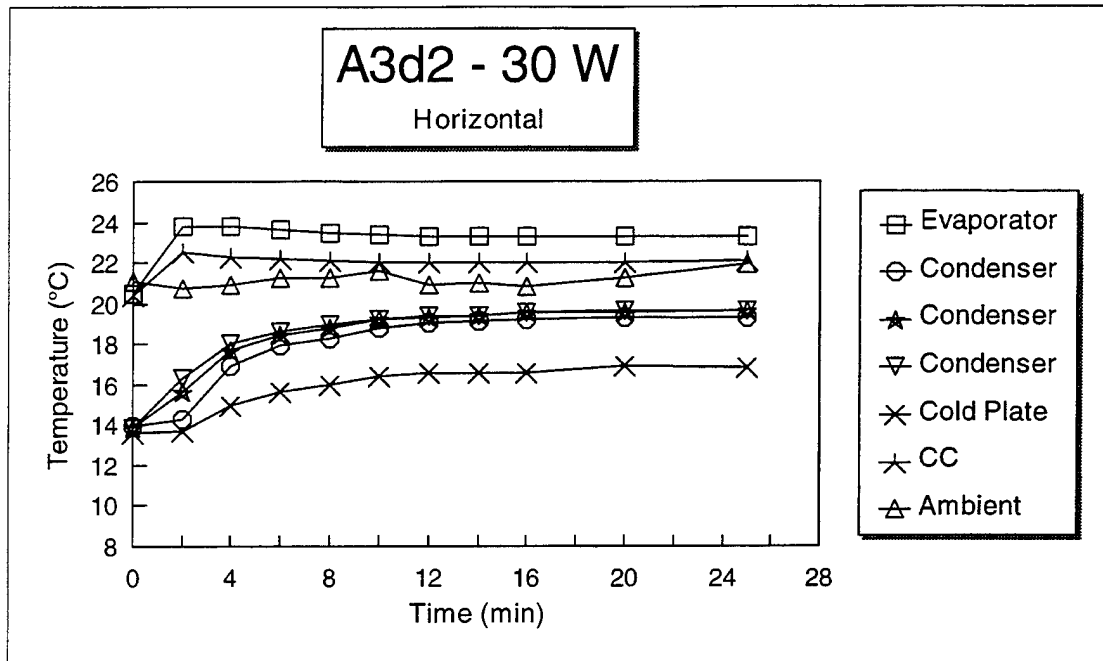


Figure 4.5. Identical Setup (30W, chiller @ 15°C) to A4b3.

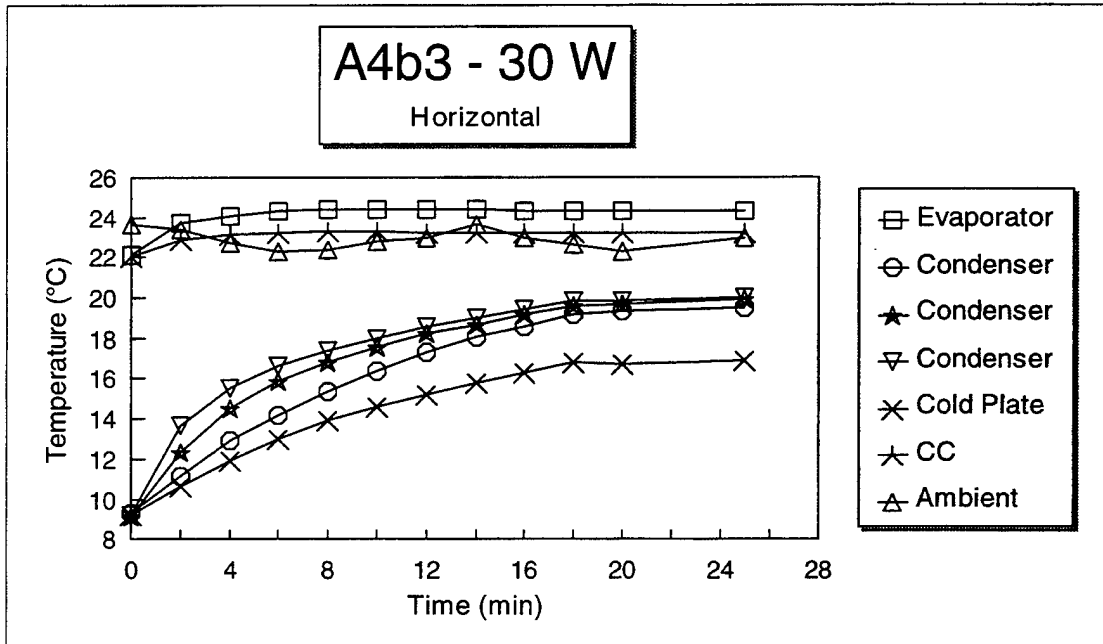


Figure 4.6. Identical Setup (30W, chiller @ 15°C) to A3d2.

a. Anomalous Runs

The runs accomplished at five watts heat load are considered anomalous, but have not been termed failures. It is still uncertain whether or not they achieved startup.

Run A3a probably did start. As shown in Fig. 4.7, the vapor line measurements show a significant excursion at the end near the condenser (the black triangle), and then remain near evaporator temperature, while the liquid line sensor nearest the condenser outlet (the + sign) shows cooler fluid moving through the line. The doubt arises in looking at the condenser and cold plate temperatures, which never show the rise normally indicating the transport of heat from the evaporator. In addition, there is no temperature separation between cold plate and condenser, something normally expected when the loop is pumping.

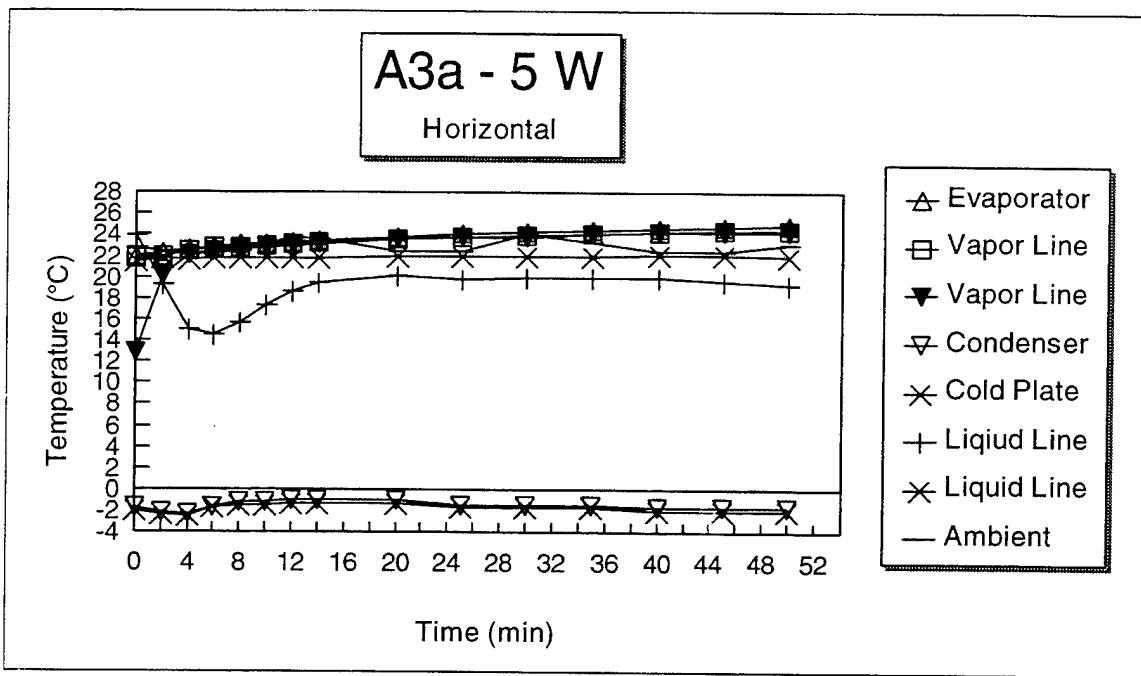


Figure 4.7. Five Watt Heat Load Run Profile.

Run A3a2, shown in Fig 4.8, is likely not to have started. The evaporator temperature met the criteria for equilibrium, but has a clear rising trend leading up to that point, and the condenser shows no change until the chiller setting is adjusted at 25 minutes. Unusual flow activity was observed, however, in the liquid and vapor lines. The nearest point to the evaporator on the vapor line (TC06) followed the evaporator temperature as expected, shown as the unfilled triangle on Fig. 4.8. The next point (TC07) is shown by the gray circle, showing a rapid rise at test initiation, followed by a drop starting at about time 16. This is hard to explain, as this point is in the middle of the

vapor line, and the "downstream" instruments did not reveal flow of cooler fluid to that point. It is possible that a slug of liquid was left in that portion of the line, and heated to the point where it began to vaporize, cooling its surroundings. The next thermocouple (TC08 - not pictured in Fig. 4.8) remained nearly isothermal at 18°C for the entire run, implying that there was no flow at all. TC09 is discussed in the following section.

Finally, the liquid line showed a rise in temperature starting at about time 12, and ending at about time 25, when the chiller setting was adjusted to 20°C. Taken as a whole, it appears that true circulation never was established, but some of the processes normally involved were in action. In any case, the LHP is evaluated as unreliable for operation below ten watts.

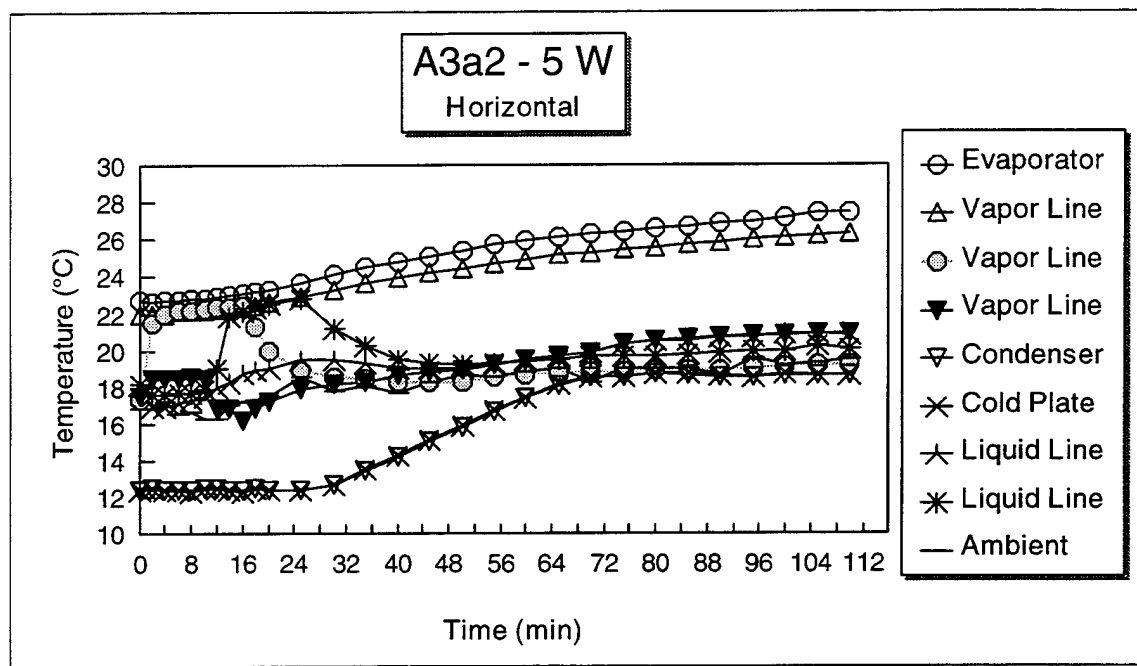


Figure 4.8. Five Watt Heat Load Run Profile.

b. Reverse Flow

The idea of complex patterns of flow is supported by the LMAG report which refers to an instance of reverse flow. Inspection of Fig. 4.8 reveals that run A3a2 appears to have experienced this phenomenon. The thermocouple on the vapor line closest to the condenser (TC09 - the black inverted triangle in Fig. 4.8) displayed a seemingly normal startup transient, but never reached the temperature of the evaporator. At 12 minutes it

showed a sharp down transient, possibly indicating a depletion of vapor from the evaporator. The downward trend bottomed out at time 16, and climbed steeply over the next 15 minutes to near the temperature that point had at equilibrium. This phenomenon was not exhibited in any of the other runs.

c. Complex Flow

The unusual activities observed in the LHP under test are hard to explain or understand. It appears, however, that the flow induced in the LHP vapor line when a load is applied is very complex, and not limited to a single phase. This is especially true at lower heat loads, when the flow velocity will be relatively small. It appears to be negligible at the higher heat loads, when high flow rates allow the first order phenomena to dominate. It will be vital to understand these low power two-phase phenomena during further study.

2. Thermal Transport

a. Operating Range

The acceptance tests from the Lavochkin Association showed 130 W as the maximum heat load tested for the test article. This test program called for testing to maximum to identify the operating range. Accordingly, successful starts were achieved at heat loads from 10 to 150 watts, with partial success at five watts. A load of 150 W may not be reliable, it was only attempted once, and is outside the design limits of the device.

When the evaporator was placed at an adverse height, the acceptance tests showed successful runs at 30 and 80 W heat load with the evaporator raised 2 m (80 in). These results could not be duplicated. Successful runs were completed at 1 m adverse, with heat loads from 20 to 100 W. There were no runs completed at 2 m adverse, but two runs were successful at 1.5 m (60 in), both within 2 w of 40 W.

Appendix C contains the complete data package, including both data collected by the author, and data collected at VTPT since then.

b. Evaporator Equilibrium Temperature

Figure 4.9 shows equilibrium temperatures for all instrumented points along the LHP for one run at each heat load. The runs were selected to be as nearly comparable as possible, by matching condenser temperatures. Note that some show very little temperature difference from the condenser outlet to the CC inlet (TC14 to TC18); others as much as four or five degrees increase. Early in the testing, environmental effects were discussed, and the conclusion was that they would be small enough to offset with insulation. Figure 4.9 would seem to contradict this idea -- the heat leak between the liquid line and the air seems significant, and effective in either direction. The vapor line was still more so assumed to be immune to the effects of its surroundings. This assumption has proven to be fairly good. The change in temperature along the vapor line is negligible, except in the five watt case, which has already been discussed as anomalous. It is interesting to note, however, that this plot displays the oddity of TC07 and TC08 having a lower temperature than TC09 which is closer to the condenser.

Appendix B, Figs. B.13 to B.16 depict equilibrium temperatures for all runs, divided up by heat load.

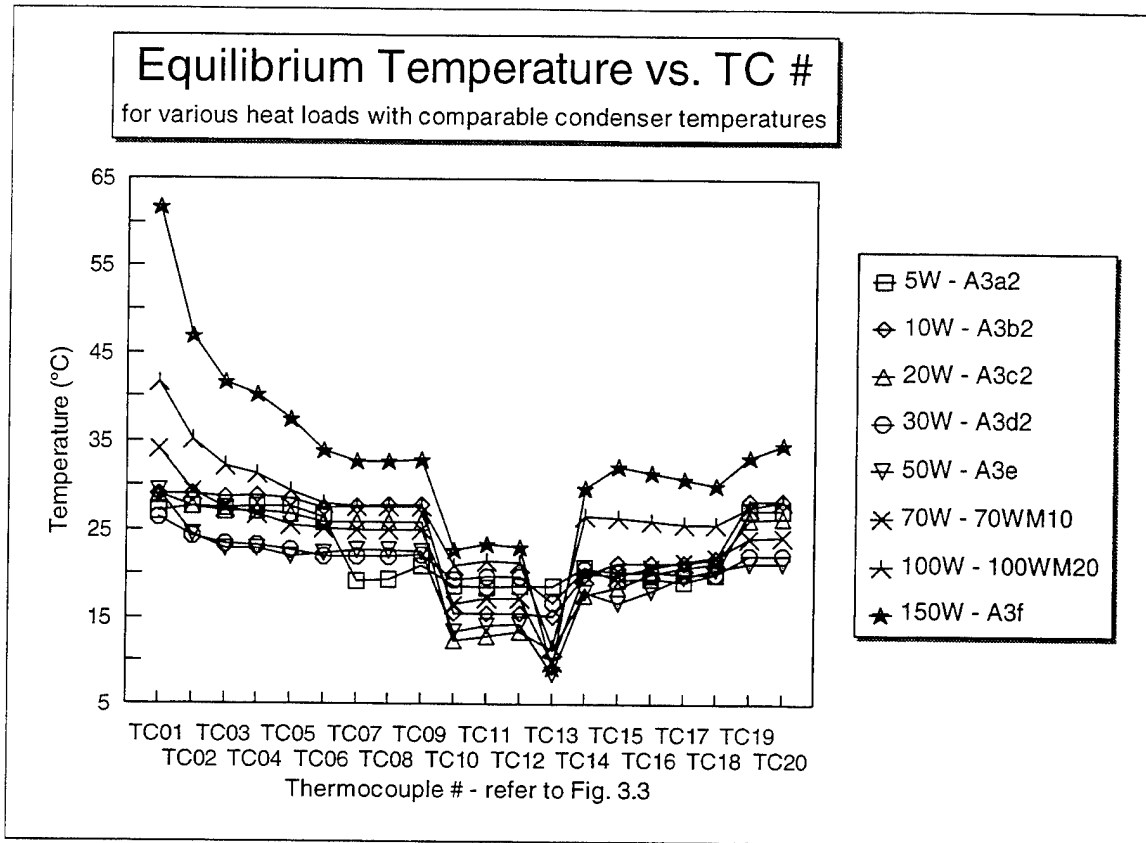


Figure 4.9. Comparison of Equilibrium Temperatures Along the Entire LHP for Various Loads.

Figure 4.10 shows a "scattergram" of all evaporator equilibrium temperatures collected. Evaporator temperature seems to depend considerably more on condenser temperature than the heat load. The best indicator of this is in the center of Fig. 4.10, where a square of 5°C can be placed around a data point from each of the heat loads except 5 W and 150 W. This shows that careful control of the condenser can be key to maintenance of evaporator temperature, even under varying load.

Figures 4.11 and 4.12 present the disproportionate variation in condenser temperature compared to evaporator temperature for 30 and 70 W. Both display very little change in evaporator temperature, even over significant rise for the condenser.

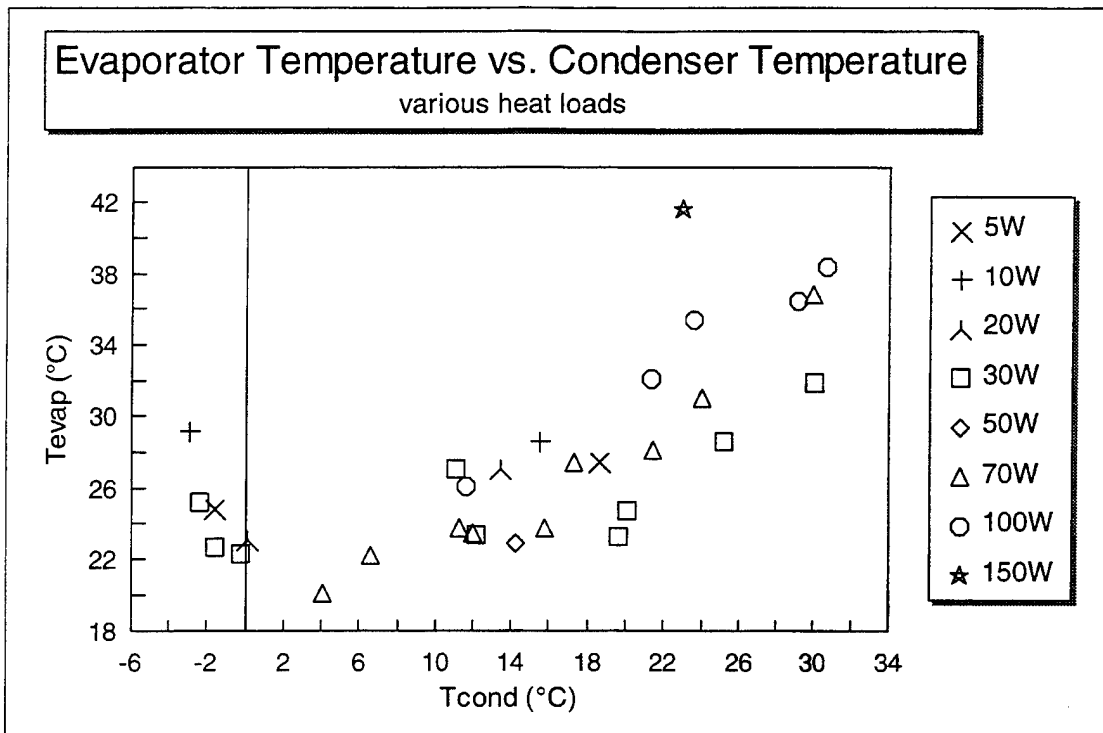


Figure 4.10. Evaporator Temperature as a Function of Condenser Temperature; Identified by Load.

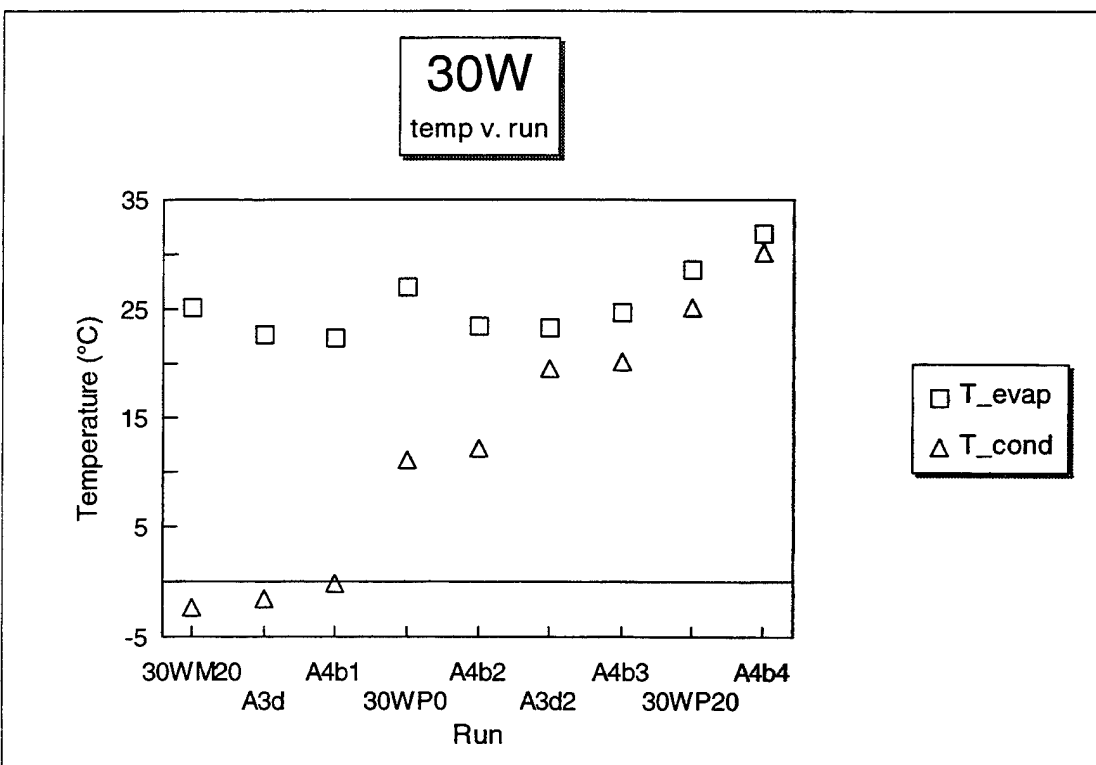


Figure 4.11. Trend of Evaporator Temperature with Increasing Condenser Temperature at 30 W.

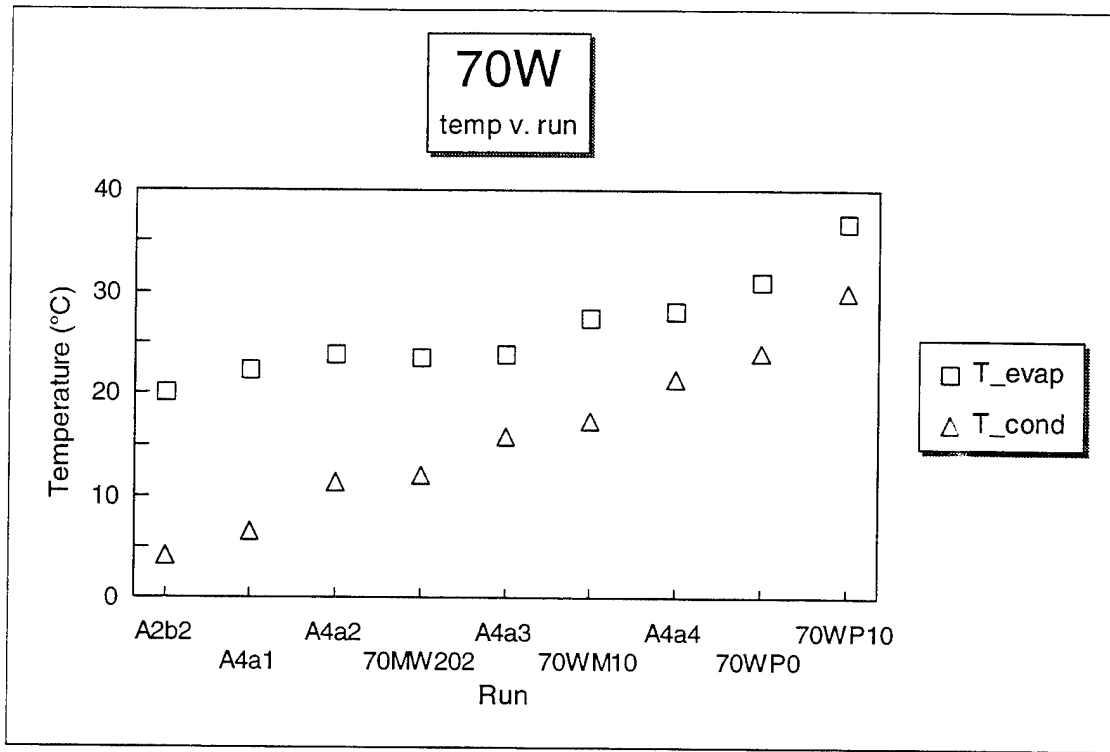


Figure 4.12. Trend of Evaporator Temperature with Increasing Condenser Temperature at 70 W.

Appendix B, Figs. B.1 to B.12 contain similar plots for all runs. The trend is consistent, though more pronounced at lower powers.

c. Delta T

Delta T (ΔT), or the temperature difference between the evaporator and the condenser, has been mentioned frequently in this thesis. In Chap. I, it was discussed as a factor which allowed the calculation of a coefficient of conductance for a heat pipe as a unit, C_{HP} . In Chap. II, it was used as one of the criteria for proper operation of the LHP (see Eqn. 2-4), and excessive delta T at low heat loads was noted as an item of concern in previous testing. Figure 4.13 shows ΔT as a function of heat load, broken out by condenser temperature. Note that there are rough groupings based on condenser temperature; i.e., data points for a T_{cond} between 10 and 15°C fall between 11 and 16°C differential, over all heat loads. LMAG results, depicted in Fig. A.6, show a definite increasing curve with increasing heat load. The results for LHP-93-2-Prop show a similar curve, for condenser temperatures in roughly the same range. Other ranges of condenser temperature show somewhat different patterns, however, such as the nearly straight line

when T_{cond} is higher (between 20 and 25°C), and the loose grouping when T_{cond} is very low (below 0°C).

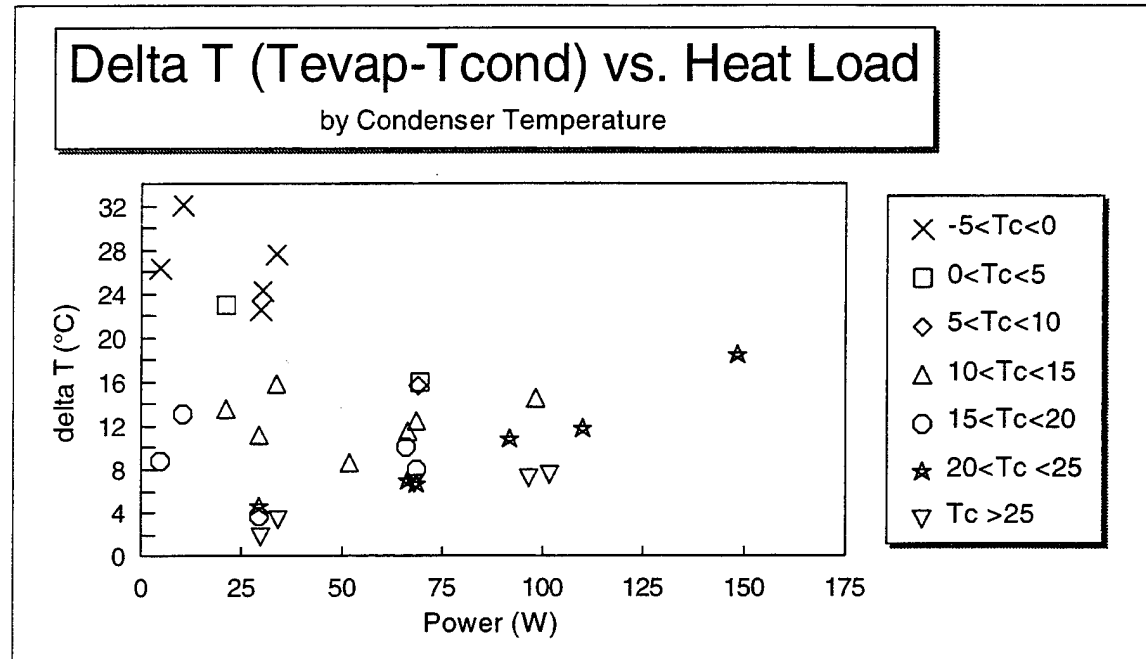


Figure 4.13. ΔT as a Function of Heat Load, Identified by Condenser Temperature.

LMAG noted high ΔT under low heat loads, which is mirrored in this data, but Fig. 4.13 shows a greater dependence on the condenser temperature, although all of the highest ΔT s shown are at low load. Fig. 4.14 shows ΔT plotted against T_{cond} , broken out to show heat load. The relationship between T_{cond} and ΔT appears more clearly in this chart, as well as the difference in flow conditions below 30 watts with a cold condenser. The main body of data in Fig. 4.14 contains data points from all heat loads, and maintains a fairly low ΔT when the condenser stays above 0°C. The condenser is never below 0°C with the higher heat loads applied, but the low loads allow considerably lower temperatures, which translate to much higher ΔT . A heat load of 150 W is an outlier in Fig. 4.14, but it should be remembered that this load is well outside the design operating range. Thirty watts is a particularly interesting data set, since it seems to be the transition point between flow conditions. While T_{cond} remains below 0°C, these runs display very high differentials, but as the condenser temperature rises, it shows the lowest of the ΔT s in the grouping. This appears to be the result of the "autoregulation" process attempting to maintain T_{evap} in a relatively narrow range, irrespective of changes to condenser temperature. It seems reasonable that, as evaporator temperature increases, evaporation

increases, and thus so does vapor flow. This would force the redistribution of working fluid, and in effect, increase transfer rate.

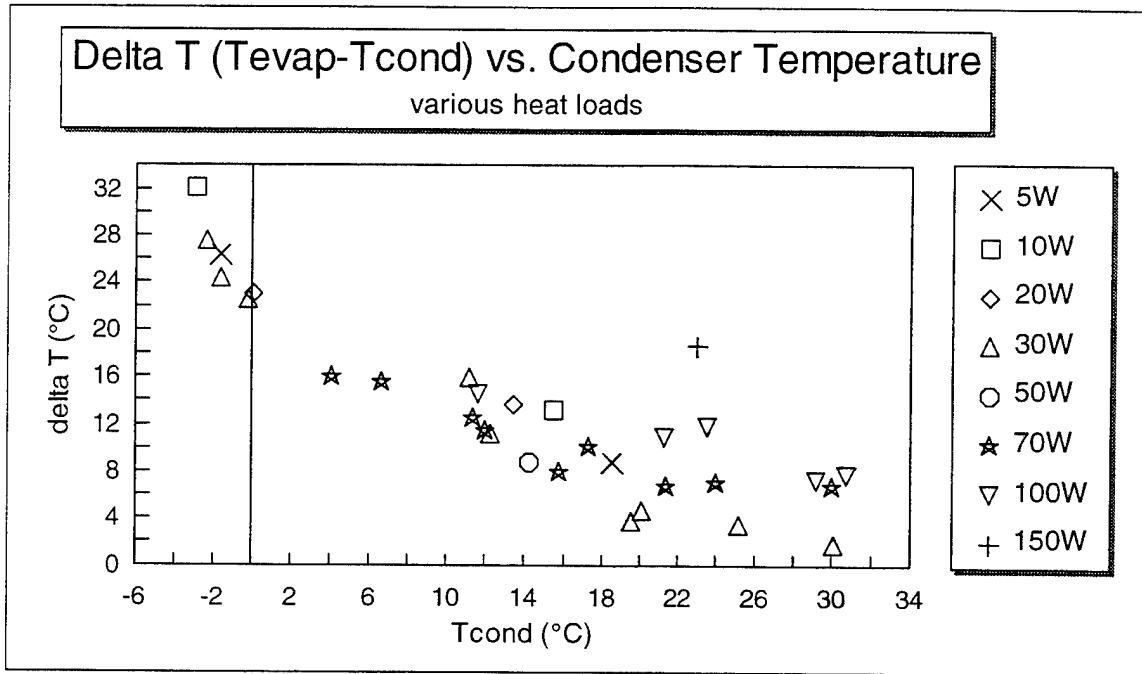


Figure 4.14. ΔT as a Function of Condenser Temperature, Identified by Heat Load.

d. Conductance Characteristics

To offset the differences imposed by differing heat loads, a coefficient of conductance was developed for the LHP at each set of data points. The coefficient, C_{HP} , was determined by rearranging Eqn. 1.8 and taking the heat load divided by ΔT . The plot of C_{HP} versus heat load is given in Fig. 4.15, and provides a reasonable match to the same range of power applied in some of the previous testing (Figs. A.2 and A.4).

Conductance Coefficient vs. Heat Load

by Condenser Temperature

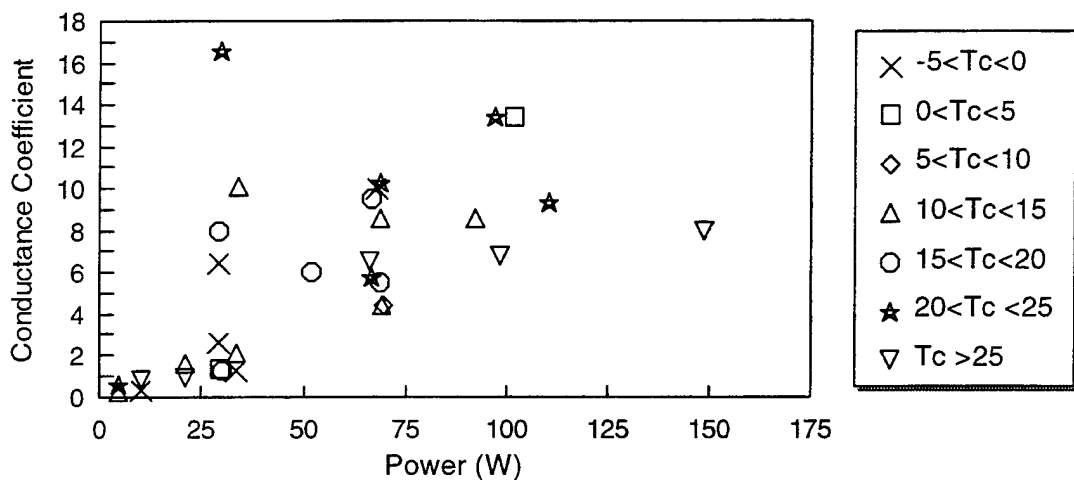


Figure 4.15. Conductance as a Function of Heat Load, Identified by Condenser Temperature.

It is interesting to note that points were again "grouped," between a coefficient of 5 and 10, and below a C_{HP} of 2. This may again show the difference in flow conditions for lower and higher loads. Figure 4.16 highlights the difference between load ranges even more prominently. The filled blocks are all at thirty watts or below, while the open blocks are above thirty. It is clear that the low power runs had C_{HP} values consistently lower than two, while the higher loads were steadily increasing from a value of five. Thirty watt runs appeared to follow both curves. This lends more support to thirty watts as a transition point between the differing flow conditions.

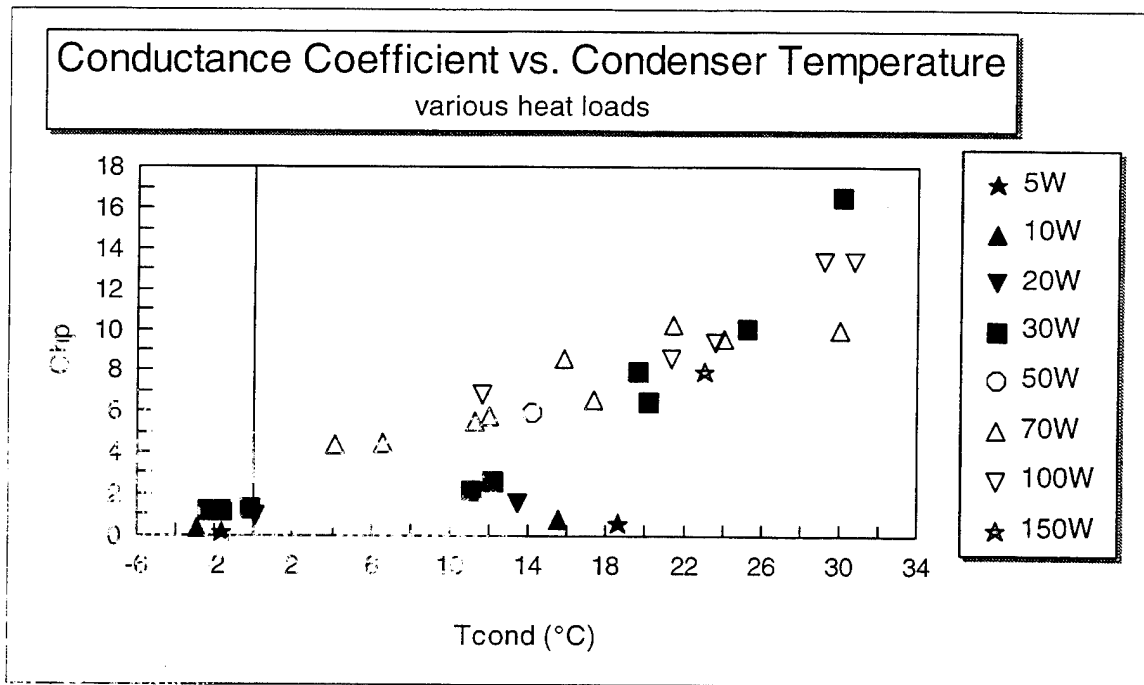


Figure 4.16. Conductance as a Function of Condenser Temperature, Identified by Heat Load.

e. Adverse Height Effects

Since failures were experienced at adverse elevations in contradiction of acceptance test sheets, the number of data points for comparison were considerably less than the LMAG results. Therefore, the multitude of curves shown in Fig. A.6. from M data could not be generated for comparison. Table 4.1 shows a listing of the failures at adverse heights.

The runs at 1 m (40 in) which failed appeared to be due to starting with 5 W (which never achieved startup), and drying out the wick. The subsequent tests were performed without returning the LHP to horizontal, and startup was not achieved at any heat load. Later, after placing the LHP horizontal and achieving startup at 70 W, successful runs were completed at 1 m. This included 10 W, although it apparently lost surface tension and ceased pumping when its evaporator reached 50°C (it displayed a sudden drop in condenser temperature, and the temperature rise at the evaporator accelerated). As evidenced by Tbl. 4.1, there were no successes at 2 m adverse, and success has only been achieved at 1.5 m within 2 W of 40 W. It has been suggested that

the acceptance testing may have been performed by starting the LHP in a horizontal orientation and raising the evaporator to the adverse height once flow had been established. This variation in procedure was not attempted since the test setup made this difficult to execute.

Date	Run #	Result	Q (W)	Position
950317	A5b	Failed To Start	69.5	80 IN Adv.
950317	A5b2	Failed To Start	71.8	80 IN Adv.
950317	A5b3	Failed To Start	71.8	80 IN Adv.
950320	A5a(5)	Failed To Start	4.84	40 IN Adv.
950320	A5a(10)	Failed To Start	10.2	40 IN Adv.
950320	A5a(20)	Failed To Start	20.7	40 IN Adv.
950320	A5a(30)	Failed To Start	29.4	40 IN Adv.
950320	A5a(50)	Failed To Start	48.7	40 IN Adv.
950320	A5a(100)	Failed To Start	93.5	40 IN Adv.
950322	A5b(100)	Failed To Start	112.9	80 IN Adv.
950322	A5b(100-2)	Failed To Start	111	80 IN Adv.
950605	JUNE05B 2 Loads	1) Successful	41.7	59.5 IN Adv.
		2) Failed To Start	88.2	
950605	JUNE05C	Failed To Start	24.1	59.5 IN Adv.
950606	JUNE06A	Failed To Start	13.9	61.5 IN Adv.
950606	JUNE06B	Failed To Start	36.7	61.5 IN Adv.
950606	JUNE06C 2 Loads	1) Successful	38.6	60 IN Adv.
		2) Failed To Start	17.2	
950606	JUNE06D	Failed To Start	54	60 IN Adv.

Table 4.1. Adverse Height Testing.

Figure 4.17 shows a comparison of evaporator temperatures for the test range of heat loads; T_{cond} is provided for comparison. The difference between horizontal and adverse tended to be between five and ten degrees, but narrowed at higher loads, something also demonstrated in previous testing. This difference may also be related to the higher flow rates associated with higher loads, which might allow better transport at a given temperature. Figure 4.18 depicts ΔT for comparable runs at each load; T_{cond} is again provided for comparison. The differentials are similar to those observed by LMAG, about 3 to 6°C. The low load cases are again the larger differences. Note that condenser temperature was a significant factor in the ΔT , even more so than load. The

apparent crossover at 100 W load deserves further investigation, as with the limited data available here, it may simply be attributable to measurement uncertainty.

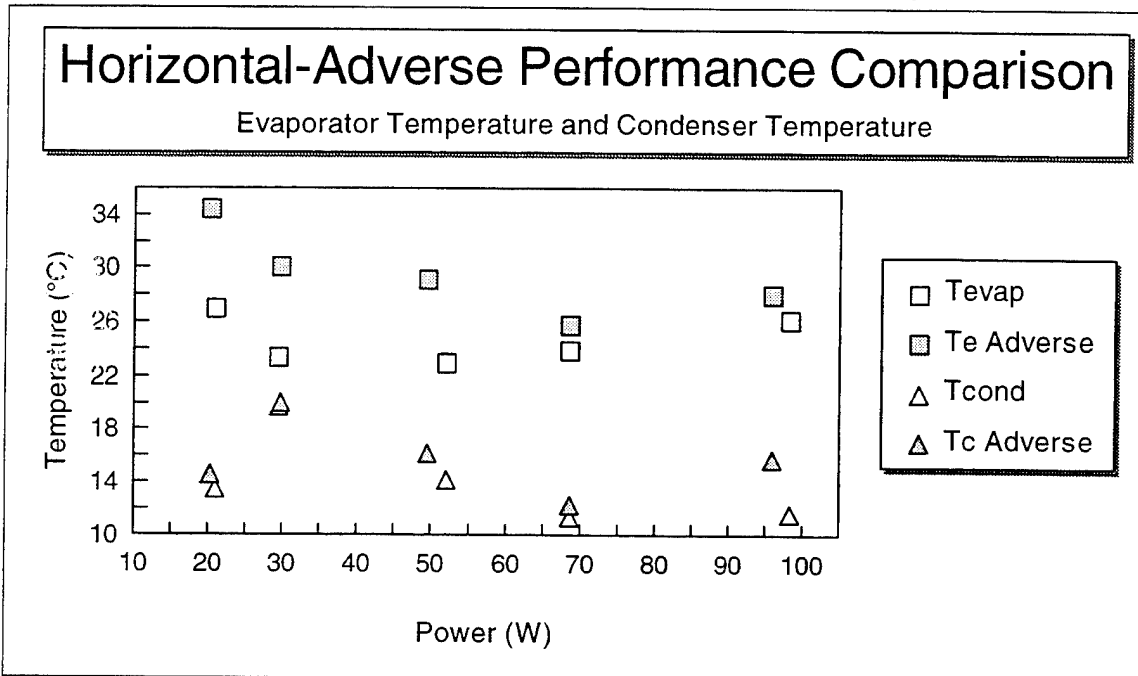


Figure 4.17. Evaporator Temperature For Horizontal and Adverse Elevated Runs with Similar Settings.

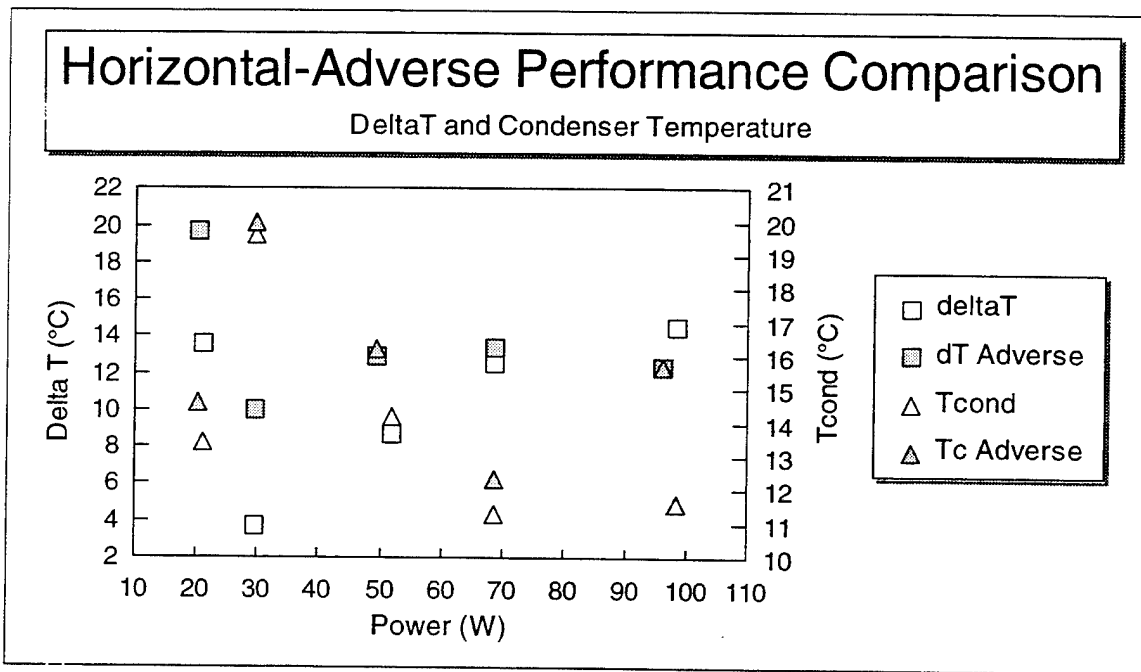


Figure 4.18. ΔT for Horizontal and Adverse Elevated Runs with Similar Settings.

Figure 4.19 compares C_{HP} for the horizontal and adverse height runs. This allows the relationship to be corrected for heat load applied. In most cases the difference between the heights is narrowed, but the 30 W case still has a significant gap; this could be more evidence of unusual flow conditions present.

From Eqn. 1-6, the adverse gravity experienced by the LHP is roughly g times the sine of the angle of the pipe from the horizontal. A height of 1 m for a 4 m total length gives an included angle of 14° , or a factor of 0.24. Thus, LHP-93-2-Prop appears capable of operation against an adverse acceleration of 0.25g.

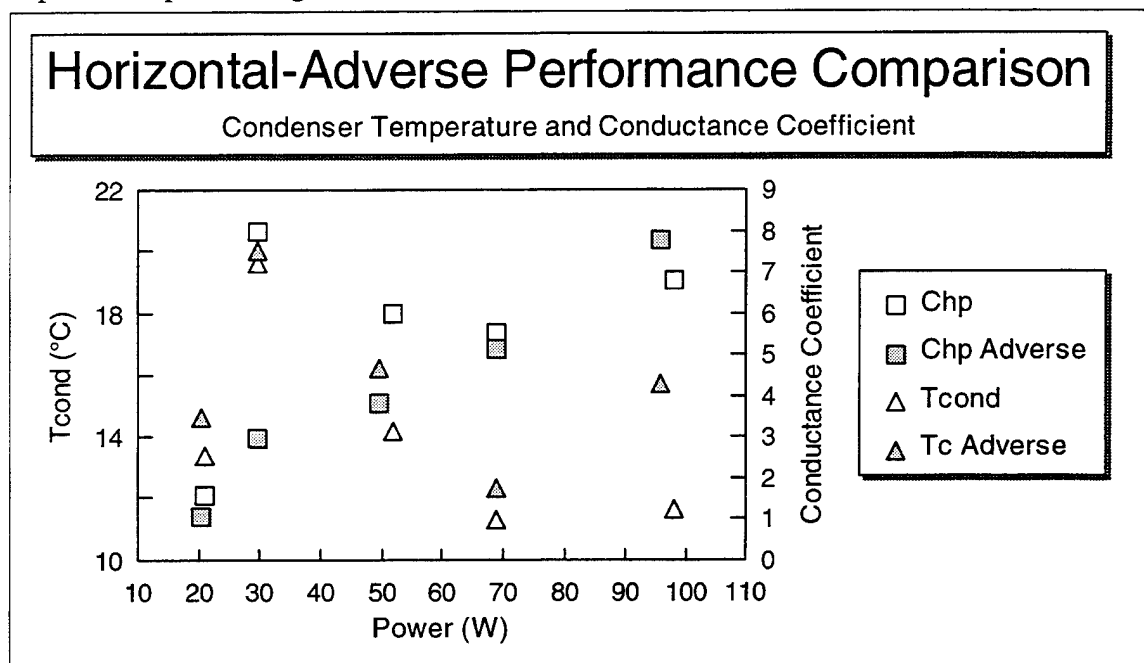


Figure 4.19. Conductance Coefficient for Horizontal and Adverse Elevated Runs with Similar Settings.

C. FAILURE MODES

LHP-93-2-Prop was shown to have two modes of failure, neither of which was completely explained. Both have operational implications for spacecraft, and thus must be investigated further and understood.

The first mode was observed in two cases both at a heat load of 70 W, which was normally seen to be the load which produced the most reliable startups and kept the evaporator in the desired temperature range most easily (without extremely low condenser

temperatures). In each case, the evaporator was slightly above ambient ($\sim 28^{\circ}\text{C}$) due to previous testing, and the condenser was at a very low temperature ($\sim 18^{\circ}\text{C}$). LMAG reported a tendency for bad starts when the condenser was "significantly colder" than the evaporator [8]. It is postulated that this tendency resulted in the failures observed. A potential explanation could be the upset of the balance described by Eqn. 2-4. When the ΔT exceeds a certain level, the conditions inside the LHP and the properties of the working fluid may make it impossible to satisfy this relation. Further investigation of this interplay is critical to ensuring reliability of the device. Internal sensors, which would allow direct perception of the physical state of the working fluid under these conditions, will likely be required to determine whether or not this hypothesis is valid, or if another explanation applies.

The second failure mode identified is the inability of LHP-93-2-Prop to operate at adverse heights greater than 1.5 m, or over any appreciable range above 1 m. This is considered a distinct mode of failure due to the acceptance test report, which documented satisfactory runs at adverse elevations of 2m. In several cases of failure, vapor flow was observed, evidenced by heating of the vapor line, but no change in liquid line temperature was observed, indicating that startup never occurred. The only situations in which these transients were not observed were the A5a series shown in Tbl. 4.1, which have been discussed as a case of initial dry out of the wick. The remaining failures appeared to be caused by insufficient vapor flow to force liquid into the CC and to the wick. It is also possible that heat leak from the evaporator to the CC created a large enough vapor bubble during the startup process to prevent resupply of liquid to the wick. This may have manifested only under adverse acceleration due to the additional time required to force liquid out of the condenser against the adverse acceleration.

D. RECOVERY MODES

To assist in recovery from failed runs, a procedure was developed to restore flow through the LHP, thereby reinstating the fluid balance required for a good start. The evaporator was returned to horizontal, cooled by blowing air on it with a fan, and the chiller setpoint was adjusted to -7°C . A heat load of 70 watts was then applied, which

provided sufficient vapor velocity to force liquid to the wick, without driving evaporator temperature too high.

Subsequent testing by VTPT personnel has suggested another method. It appears that the CC retains liquid even in a wick dry out situation. The evaporator/CC assembly was tipped evaporator down to place liquid at the wick again. Successful starts were achieved using this method after dry out.

E. EXPERIMENTAL FLAWS

1. Control of Temperature

The relationship between condenser temperature and the key parameters of evaporator temperature, delta T, and conductance coefficient showed that better control of condenser temperature would enhance the value of the results. A more robust means of providing an ultimate sink, with a relatively fine control system would allow better determination of the aforementioned relationships. Analysis of the experimental data was complicated by the difference between condenser temperatures in some cases.

2. Heat Balance

In addition, no heat balance was performed on the chiller unit to verify heat load removed from the LHP. The load values were based on the electrical power applied to the heater, and would certainly have suffered some losses, adding a source of inaccuracy to the results.

3. External Sensors

All sensors used in this experiment were thermocouples applied to the outer surface of the LHP, vice internal sensors which would directly sample the vapor and liquid temperatures. This allows the potential for environmental effects and inefficient contact to reduce measurement accuracy.

4. Temperature Sensors Only

Understanding of the obviously complex flow conditions inside the device was hampered by having only temperature sensors. this prevented true understanding of the state of the working fluid at any point or time of interest. Pressure transducers and, if practicable, vapor velocity sensors should have been incorporated into the test setup.

V. CONCLUSIONS AND RECOMMENDATIONS

A. SUITABILITY

The basic question underlying this investigation regarded the suitability of the LHP design for use in spacecraft thermal control. The secondary question was whether the LHP was sufficiently understood in operational detail to warrant the expense and difficulty of arranging flight testing. The following observations bear directly upon both of these issues.

1. Usable Operating Range and Criteria

The range over which LHP-93-2-Prop was found to be operable was from 10 watts to 150 watts. The caveat is offered that loads above the design maximum load of 100 watts were insufficiently tested to ensure reliability. This exceeded the specification requirement that it carry 100 W, and transport 30 W with ΔT less than 10°C . The condenser temperature was found to be a significant factor in the operation of the device, and an operating range between 0 and 20°C was found to provide the best results. Given these factors, the evaporator remained in the 20 to 40°C temperature range, with relatively small variation over a range of heat input and condenser temperatures.

When placed in an orientation simulating adverse acceleration, the LHP did not perform as demonstrated in the acceptance tests. It apparently could not operate at all above 1.5 m adverse, and could operate at heat loads from 20 to 100 W only at 1 m. The specification did not appear to call for any particular capability in this regard, but the design was reported to be capable of pumping against its full length. The capability provided by this design is operation under the equivalent of 0.25 g adverse acceleration.

2. Advantages

The most significant advantage of the device is its mechanical flexibility. The small diameter stainless steel vapor and liquid lines can be bent and routed into any necessary configuration. This may be of particular benefit for high density electronics

cooling, as the tubing can be configured into wiring runs. It is also under investigation at Hughes Aircraft as an enabling technology for deployable radiators for high dissipation devices such as high powered communication equipment.

The ability to operate against adverse acceleration is another significant advantage. This capability may allow significant robustness to a space vehicle under maneuver, or permit considerable latitude of installation for ground installations.

Finally, it appears to be highly reliable and self-starting. A beginning has been made on identifying causes of failure, and further investigation will enhance understanding, and permit avoidance of failure states.

3. Disadvantages

The most significant disadvantage of this LHP is the still scanty understanding of the internal condition of the working fluid under anomalous circumstances. Without a better understanding of the flow conditions which may cause failure, high risk is involved in operational use of the device.

Another disadvantage of LHP-93-2-Prop involves manufacturing reproducibility and quality assurance. It is still uncertain whether the production of the two LHPs purchased by Lockheed Martin were hand-crafted and essentially one-of-a-kind, or whether mass production reproducibility applies. The lack of understanding of the internal function of the LHP makes it difficult to know how important this is to operational reliability. It is difficult to even write a specification for tolerances for the device, since their importance is not quantitatively known. The acceptance test report included in App. B contains several errors. The document refers to the LHP in various locations as number 1, when in fact it is number 2, and the working fluid is misrepresented as Ammonia. These discrepancies, and the inability to reproduce some of the adverse height test results shown on the sheet are a warning requiring further investigation, and very solid assurances prior to operational use of the device.

B. FURTHER RESEARCH

As mentioned above, there is considerable interest in the LHP design. The experimentation at Phillips Laboratory is due to be completed and the LHP returned to LMAG as of 01 October 1995. It is likely that the Air Force will allow all further investigation to be performed by private industry. The following are issues for further investigation and recommendation for the form of that inquiry.

1. Interior Sensors

One notable shortcoming of the current experiment was that all understanding of the internal workings of the LHP was inferred from surface temperature measurements. To ensure sufficient understanding of the potential failure modes of the LHP, internal sensors should be utilized. Pressure and temperature sensors would allow direct measurement of the vapor and liquid temperatures and the pressure drops from point to point in the loop. This would permit conjectures about the reason for failed startups and about the differing nature of flow at high and low heat loads to be confirmed. These sensors might also allow sufficient information to infer the vapor and liquid velocities in the transport lines, but it might be advisable to measure these parameters as well.

2. Propylene Properties

Propylene properties are available from a variety of sources, but a careful reading will assure the reader that the majority of values provided are determined graphically or from a curve fit formula, vice experimentally. In particular, viscosity and surface tension figures were not located over a sufficient temperature range to allow use over the operating temperature range of the LHP. If propylene is to be used as a working fluid, experimentation should be performed to develop both liquid and vapor data for the temperature range from -80 to +50°C. It is possible that some further interaction with Lavochkin Association and the Institute of Thermophysics would yield further data which remains unpublished in the West.

3. Destructive Testing

Detail regarding the internal arrangement and volume of the LHP were represented to LMAG as proprietary issues. Since LMAG owns the two LHPs and they are covered under U.S. patent, the possibility of destructive testing of one of the LHPs should be considered to determine these key parameters. The internal details could answer some of the questions regarding flow conditions, and the volume would aid in determining the state of the working fluid at various points in the loop and times in the operating cycle. Testing of the alloys used in the casing and any internal fittings would allow determinations about fatigue and material incompatibility to be made prior to flight experiments.

4. Low Temperature Testing

One of the reasons cited by Yury Maidanik in a 10 March 1995 email to Don Gluck for charging one LHP with propylene was to take advantage of its relatively low melting point (-185°C) for LHP utilization at lower temperatures than other working fluids. The testing has all been performed at room temperature thus far, so the isolation of the device from the environment and the use of temperatures below 0°C should be investigated. The testing accomplished would determine if the failures observed in current testing were the result of too large a ΔT , or if there was some intrinsic reason that condenser temperatures below 0°C resulted in lower performance and higher incidence of failure.

5. Thermal Vacuum Testing

On the other end of the scale, the issue of complex patterns of flow at low heat load requires further investigation with assurance of freedom from environmental effects. Testing should be performed in a thermal vacuum chamber to allow total control over experimental parameters. This would also enable testing with ambient temperatures significantly above room temperature.

6. Tests with Vapor and Liquid Lines Coiled/Bent

Flow rate and the complexity of flow conditions seems to be a performance issue for this design. No testing has yet been accomplished regarding the effect of unusual configuration of the transport lines. No interference was observed with any testing as a result of moving or bending the lines, but they were not subjected to coiling or tight turns as might be required in operation installations. Testing should be accomplished to include moving the tubing during testing, as might be required in a deployable installation.

REFERENCE LIST

1. Agrawal, Brij N., *Design of Geosynchronous Spacecraft*. (Prentice-Hall; Englewood Cliffs, NJ: 1986).
2. Ernst, D. *Loop Heat Pipes - An Enabling Technology for Advanced Thermal Management*. (DTX Corporation; Lancaster, PA: Fall 1993).
3. Faghri, Amir. *Heat Pipe Science and Technology*. (Taylor & Francis; Washington, DC: 1995).
4. Gilmore, David G. *Satellite Thermal Control*. (The Aerospace Corp. Press; El Segundo, CA: 1994).
5. Maidanik, Yury F. "Loop Heat Pipes and Capillary Pumped Loops: Development Status in Russia," *Presentation Delivered at Ekaterinburg, 1993*.
6. Maidanik, Yury F. "Loop Heat Pipes: Design, Investigation, Prospects of Use in Aerospace Technics," *SAE Technical Paper Series*. April 1994.
7. Maidanik, Yury F. "Design and Investigation of Methods of Regulation of Loop Heat Pipes for Terrestrial and Space Application," *SAE Technical Paper Series*. June 1994.
8. Martin Marietta Astronautics Group. *Advanced Active Thermal Control Project D-19D: Loop Heat Pipe Technology Performance Evaluation* (Internal Progress Report; Denver, CO; May 1994).
9. Meyer, R., et al. *Investigation of the Heat Transfer Performance of a Capillary Pumped Loop Under Gravity*. (Paper No. 932304, 23rd International Conference on Environmental Systems; Colorado Springs, CO: July, 1993).
10. Vargaftik, N. B. *Tables on the Thermophysical Properties of Liquids and Gases*. (John Wiley and Sons; New York, NY: 1975).

BIBLIOGRAPHY

1. Incropera, Frank P. and David P. DeWitt. *Introduction to Heat Transfer*. Second Edition. (John Wiley & Sons; NY, NY: 1990).
2. Martin Marietta Corp. "Loop Heat Pipe 1993 Test Results," MM Internal Report. May 1994.
3. Van Wylen, Gordon, and others. *Fundamentals of Classical Thermodynamics*, Fourth Edition. (John Wiley & Sons; NY, NY: 1994).
4. Peterson, G. P. *An Introduction to Heat Pipes*. (John Wiley & Sons; NY, NY: 1994).

APPENDIX A. PREVIOUS LHP EXPERIMENTATION RESULTS.

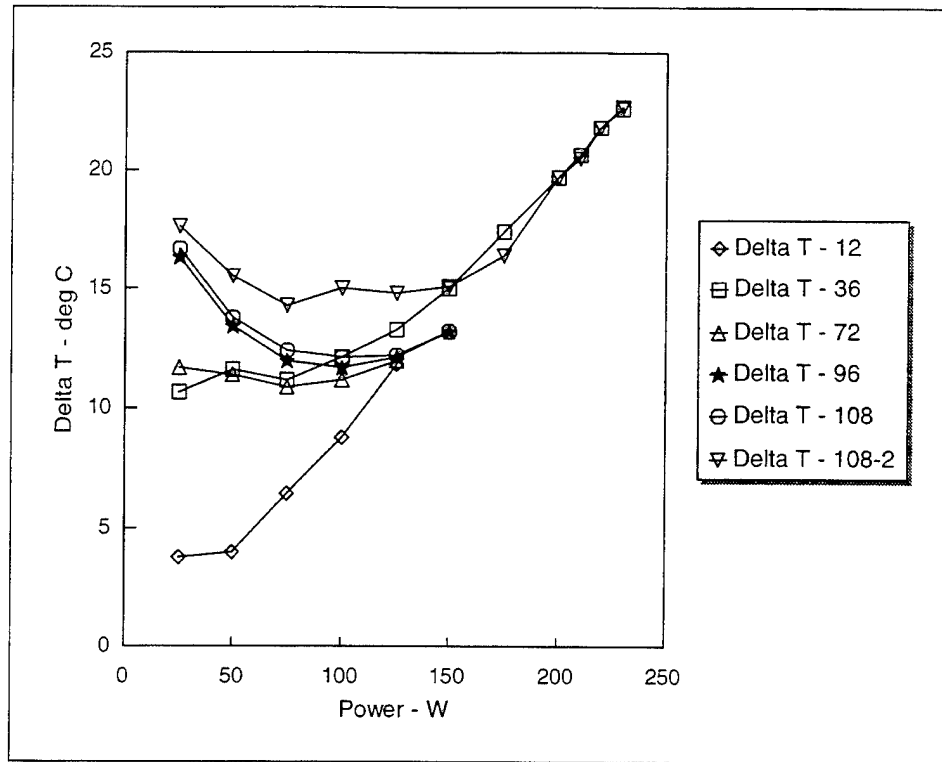


Figure A.1. Unspecified Design and Working Fluid -- Delta T vs. Power, Various Adverse Elevations.
[2]

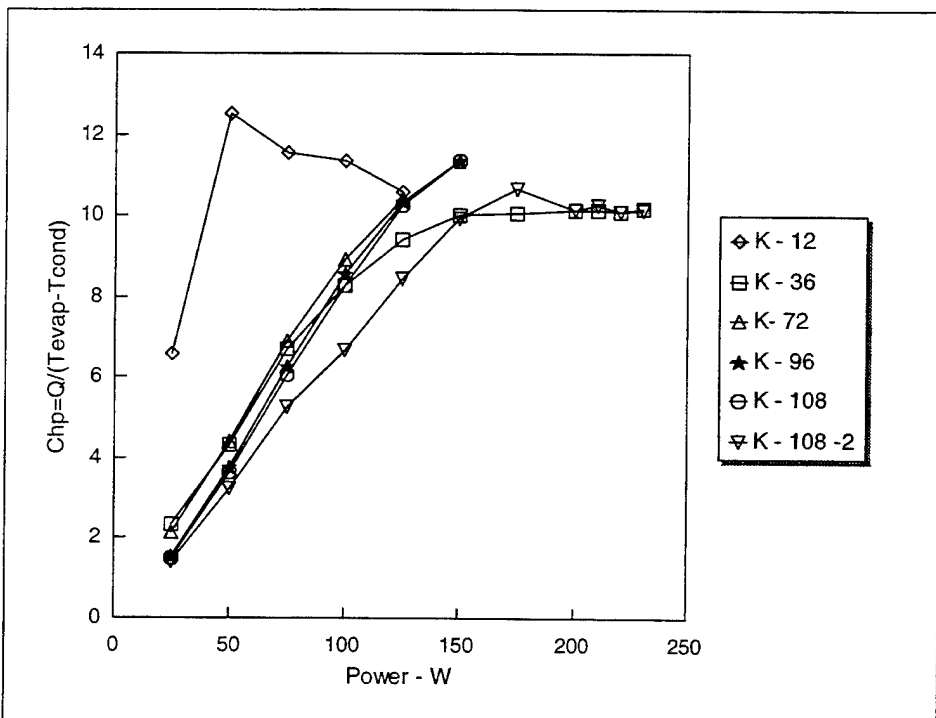


Figure A.2. Unspecified Design and Working Fluid -- Conductance Coefficient vs. Power, Various Adverse Elevations. [2]

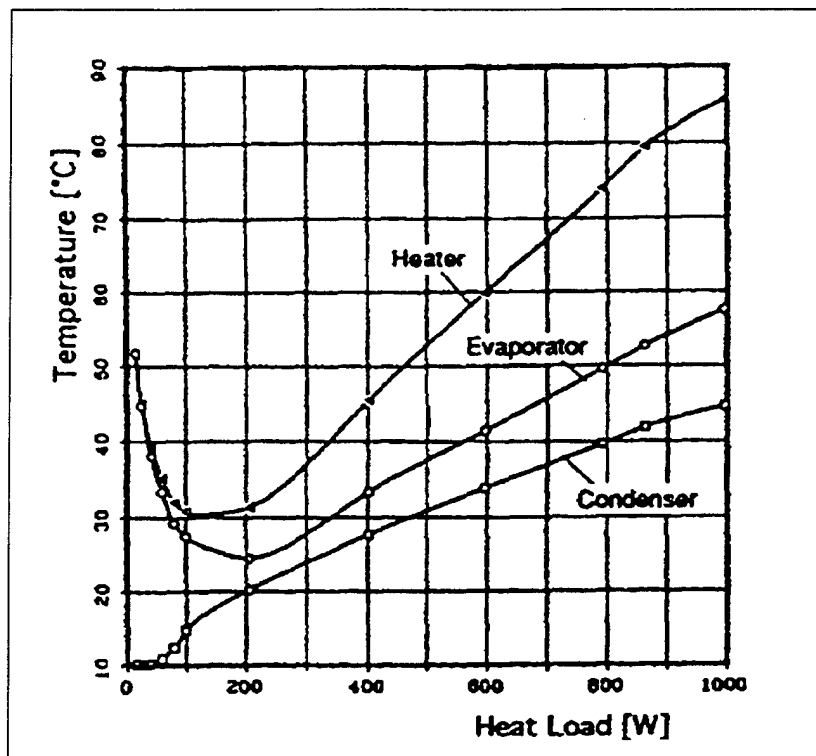


Figure A.3. German LHP Results -- Ammonia Working Fluid -- Configuration Unknown. [9]

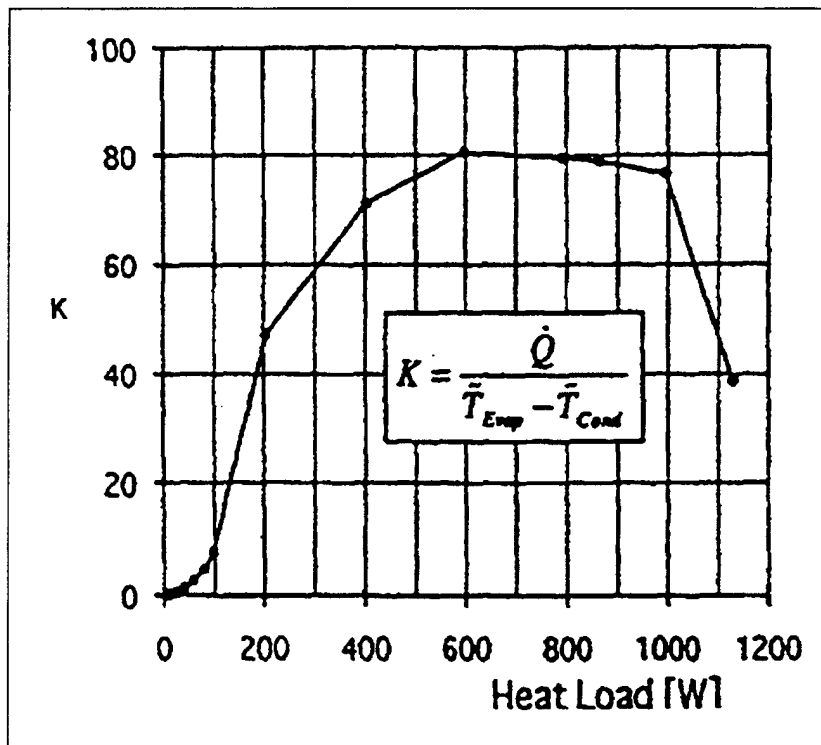


Figure A.4. German LHP Results -- Ammonia Working Fluid -- Configuration Unknown. [9]

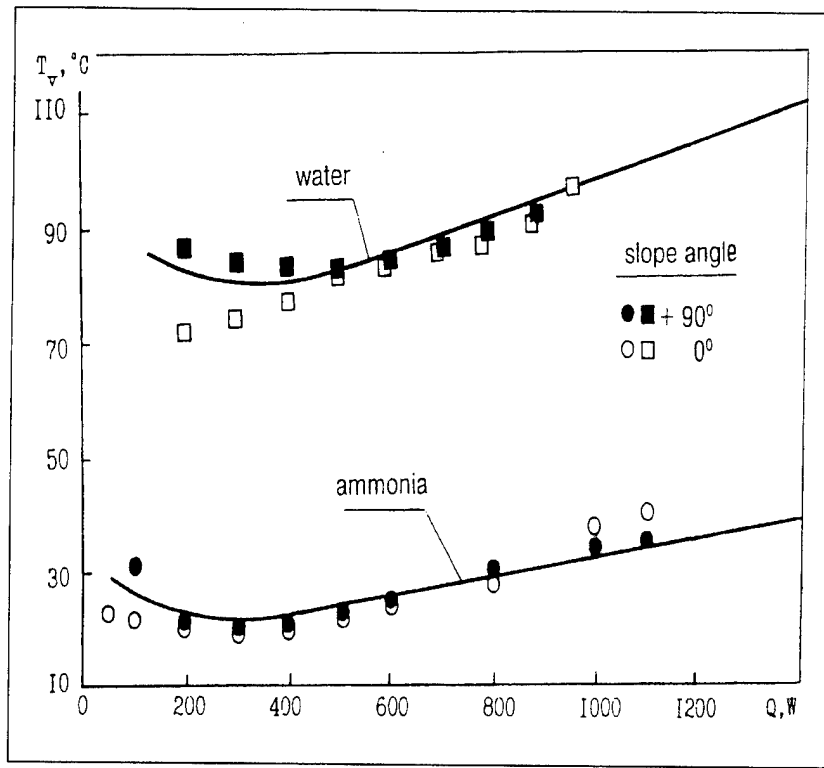


Figure A.5. Vapor (Evaporator) Temperature vs. Heat Load. Line = Calculated value at +90° (vertical orientation); dots = experimental data. Water LHP is 1.68 m; Ammonia LHP is 2.3 m. [7]

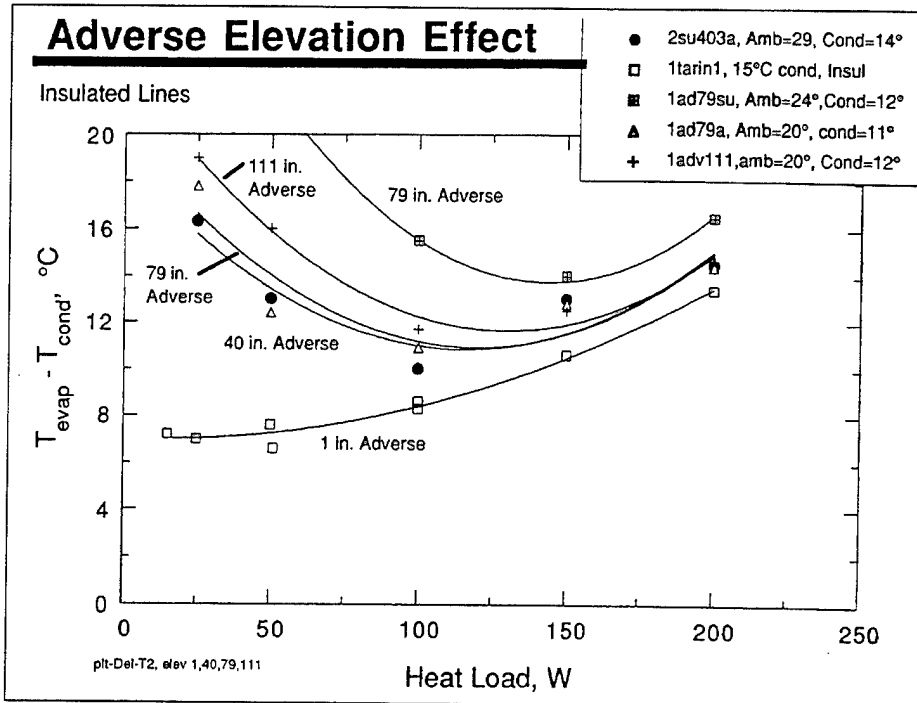


Figure A.6. Martin Marietta Astronautics Group (MMAG) Results. Ammonia-Charged LHP; otherwise Identical to Test Article. [8]

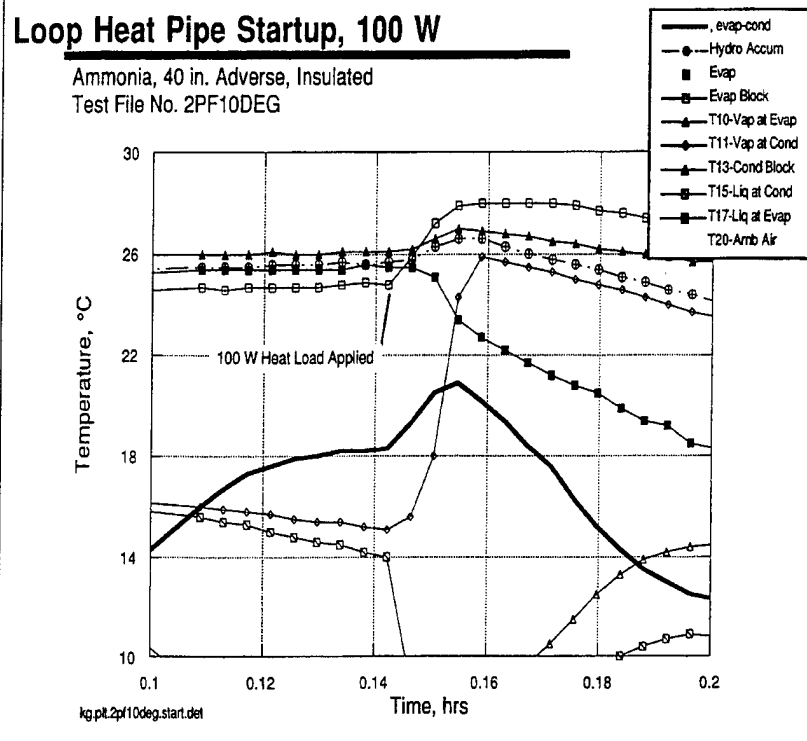


Figure A.7. LHP Startup Profile. MMAG Results. [8]

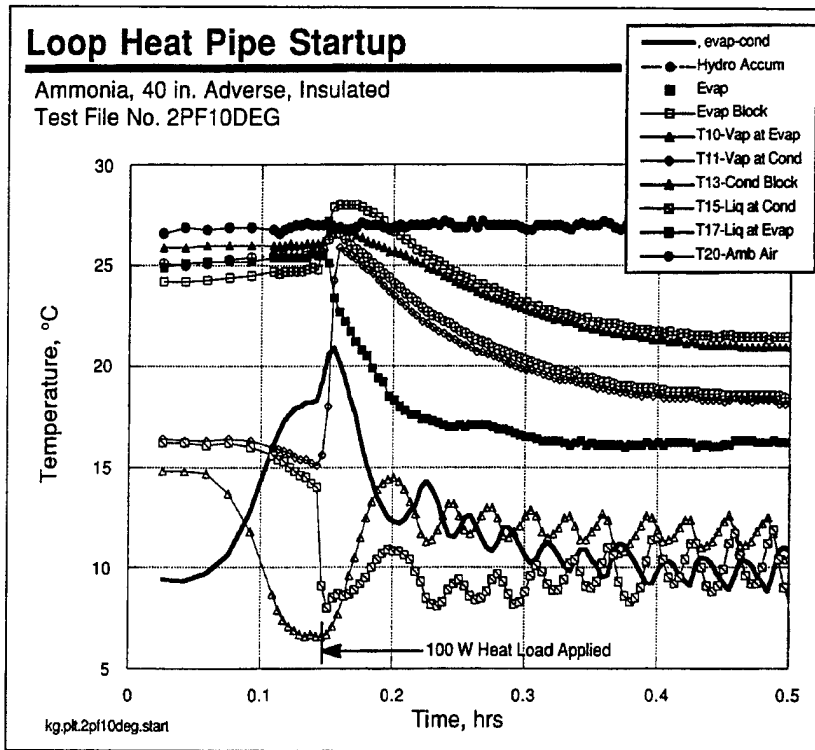


Figure A.8. LHP Run Profile. MMAG Results. [8]

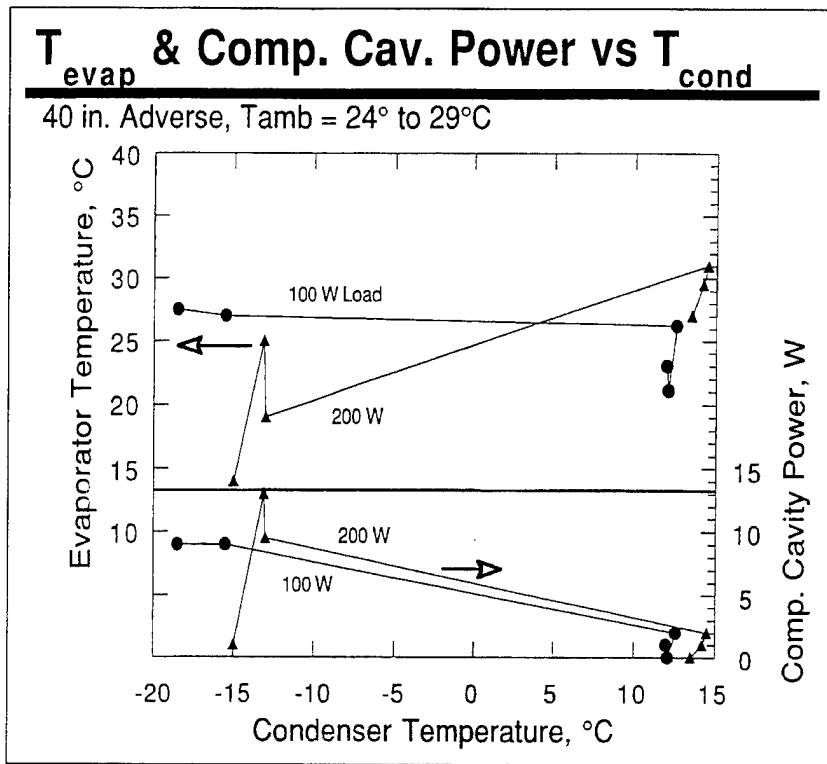


Figure A.9. MMAG Results. Displays use of CC Heating to Smooth Evaporator Temperature Response over Condenser Temperature Ranging from -18 to +13°C. [8]

APPENDIX B

LHP-93-2-PROP TEST INFORMATION, AND SELECTED RESULTS.

Test #	Purpose	Adv. Hgt. (inch)	Evap. Tilt (°)	Insul. (Y/N)	TV Y/N	Hours Btwn Tests	Evap. Load (W)	Evap. Temp. (°C)	CC Load (W)	Cond. Temp. (°C)
A1a	Baseline w/o Insul.	0	0	N	N	N/A	100	20-30	0	N/A
A1b							70			
A2a	Baseline with Insul.	0	0	Y	N	N/A	100	20-30	0	N/A
A2b							70			
A3a	Effect of Load	0	0	Y	N	N/A	5	20-30	0	N/A
A3b							10	20-30		N/A
A3c							20	20-30		N/A
A3d							30	20-30		N/A
A3e							50	20-30		N/A
A3f							150	N/A		Max Cool
A3g							200	N/A		Max Cool
A4a1	Effect of Cond. Temp.	0	0	Y	N	N/A	70	N/A	0	5
A4a2										10
A4a3										15
A4a4										20
A4b1	Effect of Cond. Temp.	0	0	Y	N	N/A	30	N/A	0	0
A4b2										5
A4b3										10
A4b4										20
A5a	Effect of Adv. Hgt.	40	0	Y	N	N/A	70	N/A		10
A5b		80								
A5c		120								

A6a	Reflux	24	0	Y	N	N/A	70	N/A		10
A6b		48								
A7a	Effect of Rotation	0	90	Y	N	N/A	70	N/A	0	10
A7b			-20							
A7c			-40							
A7d			-60							
B1	12" Adverse	12	0	Y	N	N/A	5	N/A	0	20
B2							10			
B3							20			
B4	18" Adverse	18	0	Y	N	N/A	5	N/A	0	20
B5							10			
B6							20			
B7	24" Adverse	24	0	Y	N	N/A	5	N/A	0	20
B8							10			
B9							20			
C1	Power Changes DURING Test	40	0	Y	N	N/A	100,50,20 5,20,50, 100	N/A	0	20
C2	Power Changes DURING Test	80	0	Y	N	N/A	100,50,20 5,20,50, 100	N/A	0	20
C3	Cond. Temp. Changes DURING Test	40	0	Y	N	N/A	100	N/A	0	20,5,-10, -25,-10, 5,20,35

C4	Cond. Temp.	80	0	Y	N	N/A	100	N/A	0	20,5,-10, -25,-10, 5,20,35
	Changes DURING Test									
D1	Vary CC	40	0	Y	N	N/A	100	N/A	2	20
D2									4	
3	Load								8	
4									16	
D5	Vary CC	80	0	Y	N	N/A	100	N/A	2	20
D6									4	
D7	Load								8	
D8									16	
D9	Control	40	0	Y	N	N/A	100	25	As	
D10	Evap.							32	Rqd	
D11	Temp.							40		
D12								50		
E1	Long Pause,	40	0	Y	N	24	100	N/A	0	5
E2										-10
E3	Max Load									-25
E4	Long Pause,	40	0	Y	N	24	50	N/A	0	5
E5										-10
E6	Low Load									-25
F1	Baseline	0	0	N/A	Y	N/A	100	N/A	0	20
	TV									

F2	Effect of	0	0	N/A	Y	N/A	50	N/A	0	20
F3	Load						20			
F4							7			
F5	Effect of	0	0	N/A	Y	N/A	100	N/A	0	10
F6	Cond.									0
F7	Temp.									-10
F8	Adv.	24	0	N/A	Y	N/A	100	N/A	0	20
F9	Hgt.						50			
F10							20			
F11							7			
* + is with CC down										

Table B.1. LHP-93-2-Prop Test Plan

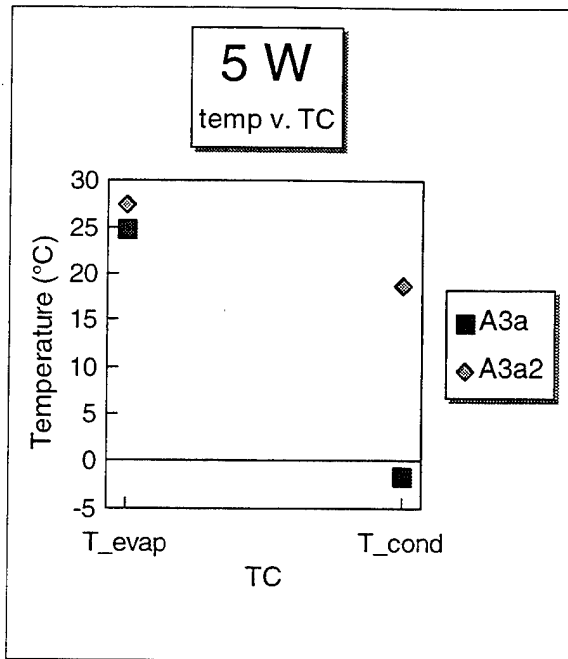


Figure B.1.

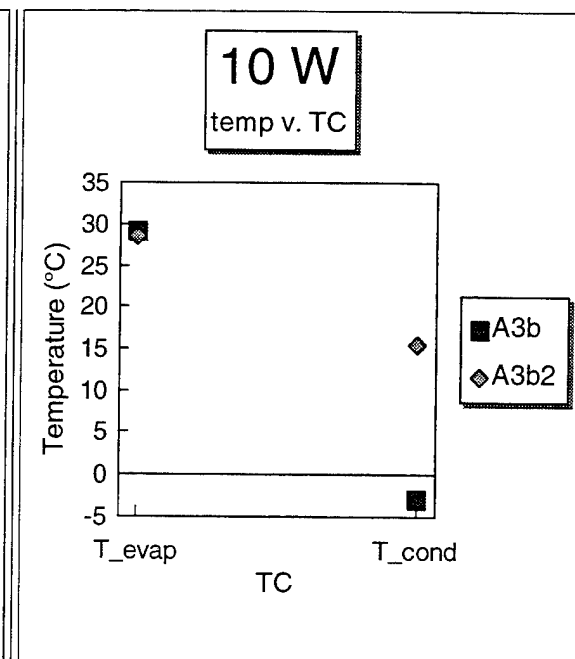


Figure B.3.

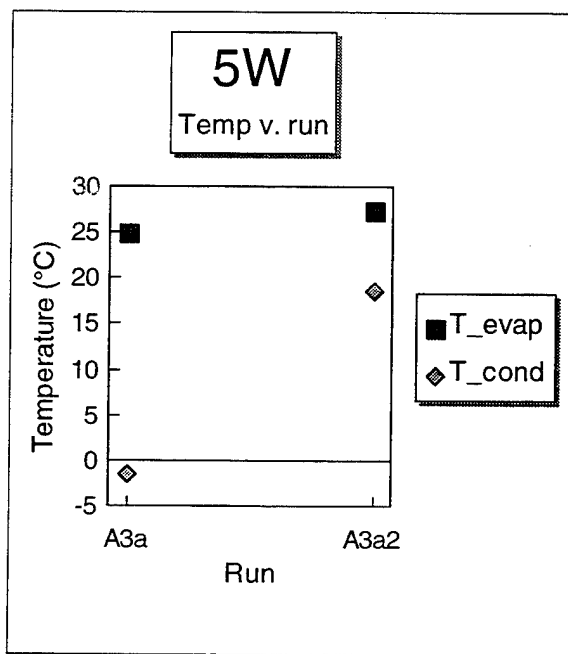


Figure B.2.

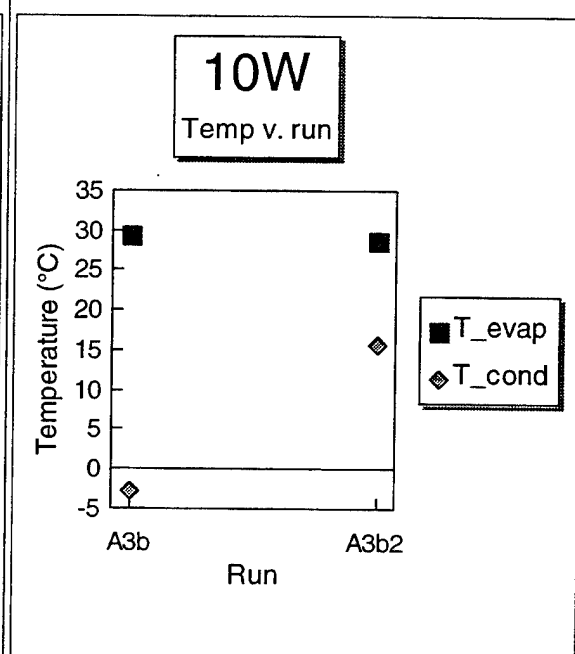


Figure B.4.

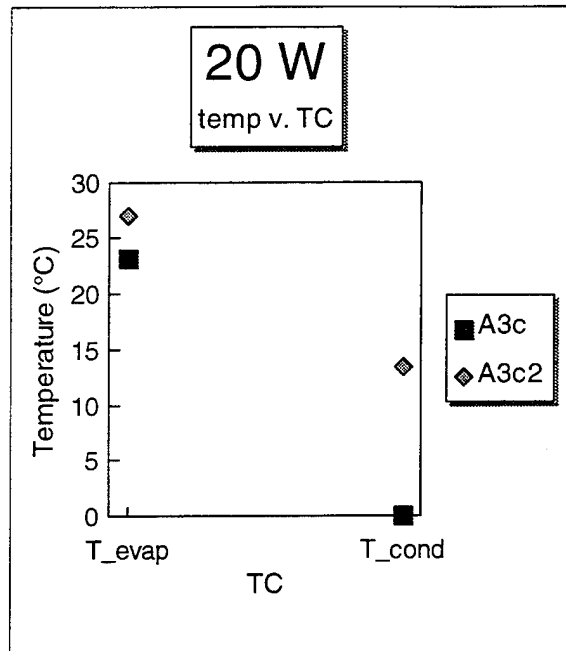


Figure B.5.

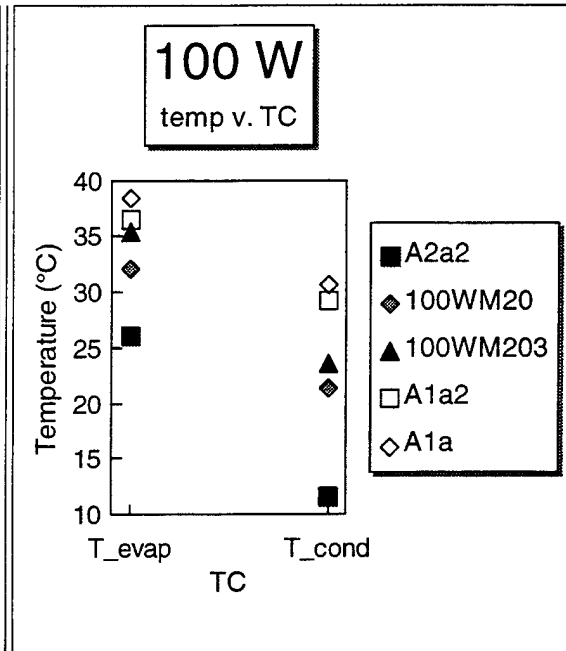


Figure B.7.

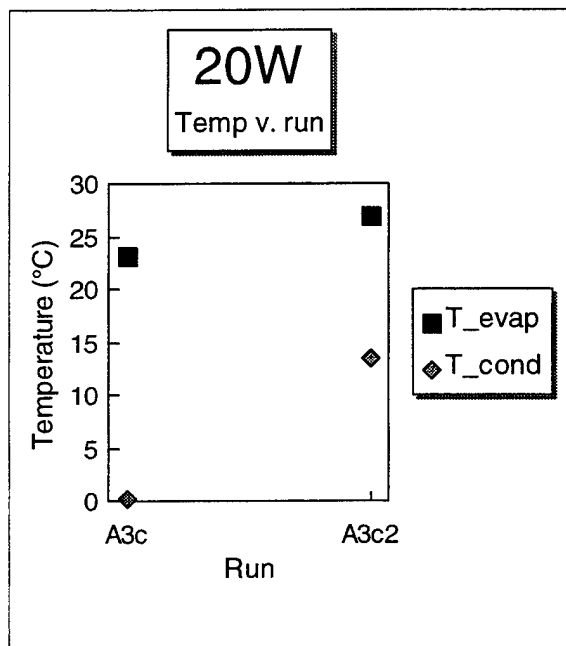


Figure B.6.

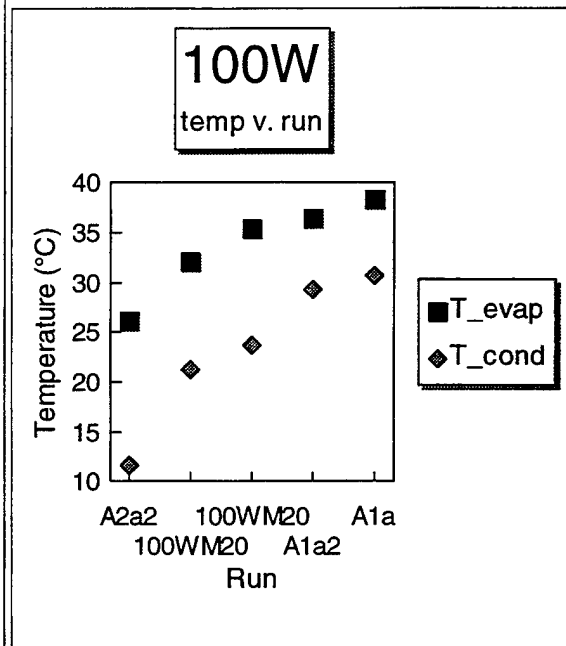


Figure B.8.

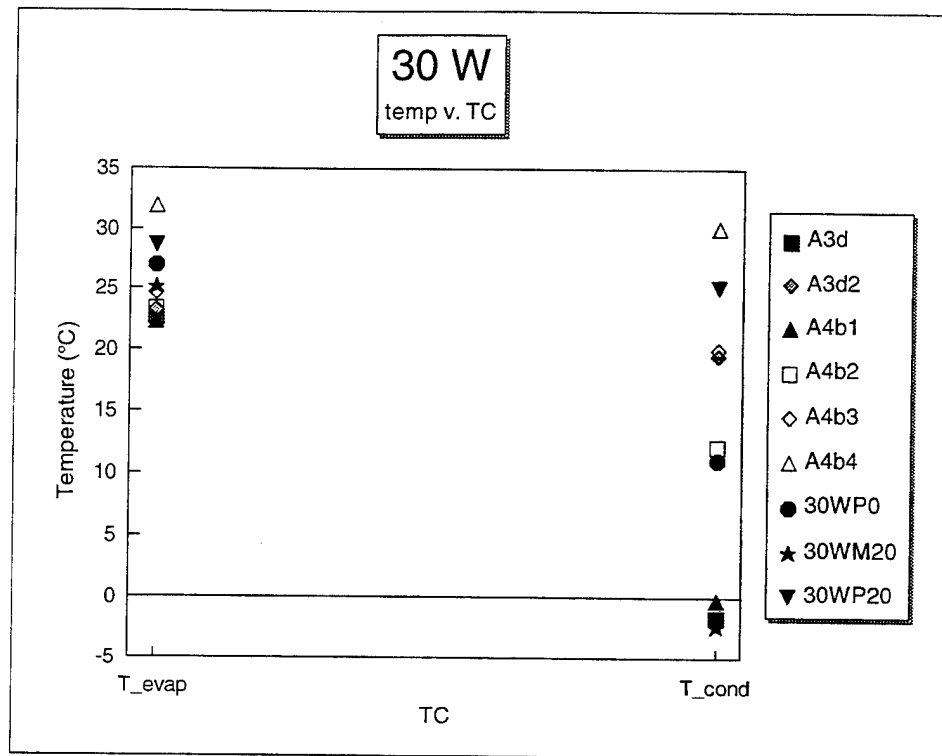


Figure B.9.

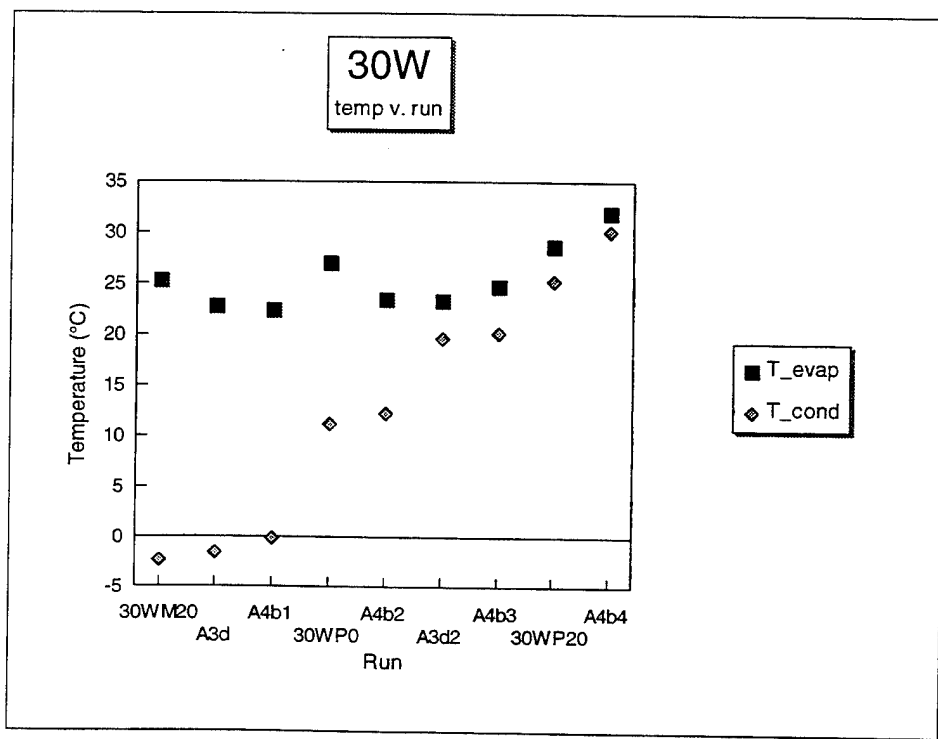


Figure B.10.

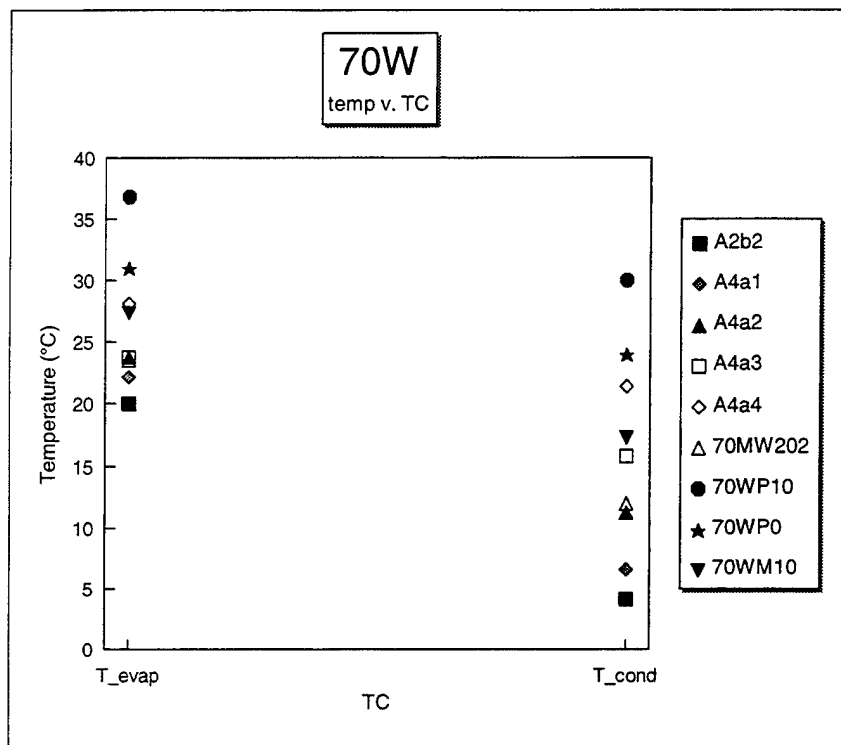


Figure B.11.

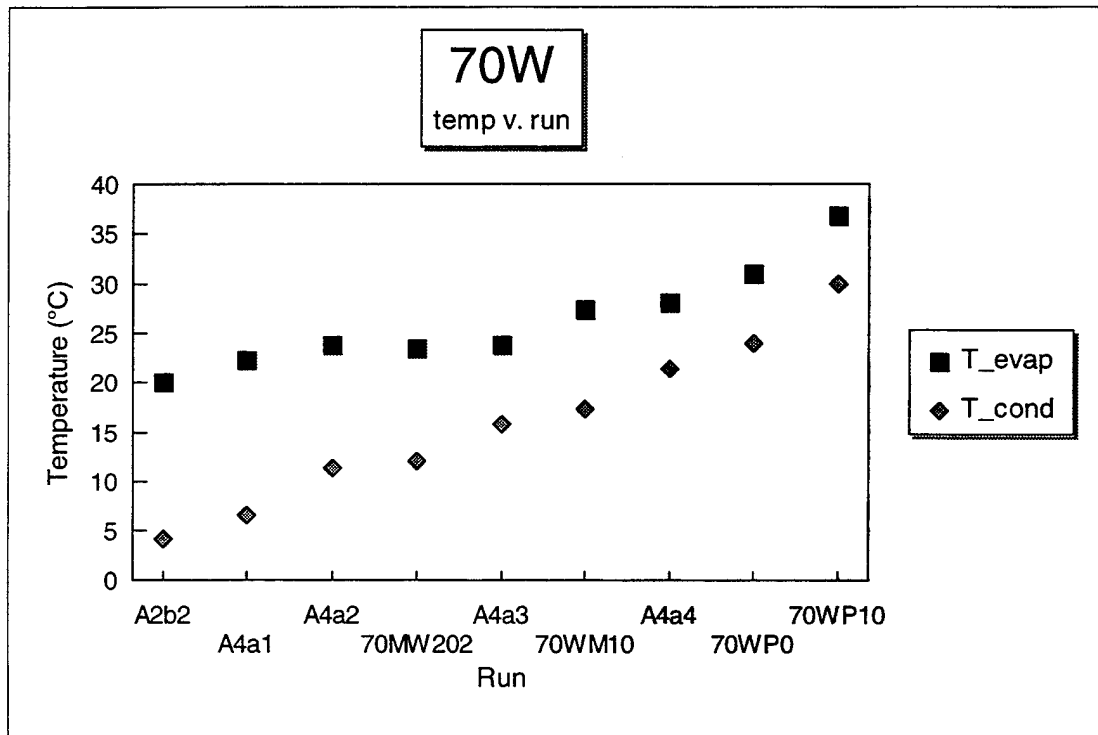


Figure B.12.

Equilibrium Temperatures
150 and 100 W Runs

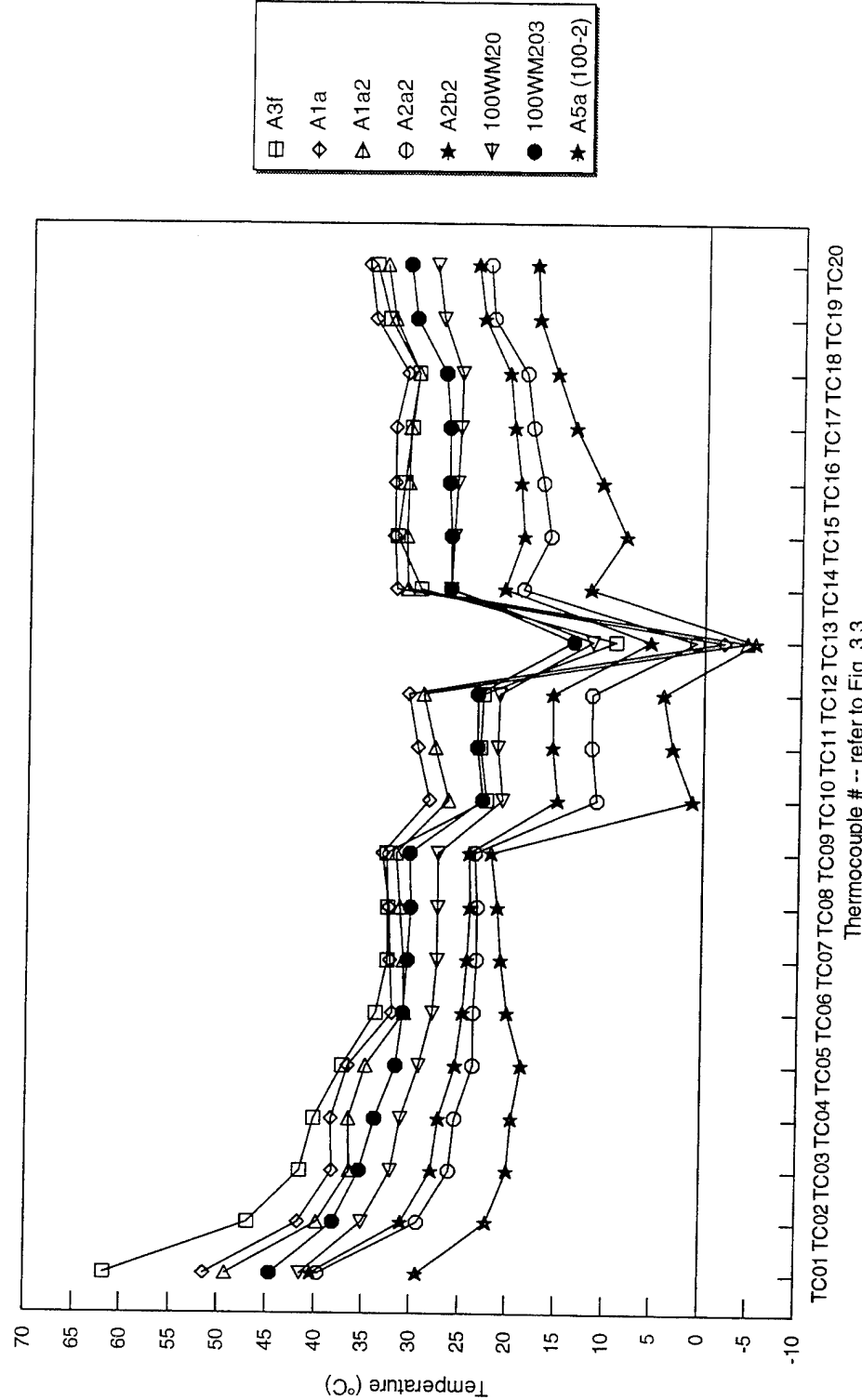


Figure B.13.

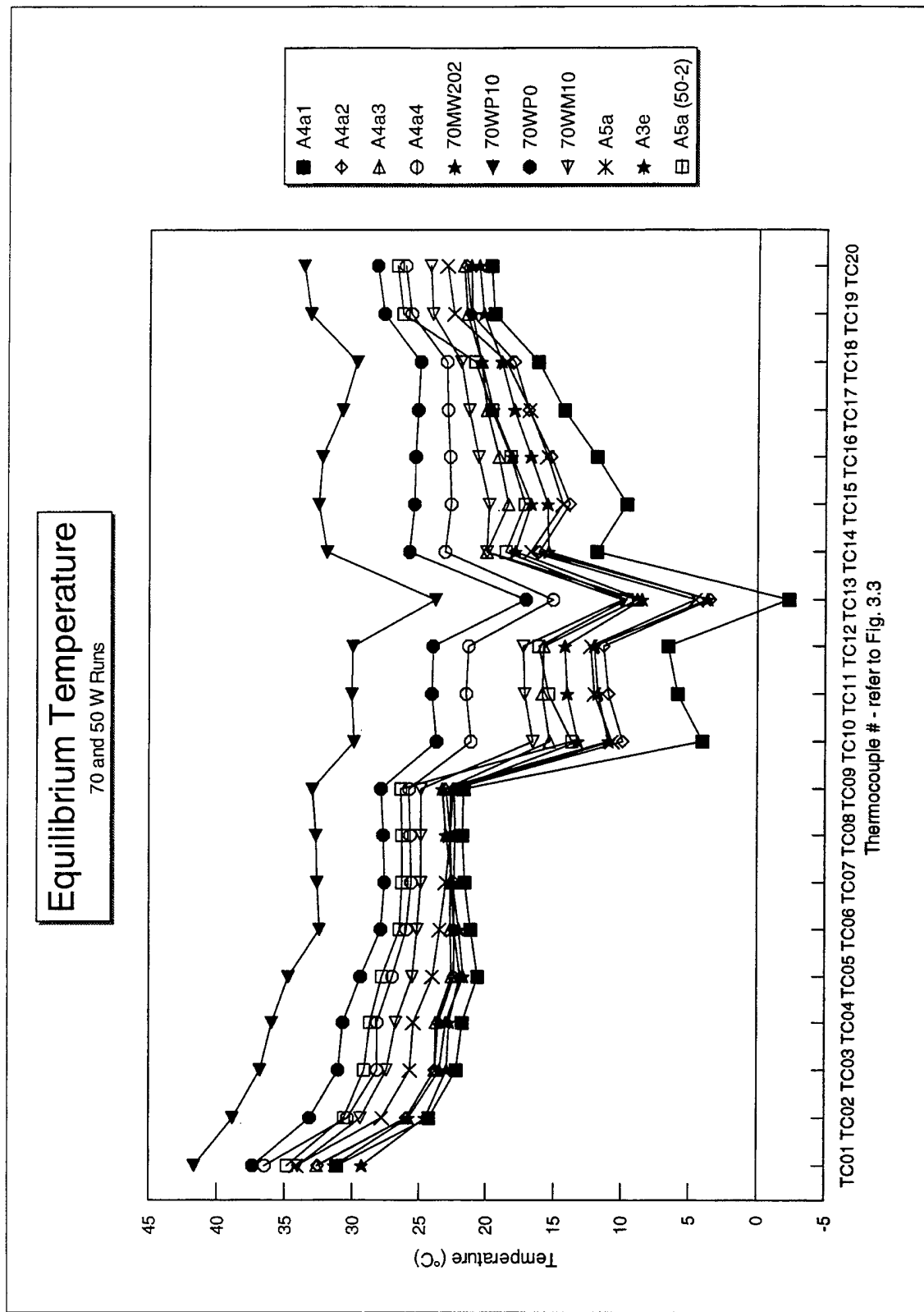


Figure B.14.

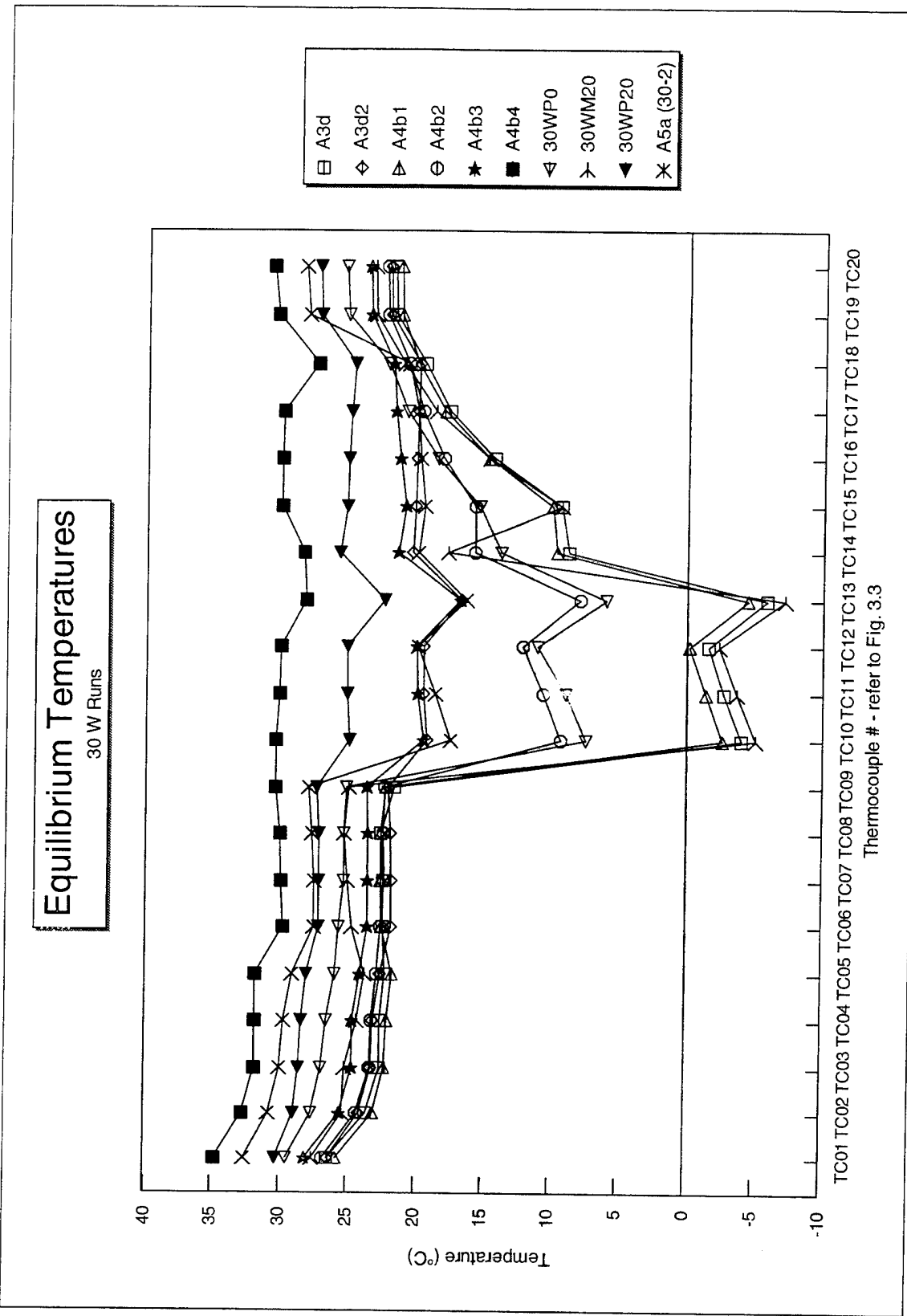


Figure B.15.

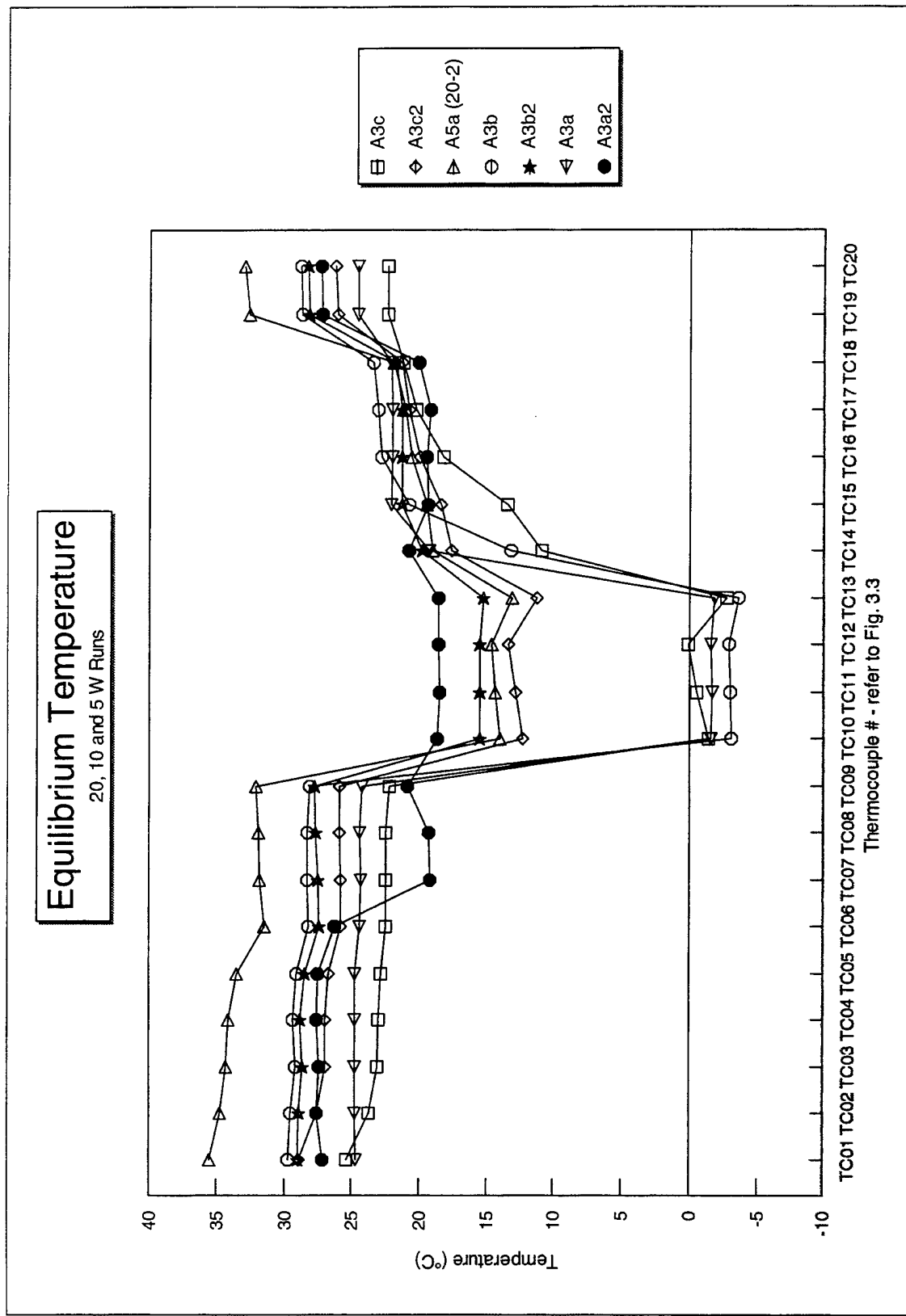
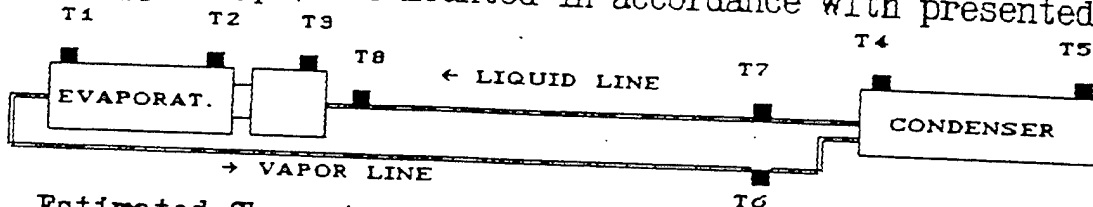


Figure B.16.

P R O T O C O L
 The results of Heat Pipe LHP-93-1-Prop
 Thermal Tests
 Heat Pipe Number 01.02

Object of Tests

Heat Pipe LHP-93-2-Prop design is based on Loop Heat Pipe. I design specification and dimensions are in accordance with contract RS3-456194. Heat Pipe is charged by propylene in volume 30.5 grams. Temperature sensors (thermal electric thermocouples copper-nickel copper type) was mounted in accordance with presented scheme.



Estimated Characteristics

In accordance with requirements of RS3-456194 heat pipe must

- transferred heat load not less 100W
- temperature difference between evaporator and condenser not more than 10 K at applied load 30 W.
(Vapor working temperature should be between 20-30°C).

Tests Results

Tests results are presented in Table. Here W - applied to the heater electric power [W], T_i - temperature of the sensors mounted places [°C], ΔT - temperature difference between evaporator and condenser [°C].

W	T_1	T_2	T_3	T_4	T_5	T_6	T_7	T_8	ΔT
34	23.4	23.8	21.8	16.3	18.1	22.2	19.0	19.3	6.4
100	24.7	25.7	21.0	6.0	11.4	21.6	18.5	18.9	-
130	32.7	35.0	27.0	8.7	16.0	28.5	27.9	27.3	-
*	30	26.5	27.6	25.0	20.7	22.3	25.8	21.7	19.2
*	80	32.1	35.1	26.3	18.7	21.2	27.6	27.1	28.2

--modes were realized with 2 meters excess of evaporator above the condenser (other modes were realized at horizontal position of heat pipe)

Conclusion.

Heat pipe LHP-93-1-Ammon, number 01.01 is in accordance with requirements of RS3-456194

Prepared Смирнова /S. Starodumova/

Checked Л. Калачёва /L. Kalachyova/

Confirmed Гончаров /K. Goncharov/

Table B.2. Data Taking Sheet.

APPENDIX C. LHP-93-2-PROP EXPERIMENTAL DATA.

Year	Month	Day	Time	Star	Power		100 W		Star Time													
					Watt	MilliWatt	Watt	MilliWatt	Watt	MilliWatt	Watt	MilliWatt	Watt	MilliWatt	Watt	MilliWatt	Watt	MilliWatt	Watt	MilliWatt	Watt	MilliWatt
1992/09																						
0	10/01	10/02	10/03	10/04	1004	1007	1008	1009	1010	1011	1012	1013	1014	1015	1016	1017	1018	1019	1020	1021	1022	
1	22.5	22.8	23.1	23.4	23.6	23.8	24.1	24.3	24.5	24.7	24.9	25.1	25.3	25.5	25.7	25.9	26.1	26.3	26.5	26.7	26.9	
2	31.1	31.4	31.7	32.0	32.3	32.6	32.9	33.1	33.3	33.5	33.7	33.9	34.1	34.3	34.5	34.7	34.9	35.1	35.3	35.5	35.7	
3	39.3	39.6	39.9	40.2	40.5	40.8	41.1	41.4	41.7	42.0	42.3	42.6	42.9	43.2	43.5	43.8	44.1	44.4	44.7	45.0	45.3	
4	47.9	48.2	48.5	48.8	49.1	49.4	49.7	50.0	50.3	50.6	50.9	51.2	51.5	51.8	52.1	52.4	52.7	53.0	53.3	53.6	53.9	
5	56.5	56.8	57.1	57.4	57.7	58.0	58.3	58.6	58.9	59.2	59.5	59.8	60.1	60.4	60.7	61.0	61.3	61.6	61.9	62.2	62.5	
6	65.1	65.4	65.7	66.0	66.3	66.6	66.9	67.2	67.5	67.8	68.1	68.4	68.7	69.0	69.3	69.6	69.9	70.2	70.5	70.8	71.1	
7	73.7	74.0	74.3	74.6	74.9	75.2	75.5	75.8	76.1	76.4	76.7	77.0	77.3	77.6	77.9	78.2	78.5	78.8	79.1	79.4	79.7	
8	82.3	82.6	82.9	83.2	83.5	83.8	84.1	84.4	84.7	85.0	85.3	85.6	85.9	86.2	86.5	86.8	87.1	87.4	87.7	88.0	88.3	
9	90.9	91.2	91.5	91.8	92.1	92.4	92.7	93.0	93.3	93.6	93.9	94.2	94.5	94.8	95.1	95.4	95.7	96.0	96.3	96.6	96.9	
10	99.5	100.0	100.5	100.8	101.3	101.6	102.1	102.4	102.7	103.0	103.3	103.6	104.0	104.3	104.7	105.0	105.3	105.6	105.9	106.2	106.5	
11	108.1	108.4	108.7	109.0	109.3	109.6	109.9	110.2	110.5	110.8	111.1	111.4	111.7	112.0	112.3	112.6	112.9	113.2	113.5	113.8	114.1	
12	116.7	117.0	117.3	117.6	117.9	118.2	118.5	118.8	119.1	119.4	119.7	120.0	120.3	120.6	120.9	121.2	121.5	121.8	122.1	122.4	122.7	
13	125.3	125.6	125.9	126.2	126.5	126.8	127.1	127.4	127.7	128.0	128.3	128.6	128.9	129.2	129.5	129.8	130.1	130.4	130.7	131.0	131.3	
14	134.0	134.3	134.6	134.9	135.2	135.5	135.8	136.1	136.4	136.7	137.0	137.3	137.6	137.9	138.2	138.5	138.8	139.1	139.4	139.7	140.0	
15	142.6	142.9	143.2	143.5	143.8	144.1	144.4	144.7	145.0	145.3	145.6	145.9	146.2	146.5	146.8	147.1	147.4	147.7	148.0	148.3	148.6	
16	151.2	151.5	151.8	152.1	152.4	152.7	153.0	153.3	153.6	153.9	154.2	154.5	154.8	155.1	155.4	155.7	156.0	156.3	156.6	156.9	157.2	
17	160.0	160.3	160.6	160.9	161.2	161.5	161.8	162.1	162.4	162.7	163.0	163.3	163.6	163.9	164.2	164.5	164.8	165.1	165.4	165.7	166.0	
18	168.6	168.9	169.2	169.5	169.8	170.1	170.4	170.7	171.0	171.3	171.6	171.9	172.2	172.5	172.8	173.1	173.4	173.7	174.0	174.3	174.6	
19	177.2	177.5	177.8	178.1	178.4	178.7	179.0	179.3	179.6	179.9	180.2	180.5	180.8	181.1	181.4	181.7	182.0	182.3	182.6	182.9	183.2	
20	185.8	186.1	186.4	186.7	187.0	187.3	187.6	187.9	188.2	188.5	188.8	189.1	189.4	189.7	190.0	190.3	190.6	190.9	191.2	191.5	191.8	
21	194.4	194.7	195.0	195.3	195.6	195.9	196.2	196.5	196.8	197.1	197.4	197.7	198.0	198.3	198.6	198.9	199.2	199.5	199.8	200.1	200.4	
22	203.0	203.3	203.6	203.9	204.2	204.5	204.8	205.1	205.4	205.7	206.0	206.3	206.6	206.9	207.2	207.5	207.8	208.1	208.4	208.7	209.0	
23	211.6	211.9	212.2	212.5	212.8	213.1	213.4	213.7	214.0	214.3	214.6	214.9	215.2	215.5	215.8	216.1	216.4	216.7	217.0	217.3	217.6	
24	220.2	220.5	220.8	221.1	221.4	221.7	222.0	222.3	222.6	222.9	223.2	223.5	223.8	224.1	224.4	224.7	225.0	225.3	225.6	225.9	226.2	
25	228.8	229.1	229.4	229.7	230.0	230.3	230.6	230.9	231.2	231.5	231.8	232.1	232.4	232.7	233.0	233.3	233.6	233.9	234.2	234.5	234.8	
26	237.4	237.7	238.0	238.3	238.6	238.9	239.2	239.5	239.8	240.1	240.4	240.7	241.0	241.3	241.6	241.9	242.2	242.5	242.8	243.1	243.4	
27	246.0	246.3	246.6	246.9	247.2	247.5	247.8	248.1	248.4	248.7	249.0	249.3	249.6	249.9	250.2	250.5	250.8	251.1	251.4	251.7	252.0	
28	254.6	254.9	255.2	255.5	255.8	256.1	256.4	256.7	257.0	257.3	257.6	257.9	258.2	258.5	258.8	259.1	259.4	259.7	260.0	260.3	260.6	
29	259.1	259.4	259.7	260.0	260.3	260.6	260.9	261.2	261.5	261.8	262.1	262.4	262.7	263.0	263.3	263.6	263.9	264.2	264.5	264.8	265.1	
30	267.7	268.0	268.3	268.6	268.9	269.2	269.5	269.8	270.1	270.4	270.7	271.0	271.3	271.6	271.9	272.2	272.5	272.8	273.1	273.4	273.7	
31	276.3	276.6	276.9	277.2	277.5	277.8	278.1	278.4	278.7	279.0	279.3	279.6	279.9	280.2	280.5	280.8	281.1	281.4	281.7	282.0	282.3	
32	284.9	285.2	285.5	285.8	286.1	286.4	286.7	287.0	287.3	287.6	287.9	288.2	288.5	288.8	289.1	289.4	289.7	290.0	290.3	290.6	290.9	
33	289.5	290.2	290.9	291.6	292.3	293.0	293.7	294.4	295.1	295.8	296.5	297.2	297.9	298.6	299.3	300.0	300.7	301.4	302.1	302.8	303.5	
34	303.1	303.8	304.5	305.2	305.9	306.6	307.3	308.0	308.7	309.4	310.1	310.8	311.5	312.2	312.9	313.6	314.3	315.0	315.7	316.4	317.1	
35	312.7	313.4	314.1	314.8	315.5	316.2	316.9	317.6	318.3	319.0	319.7	320.4	321.1	321.8	322.5	323.2	323.9	324.6	325.3	326.0	326.7	
36	321.3	321.6	321.9	322.2	322.5	322.8	323.1	323.4	323.7	324.0	324.3	324.6	324.9	325.2	325.5	325.8	326.1	326.4	326.7	327.0	327.3	
37	330.9	331.2	331.5	331.8	332.1	332.4	332.7	333.0	333.3	333.6	333.9	334.2	334.5	334.8	335.1	335.4	335.7	336.0	336.3	336.6	336.9	
38	340.5	340.8	341.1	341.4	341.7	342.0	342.3	342.6	342.9	343.2	343.5	343.8	344.1	344.4	344.7	345.0	345.3	345.6	345.9	346.2	346.5	
39	350.1	350.4	350.7	351.0	351.3	351.6	351.9	352.2	352.5	352.8	353.1	353.4	353.7	354.0	354.3	354.6	354.9	355.2	355.5	355.8	356.1	
40	359.7	360.0	360.3	360.6	360.9	361.2	361.5	361.8	362.1	362.4	362.7	363.0	363.3	363.6	363.9	364.2	364.5	364.8	365.1	365.4	365.7	
41	379.3	379.6	380.1	380.4	380.7	381.0	381.3	381.6	381.9	382.2	382.5	382.8	383.1	383.4	383.7	384.0	384.3	384.6	384.9	385.2	385.5	
42	388.9	390.2	391.5	392.8	394.1	395.4	396.7	398.0	399.3	400.6	401.9	403.2	404.5	405.8	407.1	408.4	409.7	411.0	412.3	413.6	414.9	
43	418.5	419.8	421.1	422.4	423.7	425.0	426.3	427.6	428.9	430.2	431.5	432.8	434.1	435.4	436.7	438.0	439.3	440.6	441.9	443.2	444.5	
44	427.1	428.4	429.7	431.0	432.3	433.6	434.9	436.2	437.5	438.8	439.1	440.4	441.7	443.0	444.3	445.6	446.9	448.2	449.5	450.8	452.1	
45	435.7	437.0	438.3	439.6	440.9	442.2	443.5	444.8	446.1	447.4	448.7	449.0	450.3	451.6	452.9	454.2	455.5	456.8	458.1	459.4	460.7	
46	465.3	466.6	467.9	469.2	470.5	471.8	473.1	474.4	475.7	477.0	478.3	479.6	480.9	482.2	483.5	484.8	486.1	487.4	488.7	489.0	490.3	
47	474.9	476.2	477.5	478.8	479.1	479.4	479.7	480.0	480.3	480.6	480.9	481.2	481.5	481.8	482.1	482.4	482.7	483.0	483.3	483.6	483.9	
48	483.5	484.8	486.1	487.4	488.7	489.0	489.3	489.6	489.9	490.2	490.5	490.8	491.1	491.4	491.7	492.0	492.3	492.6	492.9	493.2	493.5	
49	492.1	493.4	494.7	496.0	497.3	498.6	499.9	501.2	502.5	503.8	505.1	506.4	507.7	509.0	510.3	511.6	512.9	514.2	515.5	516.8	518.1	
50	500.7	502.0	503.3	504.6	505.9	507.2	508.5	509.8	511.1	512.4	513.7	515.0	516.3	517.6	518.9	520.2	521.5	522.8	524.1	525.4	526.7	
51	519.3	520.6	521.9	523.2	524.5	525.8	527.1															

Fam.	A ₁	A ₂	D ₁₂	S ₂₂₁₀	1953				1954				1955			
					P ₁₂	S ₁₂	S ₁₂ t.m.	P ₁₂	S ₁₂	S ₁₂ t.m.	P ₁₂	S ₁₂	S ₁₂ t.m.	P ₁₂	S ₁₂	S ₁₂ t.m.
0	101	102	103	104	105	106	107	108	109	110	111	112	113	114	115	116
0	218	219	220	221	222	223	224	225	226	227	228	229	230	231	232	233
2	222	223	224	225	226	227	228	229	230	231	232	233	234	235	236	237
4	226	227	228	229	230	231	232	233	234	235	236	237	238	239	240	241
6	230	231	232	233	234	235	236	237	238	239	240	241	242	243	244	245
8	234	235	236	237	238	239	240	241	242	243	244	245	246	247	248	249
0	238	239	240	241	242	243	244	245	246	247	248	249	250	251	252	253
1	242	243	244	245	246	247	248	249	250	251	252	253	254	255	256	257
3	246	247	248	249	250	251	252	253	254	255	256	257	258	259	260	261
5	250	251	252	253	254	255	256	257	258	259	260	261	262	263	264	265
7	254	255	256	257	258	259	260	261	262	263	264	265	266	267	268	269
9	258	259	260	261	262	263	264	265	266	267	268	269	270	271	272	273
1	262	263	264	265	266	267	268	269	270	271	272	273	274	275	276	277
3	266	267	268	269	270	271	272	273	274	275	276	277	278	279	280	281
5	270	271	272	273	274	275	276	277	278	279	280	281	282	283	284	285
7	274	275	276	277	278	279	280	281	282	283	284	285	286	287	288	289
9	278	279	280	281	282	283	284	285	286	287	288	289	290	291	292	293
1	282	283	284	285	286	287	288	289	290	291	292	293	294	295	296	297
3	286	287	288	289	290	291	292	293	294	295	296	297	298	299	300	301
5	290	291	292	293	294	295	296	297	298	299	300	301	302	303	304	305
7	294	295	296	297	298	299	300	301	302	303	304	305	306	307	308	309
9	298	299	300	301	302	303	304	305	306	307	308	309	310	311	312	313
1	302	303	304	305	306	307	308	309	310	311	312	313	314	315	316	317
3	306	307	308	309	310	311	312	313	314	315	316	317	318	319	320	321
5	310	311	312	313	314	315	316	317	318	319	320	321	322	323	324	325
7	314	315	316	317	318	319	320	321	322	323	324	325	326	327	328	329
9	318	319	320	321	322	323	324	325	326	327	328	329	330	331	332	333
1	322	323	324	325	326	327	328	329	330	331	332	333	334	335	336	337
3	326	327	328	329	330	331	332	333	334	335	336	337	338	339	340	341
5	330	331	332	333	334	335	336	337	338	339	340	341	342	343	344	345
7	334	335	336	337	338	339	340	341	342	343	344	345	346	347	348	349
9	338	339	340	341	342	343	344	345	346	347	348	349	350	351	352	353
1	342	343	344	345	346	347	348	349	350	351	352	353	354	355	356	357
3	346	347	348	349	350	351	352	353	354	355	356	357	358	359	360	361
5	350	351	352	353	354	355	356	357	358	359	360	361	362	363	364	365
7	354	355	356	357	358	359	360	361	362	363	364	365	366	367	368	369
9	358	359	360	361	362	363	364	365	366	367	368	369	370	371	372	373
1	362	363	364	365	366	367	368	369	370	371	372	373	374	375	376	377
3	366	367	368	369	370	371	372	373	374	375	376	377	378	379	380	381
5	370	371	372	373	374	375	376	377	378	379	380	381	382	383	384	385
7	374	375	376	377	378	379	380	381	382	383	384	385	386	387	388	389
9	378	379	380	381	382	383	384	385	386	387	388	389	390	391	392	393
1	382	383	384	385	386	387	388	389	390	391	392	393	394	395	396	397
3	386	387	388	389	390	391	392	393	394	395	396	397	398	399	400	401
5	390	391	392	393	394	395	396	397	398	399	400	401	402	403	404	405
7	394	395	396	397	398	399	400	401	402	403	404	405	406	407	408	409
9	398	399	400	401	402	403	404	405	406	407	408	409	410	411	412	413
1	402	403	404	405	406	407	408	409	410	411	412	413	414	415	416	417
3	406	407	408	409	410	411	412	413	414	415	416	417	418	419	420	421
5	410	411	412	413	414	415	416	417	418	419	420	421	422	423	424	425
7	414	415	416	417	418	419	420	421	422	423	424	425	426	427	428	429
9	418	419	420	421	422	423	424	425	426	427	428	429	430	431	432	433
1	422	423	424	425	426	427	428	429	430	431	432	433	434	435	436	437
3	426	427	428	429	430	431	432	433	434	435	436	437	438	439	440	441
5	430	431	432	433	434	435	436	437	438	439	440	441	442	443	444	445
7	434	435	436	437	438	439	440	441	442	443	444	445	446	447	448	449
9	438	439	440	441	442	443	444	445	446	447	448	449	450	451	452	453
1	442	443	444	445	446	447	448	449	450	451	452	453	454	455	456	457
3	446	447	448	449	450	451	452	453	454	455	456	457	458	459	460	461
5	450	451	452	453	454	455	456	457	458	459	460	461	462	463	464	465
7	454	455	456	457	458	459	460	461	462	463	464	465	466	467	468	469
9	458	459	460	461	462	463	464	465	466	467	468	469	470	471	472	473
1	462	463	464	465	466	467	468	469	470	471	472	473	474	475	476	477
3	466	467	468	469	470	471	472	473	474	475	476	477	478	479	480	481
5	470	471	472	473	474	475	476	477	478	479	480	481	482	483	484	485
7	474	475	476	477	478	479	480	481	482	483	484	485	486	487	488	489
9	478	479	480	481	482	483	484	485	486	487	488	489	490	491	492	493
1	482	483	484	485	486	487	488	489	490	491	492	493	494	495	496	497
3	486	487	488	489	490	491	492	493	494	495	496	497	498	499	500	501
5	490	491	492	493	494	495	496	497	498	499	500	501	502	503	504	505
7	494	495	496	497	498	499	500	501	502	503	504	505	506	507	508	509
9	498	499	500	501	502	503	504	505	506	507	508	509	510	511	512	513
1	502	503	504	505	506	507	508	509	510	511	512	513	514	515	516	517
3	506	507	508	509	510	511	512	513	514	515	516	517	518	519	520	521
5	510	511	512	513	514	515	516	517	518	519	520	521	522	523	524	525
7	514	515	516	517	518	519	520	521	522	523	524	525	526	527	528	529
9	518	519	520	521	522	523	524	525	526	527	528	529	530	531	532	533
1	522	523	524	525	526	527	528	529	530	531	532	533	534	535	536	537
3	526	527	528	529	530	531	532	533	534	535	536	537	538	539	540	541
5	530	531	532	533	534	535	536	537	538	539	540	541	542	543	544	545
7	534	535	536	537	538	539	540	541	542	543	544	545	546	547	548	549
9	538	539	540	541	542	543	544	545	546	547	548	549	550	551	552	553
1	542	543	544	545	546	547	548	549	550	551	552	553	554	555		

Date	Species	Time																				
		Start	End																			
1991	920314																					
10/01	10/02	10/03	10/04	10/05	10/06	10/07	10/08	10/09	10/10	10/11	10/12	10/13	10/14	10/15	10/16	10/17	10/18	10/19	10/20	10/21	10/22	
2	21.1	21.2	21.3	21.4	21.5	21.6	21.7	21.8	21.9	22.0	22.1	22.2	22.3	22.4	22.5	22.6	22.7	22.8	22.9	23.0	23.1	23.2
3	22.1	22.2	22.3	22.4	22.5	22.6	22.7	22.8	22.9	23.0	23.1	23.2	23.3	23.4	23.5	23.6	23.7	23.8	23.9	24.0	24.1	24.2
4	23.1	23.2	23.3	23.4	23.5	23.6	23.7	23.8	23.9	24.0	24.1	24.2	24.3	24.4	24.5	24.6	24.7	24.8	24.9	25.0	25.1	25.2
5	24.1	24.2	24.3	24.4	24.5	24.6	24.7	24.8	24.9	25.0	25.1	25.2	25.3	25.4	25.5	25.6	25.7	25.8	25.9	26.0	26.1	26.2
6	25.1	25.2	25.3	25.4	25.5	25.6	25.7	25.8	25.9	26.0	26.1	26.2	26.3	26.4	26.5	26.6	26.7	26.8	26.9	27.0	27.1	27.2
7	26.1	26.2	26.3	26.4	26.5	26.6	26.7	26.8	26.9	27.0	27.1	27.2	27.3	27.4	27.5	27.6	27.7	27.8	27.9	28.0	28.1	28.2
8	27.1	27.2	27.3	27.4	27.5	27.6	27.7	27.8	27.9	28.0	28.1	28.2	28.3	28.4	28.5	28.6	28.7	28.8	28.9	29.0	29.1	29.2
9	28.1	28.2	28.3	28.4	28.5	28.6	28.7	28.8	28.9	29.0	29.1	29.2	29.3	29.4	29.5	29.6	29.7	29.8	29.9	30.0	30.1	30.2
10	29.1	29.2	29.3	29.4	29.5	29.6	29.7	29.8	29.9	30.0	30.1	30.2	30.3	30.4	30.5	30.6	30.7	30.8	30.9	31.0	31.1	31.2
11	30.1	30.2	30.3	30.4	30.5	30.6	30.7	30.8	30.9	31.0	31.1	31.2	31.3	31.4	31.5	31.6	31.7	31.8	31.9	32.0	32.1	32.2
12	31.1	31.2	31.3	31.4	31.5	31.6	31.7	31.8	31.9	32.0	32.1	32.2	32.3	32.4	32.5	32.6	32.7	32.8	32.9	33.0	33.1	33.2
13	32.1	32.2	32.3	32.4	32.5	32.6	32.7	32.8	32.9	33.0	33.1	33.2	33.3	33.4	33.5	33.6	33.7	33.8	33.9	34.0	34.1	34.2
14	33.1	33.2	33.3	33.4	33.5	33.6	33.7	33.8	33.9	34.0	34.1	34.2	34.3	34.4	34.5	34.6	34.7	34.8	34.9	35.0	35.1	35.2
15	34.1	34.2	34.3	34.4	34.5	34.6	34.7	34.8	34.9	35.0	35.1	35.2	35.3	35.4	35.5	35.6	35.7	35.8	35.9	36.0	36.1	36.2
16	35.1	35.2	35.3	35.4	35.5	35.6	35.7	35.8	35.9	36.0	36.1	36.2	36.3	36.4	36.5	36.6	36.7	36.8	36.9	37.0	37.1	37.2
17	36.1	36.2	36.3	36.4	36.5	36.6	36.7	36.8	36.9	37.0	37.1	37.2	37.3	37.4	37.5	37.6	37.7	37.8	37.9	38.0	38.1	38.2
18	37.1	37.2	37.3	37.4	37.5	37.6	37.7	37.8	37.9	38.0	38.1	38.2	38.3	38.4	38.5	38.6	38.7	38.8	38.9	39.0	39.1	39.2
19	38.1	38.2	38.3	38.4	38.5	38.6	38.7	38.8	38.9	39.0	39.1	39.2	39.3	39.4	39.5	39.6	39.7	39.8	39.9	40.0	40.1	40.2
20	39.1	39.2	39.3	39.4	39.5	39.6	39.7	39.8	39.9	40.0	40.1	40.2	40.3	40.4	40.5	40.6	40.7	40.8	40.9	41.0	41.1	41.2
21	40.1	40.2	40.3	40.4	40.5	40.6	40.7	40.8	40.9	41.0	41.1	41.2	41.3	41.4	41.5	41.6	41.7	41.8	41.9	42.0	42.1	42.2
22	41.1	41.2	41.3	41.4	41.5	41.6	41.7	41.8	41.9	42.0	42.1	42.2	42.3	42.4	42.5	42.6	42.7	42.8	42.9	43.0	43.1	43.2
23	42.1	42.2	42.3	42.4	42.5	42.6	42.7	42.8	42.9	43.0	43.1	43.2	43.3	43.4	43.5	43.6	43.7	43.8	43.9	44.0	44.1	44.2
24	43.1	43.2	43.3	43.4	43.5	43.6	43.7	43.8	43.9	44.0	44.1	44.2	44.3	44.4	44.5	44.6	44.7	44.8	44.9	45.0	45.1	45.2
25	44.1	44.2	44.3	44.4	44.5	44.6	44.7	44.8	44.9	45.0	45.1	45.2	45.3	45.4	45.5	45.6	45.7	45.8	45.9	46.0	46.1	46.2
26	45.1	45.2	45.3	45.4	45.5	45.6	45.7	45.8	45.9	46.0	46.1	46.2	46.3	46.4	46.5	46.6	46.7	46.8	46.9	47.0	47.1	47.2
27	46.1	46.2	46.3	46.4	46.5	46.6	46.7	46.8	46.9	47.0	47.1	47.2	47.3	47.4	47.5	47.6	47.7	47.8	47.9	48.0	48.1	48.2
28	47.1	47.2	47.3	47.4	47.5	47.6	47.7	47.8	47.9	48.0	48.1	48.2	48.3	48.4	48.5	48.6	48.7	48.8	48.9	49.0	49.1	49.2
29	48.1	48.2	48.3	48.4	48.5	48.6	48.7	48.8	48.9	49.0	49.1	49.2	49.3	49.4	49.5	49.6	49.7	49.8	49.9	50.0	50.1	50.2
30	49.1	49.2	49.3	49.4	49.5	49.6	49.7	49.8	49.9	50.0	50.1	50.2	50.3	50.4	50.5	50.6	50.7	50.8	50.9	51.0	51.1	51.2
31	50.1	50.2	50.3	50.4	50.5	50.6	50.7	50.8	50.9	51.0	51.1	51.2	51.3	51.4	51.5	51.6	51.7	51.8	51.9	52.0	52.1	52.2
32	51.1	51.2	51.3	51.4	51.5	51.6	51.7	51.8	51.9	52.0	52.1	52.2	52.3	52.4	52.5	52.6	52.7	52.8	52.9	53.0	53.1	53.2
33	52.1	52.2	52.3	52.4	52.5	52.6	52.7	52.8	52.9	53.0	53.1	53.2	53.3	53.4	53.5	53.6	53.7	53.8	53.9	54.0	54.1	54.2
34	53.1	53.2	53.3	53.4	53.5	53.6	53.7	53.8	53.9	54.0	54.1	54.2	54.3	54.4	54.5	54.6	54.7	54.8	54.9	55.0	55.1	55.2
35	54.1	54.2	54.3	54.4	54.5	54.6	54.7	54.8	54.9	55.0	55.1	55.2	55.3	55.4	55.5	55.6	55.7	55.8	55.9	56.0	56.1	56.2
36	55.1	55.2	55.3	55.4	55.5	55.6	55.7	55.8	55.9	56.0	56.1	56.2	56.3	56.4	56.5	56.6	56.7	56.8	56.9	57.0	57.1	57.2
37	56.1	56.2	56.3	56.4	56.5	56.6	56.7	56.8	56.9	57.0	57.1	57.2	57.3	57.4	57.5	57.6	57.7	57.8	57.9	58.0	58.1	58.2
38	58.1	58.2	58.3	58.4	58.5	58.6	58.7	58.8	58.9	59.0	59.1	59.2	59.3	59.4	59.5	59.6	59.7	59.8	59.9	60.0	60.1	60.2
39	59.1	59.2	59.3	59.4	59.5	59.6	59.7	59.8	59.9	60.0	60.1	60.2	60.3	60.4	60.5	60.6	60.7	60.8	60.9	61.0	61.1	61.2
40	60.1	60.2	60.3	60.4	60.5	60.6	60.7	60.8	60.9	61.0	61.1	61.2	61.3	61.4	61.5	61.6	61.7	61.8	61.9	62.0	62.1	62.2
41	61.1	61.2	61.3	61.4	61.5	61.6	61.7	61.8	61.9	62.0	62.1	62.2	62.3	62.4	62.5	62.6	62.7	62.8	62.9	63.0	63.1	63.2
42	62.1	62.2	62.3	62.4	62.5	62.6	62.7	62.8	62.9	63.0	63.1	63.2	63.3	63.4	63.5	63.6	63.7	63.8	63.9	64.0	64.1	64.2
43	63.1	63.2	63.3	63.4	63.5	63.6	63.7	63.8	63.9	64.0	64.1	64.2	64.3	64.4	64.5	64.6	64.7	64.8	64.9	65.0	65.1	65.2
44	64.1	64.2	64.3	64.4	64.5	64.6	64.7	64.8	64.9	65.0	65.1	65.2	65.3	65.4	65.5	65.6	65.7	65.8	65.9	66.0	66.1	66.2
45	65.1	65.2	65.3	65.4	65.5	65.6	65.7	65.8	65.9	66.0	66.1	66.2	66.3	66.4	66.5	66.6	66.7	66.8	66.9	67.0	67.1	67.2
46	66.1	66.2	66.3	66.4	66.5	66.6	66.7	66.8	66.9	67.0	67.1	67.2	67.3	67.4	67.5	67.6	67.7	67.8	67.9	68.0	68.1	68.2
47	67.1	67.2	67.3	67.4	67.5	67.6	67.7	67.8	67.9	68.0	68.1	68.2	68.3	68.4	68.5	68.6	68.7	68.8	68.9	69.0	69.1	69.2
48	68.1	68.2	68.3	68.4	68.5	68.6	68.7	68.8	68.9	69.0	69.1	69.2	69.3	69.4	69.5	69.6	69.7	69.8	69.9	70.0	70.1	70.2
49	69.1	69.2	69.3	69.4	69.5	69.6	69.7	69.8	69.9	70.0	70.1	70.2	70.3	70.4	70.5	70.6	70.7	70.8	70.9	71.0	71.1	71.2
50	70.1	70.2	70.3	70.4	70.5	70.6	70.7	70.8	70.9	71.0	71.1	71.2	71.3	71.4	71.5	71.6	71.7	71.8	71.9	72.0	72.1	72.2
51	71.1	71.2	71.3	71.4	71.5	71.6	71.7	71.8	71.9	72.0	72.1	72.2	72.3	72.4	72.5	72.6	72.7	72.8	72.9	73.0	73.1	73.2
52	72.1	72.2	72.3	72.4	72.5	72.6	72.7	72.8	72.9	73.0	73.1	73.2	73.3	73.4	73.5	73.6	73.7	73.8	73.9	74.0	74.1	74.2
53	73.1	73.2	73.3	73.4	73.5	73.6	73.7	73.8	73.9	74.0	74.1	74.2	74.3	74.4	74.5	74.6	74.7	74.8	74.9	75.0	75.1	75.2
54	74.1	74.2	74.3	74.4	74.5	74.6	74.7	74.8	74.9	75.0	75.1	75.2	75.3	75.4	75.5	75.6	75.7	75.8	75.9	76.0	76.1	76.2
55	75.1	75.2	75.3	75.4	75.5	75.6	75.7	75.8	75.9													

Gal	Ab4		Pm		D/W		S&L		1903													
	1021	1020	1024	1023	1027	1028	1028	1029	1021	1022	1023	1024	1021	1022	1023	1024	1021	1022	1023	1024	1021	1022
0	22.8	22.7	22.8	22.7	22.8	22.8	22.8	22.8	19.6	19.4	19.5	19.6	22.6	22.7	22.6	22.6	22.6	22.7	22.6	22.6	22.6	22.6
2	28.2	28.4	28.3	28.5	28.6	28.5	28.4	28.4	24.4	24.5	24.6	24.7	22.6	22.5	22.5	22.5	22.6	22.5	22.5	22.5	22.5	22.5
4	26.9	26.6	26.5	26.6	25.6	25.6	25.6	25.6	24.5	24.5	24.5	24.7	22.4	22.4	22.4	22.4	22.3	22.3	22.3	22.3	22.3	22.3
6	22.2	22.0	22.0	22.0	22.0	22.0	22.0	22.0	24.7	24.7	24.7	24.7	23.4	23.4	23.4	23.4	23.1	23.1	23.1	23.1	23.1	23.1
8	25.5	25.2	25.2	25.3	25.3	25.3	25.3	25.3	24.9	24.9	24.9	25.0	23.5	23.5	23.5	23.5	23.8	23.8	23.8	23.8	23.8	23.8
10	21.7	21.6	21.6	21.6	21.5	21.5	21.5	21.5	25.1	25.1	25.1	25.1	24.4	24.4	24.4	24.4	23.5	23.5	23.5	23.5	23.5	23.5
12	20.8	20.7	20.7	20.7	20.6	20.6	20.6	20.6	25.1	25.1	25.1	25.1	24.6	24.6	24.6	24.6	23.5	23.5	23.5	23.5	23.5	23.5
14	22.0	22.1	22.1	22.1	22.1	22.1	22.1	22.1	24.5	24.5	24.5	24.5	23.0	23.0	23.0	23.0	22.1	22.1	22.1	22.1	22.1	22.1
16	20.1	20.2	20.2	20.2	20.3	20.3	20.3	20.3	21.3	21.3	21.3	21.3	20.5	20.5	20.5	20.5	20.5	20.5	20.5	20.5	20.5	20.5
18	26.7	26.6	26.5	26.6	27.1	27.1	27.1	27.1	28.1	28.1	28.1	28.1	25.9	25.9	25.9	25.9	26.1	26.1	26.1	26.1	26.1	26.1
20	26.9	26.8	26.8	26.8	27.0	27.0	27.0	27.0	28.4	28.4	28.4	28.4	26.2	26.2	26.2	26.2	24.3	24.3	24.3	24.3	24.3	24.3
22	21.5	21.4	21.4	21.5	21.5	21.5	21.5	21.5	28.8	28.8	28.8	28.8	28.0	28.0	28.0	28.0	27	27	27	27	27	27
24	31.2	30.1	30.1	30.1	29.2	29.3	29.3	29.3	27.6	27.7	27.7	27.7	27.6	27.6	27.6	27.6	27.6	27.6	27.6	27.6	27.6	27.6
26	32.4	32.1	32.1	32.1	32.0	32.0	32.0	32.0	28.1	28.2	28.2	28.2	28.3	28.3	28.3	28.3	28.4	28.4	28.4	28.4	28.4	28.4
28	23.4	23.4	23.4	23.4	23.4	23.4	23.4	23.4	28.8	28.8	28.8	28.8	28.0	28.0	28.0	28.0	28.1	28.1	28.1	28.1	28.1	28.1
30	23.1	23.1	23.1	23.1	23.1	23.1	23.1	23.1	28.8	28.8	28.8	28.8	28.0	28.0	28.0	28.0	28.1	28.1	28.1	28.1	28.1	28.1
32	21.1	21.1	21.1	21.1	21.1	21.1	21.1	21.1	28.8	28.8	28.8	28.8	28.0	28.0	28.0	28.0	28.1	28.1	28.1	28.1	28.1	28.1
34	21.0	21.0	21.0	21.0	21.0	21.0	21.0	21.0	28.8	28.8	28.8	28.8	28.0	28.0	28.0	28.0	28.1	28.1	28.1	28.1	28.1	28.1
36	22.1	22.1	22.1	22.1	22.1	22.1	22.1	22.1	28.8	28.8	28.8	28.8	28.0	28.0	28.0	28.0	28.1	28.1	28.1	28.1	28.1	28.1
38	21.9	21.9	21.9	21.9	21.9	21.9	21.9	21.9	28.8	28.8	28.8	28.8	28.0	28.0	28.0	28.0	28.1	28.1	28.1	28.1	28.1	28.1
40	21.9	21.9	21.9	21.9	21.9	21.9	21.9	21.9	28.8	28.8	28.8	28.8	28.0	28.0	28.0	28.0	28.1	28.1	28.1	28.1	28.1	28.1
42	21.9	21.9	21.9	21.9	21.9	21.9	21.9	21.9	28.8	28.8	28.8	28.8	28.0	28.0	28.0	28.0	28.1	28.1	28.1	28.1	28.1	28.1
44	21.9	21.9	21.9	21.9	21.9	21.9	21.9	21.9	28.8	28.8	28.8	28.8	28.0	28.0	28.0	28.0	28.1	28.1	28.1	28.1	28.1	28.1
46	21.9	21.9	21.9	21.9	21.9	21.9	21.9	21.9	28.8	28.8	28.8	28.8	28.0	28.0	28.0	28.0	28.1	28.1	28.1	28.1	28.1	28.1
48	21.9	21.9	21.9	21.9	21.9	21.9	21.9	21.9	28.8	28.8	28.8	28.8	28.0	28.0	28.0	28.0	28.1	28.1	28.1	28.1	28.1	28.1
50	21.9	21.9	21.9	21.9	21.9	21.9	21.9	21.9	28.8	28.8	28.8	28.8	28.0	28.0	28.0	28.0	28.1	28.1	28.1	28.1	28.1	28.1
52	21.9	21.9	21.9	21.9	21.9	21.9	21.9	21.9	28.8	28.8	28.8	28.8	28.0	28.0	28.0	28.0	28.1	28.1	28.1	28.1	28.1	28.1
54	21.9	21.9	21.9	21.9	21.9	21.9	21.9	21.9	28.8	28.8	28.8	28.8	28.0	28.0	28.0	28.0	28.1	28.1	28.1	28.1	28.1	28.1
56	21.9	21.9	21.9	21.9	21.9	21.9	21.9	21.9	28.8	28.8	28.8	28.8	28.0	28.0	28.0	28.0	28.1	28.1	28.1	28.1	28.1	28.1
58	21.9	21.9	21.9	21.9	21.9	21.9	21.9	21.9	28.8	28.8	28.8	28.8	28.0	28.0	28.0	28.0	28.1	28.1	28.1	28.1	28.1	28.1
60	21.9	21.9	21.9	21.9	21.9	21.9	21.9	21.9	28.8	28.8	28.8	28.8	28.0	28.0	28.0	28.0	28.1	28.1	28.1	28.1	28.1	28.1
62	21.9	21.9	21.9	21.9	21.9	21.9	21.9	21.9	28.8	28.8	28.8	28.8	28.0	28.0	28.0	28.0	28.1	28.1	28.1	28.1	28.1	28.1
64	21.9	21.9	21.9	21.9	21.9	21.9	21.9	21.9	28.8	28.8	28.8	28.8	28.0	28.0	28.0	28.0	28.1	28.1	28.1	28.1	28.1	28.1
66	21.9	21.9	21.9	21.9	21.9	21.9	21.9	21.9	28.8	28.8	28.8	28.8	28.0	28.0	28.0	28.0	28.1	28.1	28.1	28.1	28.1	28.1
68	21.9	21.9	21.9	21.9	21.9	21.9	21.9	21.9	28.8	28.8	28.8	28.8	28.0	28.0	28.0	28.0	28.1	28.1	28.1	28.1	28.1	28.1
70	21.9	21.9	21.9	21.9	21.9	21.9	21.9	21.9	28.8	28.8	28.8	28.8	28.0	28.0	28.0	28.0	28.1	28.1	28.1	28.1	28.1	28.1

Date	A ₃ (12,2)																				
	Obs	Actual																			
1962/01/01	95221	95221	1000	1000	1000	1000	1000	1000	1000	1000	1000	1000	1000	1000	1000	1000	1000	1000	1000	1000	1000
1	101	102	103	104	105	106	107	108	109	110	111	112	113	114	115	116	117	118	119	120	121
2	201	202	203	204	205	206	207	208	209	210	211	212	213	214	215	216	217	218	219	220	221
3	301	302	303	304	305	306	307	308	309	310	311	312	313	314	315	316	317	318	319	320	321
4	401	402	403	404	405	406	407	408	409	410	411	412	413	414	415	416	417	418	419	420	421
5	501	502	503	504	505	506	507	508	509	510	511	512	513	514	515	516	517	518	519	520	521
6	601	602	603	604	605	606	607	608	609	610	611	612	613	614	615	616	617	618	619	620	621
7	701	702	703	704	705	706	707	708	709	710	711	712	713	714	715	716	717	718	719	720	721
8	801	802	803	804	805	806	807	808	809	810	811	812	813	814	815	816	817	818	819	820	821
9	901	902	903	904	905	906	907	908	909	910	911	912	913	914	915	916	917	918	919	920	921
10	1001	1002	1003	1004	1005	1006	1007	1008	1009	1010	1011	1012	1013	1014	1015	1016	1017	1018	1019	1020	1021
11	1101	1102	1103	1104	1105	1106	1107	1108	1109	1110	1111	1112	1113	1114	1115	1116	1117	1118	1119	1120	1121
12	1201	1202	1203	1204	1205	1206	1207	1208	1209	1210	1211	1212	1213	1214	1215	1216	1217	1218	1219	1220	1221
13	1301	1302	1303	1304	1305	1306	1307	1308	1309	1310	1311	1312	1313	1314	1315	1316	1317	1318	1319	1320	1321
14	1401	1402	1403	1404	1405	1406	1407	1408	1409	1410	1411	1412	1413	1414	1415	1416	1417	1418	1419	1420	1421
15	1501	1502	1503	1504	1505	1506	1507	1508	1509	1510	1511	1512	1513	1514	1515	1516	1517	1518	1519	1520	1521
16	1601	1602	1603	1604	1605	1606	1607	1608	1609	1610	1611	1612	1613	1614	1615	1616	1617	1618	1619	1620	1621
17	1701	1702	1703	1704	1705	1706	1707	1708	1709	1710	1711	1712	1713	1714	1715	1716	1717	1718	1719	1720	1721
18	1801	1802	1803	1804	1805	1806	1807	1808	1809	1810	1811	1812	1813	1814	1815	1816	1817	1818	1819	1820	1821
19	1901	1902	1903	1904	1905	1906	1907	1908	1909	1910	1911	1912	1913	1914	1915	1916	1917	1918	1919	1920	1921
20	2001	2002	2003	2004	2005	2006	2007	2008	2009	2010	2011	2012	2013	2014	2015	2016	2017	2018	2019	2020	2021
21	2101	2102	2103	2104	2105	2106	2107	2108	2109	2110	2111	2112	2113	2114	2115	2116	2117	2118	2119	2120	2121
22	2201	2202	2203	2204	2205	2206	2207	2208	2209	2210	2211	2212	2213	2214	2215	2216	2217	2218	2219	2220	2221
23	2301	2302	2303	2304	2305	2306	2307	2308	2309	2310	2311	2312	2313	2314	2315	2316	2317	2318	2319	2320	2321
24	2401	2402	2403	2404	2405	2406	2407	2408	2409	2410	2411	2412	2413	2414	2415	2416	2417	2418	2419	2420	2421
25	2501	2502	2503	2504	2505	2506	2507	2508	2509	2510	2511	2512	2513	2514	2515	2516	2517	2518	2519	2520	2521
26	2601	2602	2603	2604	2605	2606	2607	2608	2609	2610	2611	2612	2613	2614	2615	2616	2617	2618	2619	2620	2621
27	2701	2702	2703	2704	2705	2706	2707	2708	2709	2710	2711	2712	2713	2714	2715	2716	2717	2718	2719	2720	2721
28	2801	2802	2803	2804	2805	2806	2807	2808	2809	2810	2811	2812	2813	2814	2815	2816	2817	2818	2819	2820	2821
29	2901	2902	2903	2904	2905	2906	2907	2908	2909	2910	2911	2912	2913	2914	2915	2916	2917	2918	2919	2920	2921
30	3001	3002	3003	3004	3005	3006	3007	3008	3009	3010	3011	3012	3013	3014	3015	3016	3017	3018	3019	3020	3021
31	3101	3102	3103	3104	3105	3106	3107	3108	3109	3110	3111	3112	3113	3114	3115	3116	3117	3118	3119	3120	3121
32	3201	3202	3203	3204	3205	3206	3207	3208	3209	3210	3211	3212	3213	3214	3215	3216	3217	3218	3219	3220	3221
33	3301	3302	3303	3304	3305	3306	3307	3308	3309	3310	3311	3312	3313	3314	3315	3316	3317	3318	3319	3320	3321
34	3401	3402	3403	3404	3405	3406	3407	3408	3409	3410	3411	3412	3413	3414	3415	3416	3417	3418	3419	3420	3421
35	3501	3502	3503	3504	3505	3506	3507	3508	3509	3510	3511	3512	3513	3514	3515	3516	3517	3518	3519	3520	3521
36	3601	3602	3603	3604	3605	3606	3607	3608	3609	3610	3611	3612	3613	3614	3615	3616	3617	3618	3619	3620	3621
37	3701	3702	3703	3704	3705	3706	3707	3708	3709	3710	3711	3712	3713	3714	3715	3716	3717	3718	3719	3720	3721
38	3801	3802	3803	3804	3805	3806	3807	3808	3809	3810	3811	3812	3813	3814	3815	3816	3817	3818	3819	3820	3821
39	3901	3902	3903	3904	3905	3906	3907	3908	3909	3910	3911	3912	3913	3914	3915	3916	3917	3918	3919	3920	3921
40	4001	4002	4003	4004	4005	4006	4007	4008	4009	4010	4011	4012	4013	4014	4015	4016	4017	4018	4019	4020	4021

INITIAL DISTRIBUTION LIST

	Number of Copies
1. Defense Technical Information Center Cameron Station Alexandria, VA 22304-6145	2
2. Library, Code 52 Naval Postgraduate School Monterey, CA 93943-5101	2
3. Dr. Matthew D. Kelleher Chairman, Department of Mechanical Engineering Code ME/KK Naval Postgraduate School Monterey, CA 93943-5002	2
4. Dr. Paul J. Marto Dean Of Research Code 09 Naval Postgraduate School Monterey, CA 93943-5002	2
5. Dr. Conrad F. Newberry Department of Aeronautics and Astronautics Code AA/NE Naval Postgraduate School Monterey, CA 93943-5002	2
6. Dr. Dan C. Boger Academic Associate, Space Systems Academic Group Code SM/BO Naval Postgraduate School Monterey, CA 93943-5002	2
7. Dr. Daniel J. Collins Chairman, Department of Aeronautical and Astronautical Engineering Code AA/CO Naval Postgraduate School Monterey, CA 93943-5002	2

8. Dr. Rudolph Panholzer 2
Chairman, Space Systems Academic Group
Code SP/PZ
Naval Postgraduate School
Monterey, CA 93943-5002

9. Captain Scott Thompson 1
Office of the Chief of Naval Operations
Code N63, Room 4E679 The Pentagon
Washington, DC 20350-2000

10. LT J.A. Gherlone, Jr., USN 2
41 Clintonville Rd.
North Haven, CT 06473

11. Dr. Donald Gluck 2
Philips Laboratory, VTPT
3550 Aberdeen Ave, S.E.
Bldg. 30117
Kirtland AFB, NM 87117-5776

12. Lt. Col. David H. Kristensen, USAF 1
Chief, Space Power and Thermal Management Division
Philips Laboratory, VTP
3550 Aberdeen Ave, S.E.
Bldg. 30117
Kirtland AFB, NM 87117-5776

13. Capt. Jeff Wiese, USAF 1
Chief, Space Thermal Technologies Branch
Philips Laboratory, VTPT
3550 Aberdeen Ave, S.E.
Bldg. 30117
Kirtland AFB, NM 87117-5776

14. Lt. Eric Critchley 1
Project Officer
Philips Laboratory, VTPT
3550 Aberdeen Ave, S.E.
Bldg. 30117
Kirtland AFB, NM 87117-5776

15. Jane Baumann	1
Lockheed Martin Astronautics Group	
P.O. Box 179	
Denver, CO 80201	
16. Roger Giellis	1
Lockheed Martin Astronautics Group	
P.O. Box 179	
Denver, CO 80201	
17. Brent Cullimore	1
Cullimore and Ring Technologies	
49 Dawn Heath Circle	
Littleton, CO 80127-4303	
18. Dr. Walter Bienert	1
President, Dynatherm Corporation	
1 Beaver Ct.	
P.O. Box 398	
Hunt Valley, MD 21030	
19. Nelson Hyman	1
Naval Research Laboratory	
Code 8222	
Washington, DC 20375-5000	
20. Ted Swanson	1
NASA Goddard Space Flight Center	
Code 724	
Greenbelt, MD 20771	